Break-up in formation of small bubbles

Pengbo Chu

Department of Mining and Materials Engineering
McGill University
Montreal, Canada

A thesis submitted to McGill University in partial fulfillment of the requirements of the degree of Doctor of Philosophy

April 2017

Abstract

Small bubbles, ca. 1 mm in diameter, play a key role in froth flotation. They not only form bubble swarms to provide large interfacial area for collecting and transporting attached mineral particles, but also rise at reduced velocities to increase bubble/particle collision frequency. Generation of small bubbles is usually accomplished by the use of surfactants called frothers, or sometimes by the presence of some inorganic salts. Understanding the action of these solutes, however, remains obscure. A common explanation is that the solutes inhibit coalescence, which can certainly be demonstrated, for example, by slowly bringing two bubbles into contact. But the fact that salts and many frothers are poor at building froth suggests they do not exhibit strong coalescence inhibition properties. This thesis postulates that the solutes may have a direct impact on break-up of the air mass.

Break-up and coalescence are simultaneous events that are coupled. To investigate a role of solutes in break-up, a break-up only system is required. In this thesis two experimental techniques are developed allowing break-up to be isolated from coalescence.

The first technique is to generate single air bubbles through break-away from an underwater capillary under quasi-static conditions. The break-away process is monitored using a passive acoustic technique and high speed cinematography. The image results show that break-away results in a liquid jet which is formed independent of the addition of frothers. Combining visual and the acoustic results suggested that the decay of the jet is associated with two mechanisms, acoustic emission and development of surface waves. The dissipation rate of the two mechanisms is characterized by their damping ratio. An increase in frother concentration leads to a decrease in the acoustic damping ratio and to an increase in damping of the surface wave.

The second experimental technique is a set-up devised to mimic break-up of the air cavity behind an impeller blade in a mechanical cell. In this case, single air bubbles are produced through mechanically-induced deformation of a trapped air volume. The first experiments showed that the size of the generated bubble is strongly affected by the presence of frother, but weakly by the input mechanical energy and the volume of trapped air. A second test series showed that an increase in frother concentration initially decreased the bubble size to a minimum then it increased. A critical break-up concentration (CBC) was introduced referring to the concentration corresponding to the minimum bubble size. In the last experimental series it was observed that the time taken for a bubble to form decreased in the presence of frother and salt. The hypothesis is that the presence of frother and salt accelerates break-up, interpreted as an added energy term derived from the solutes.

The thesis provides evidence that the presence of frother does reduce the size of bubble formed at break-up. A proposed explanation is that surface tension gradients induced by the frother play a role in the formation and size of interfacial instabilities (i.e., surface waves), that control the break-up bubble size.

Résumé

Les petites bulles (<1 mm) jouent un rôle clé dans la flottation par mousse. En plus de former des essaims fournissant une grande aire interfaciale pour l'attachement et le transport des particules minérales, elles montent à une vitesse réduite ce qui augmente la fréquence de collision entre les bulles et les particules. La production de petites bulles est habituellement réalisée par l'utilisation d'agents de surface nommés moussants, ou bien par la présence de sels inorganiques. La compréhension de l'action des ces solutés n'est pas encore bien définie. Une explication simple est l'inhibition de la coalescence par les solutés qui peut facilement être démontré, par exemple, en approchant doucement deux bulle jusqu'au contact. Cependant, le fait que les sels et plusieurs agents moussants ont une faible capacité à construire une mousse suggère que ceux-ci n'ont pas d'effet important sur l'inhibition de la coalescence. Cette thèse postule que les solutés ont peut-être un effet direct sur la rupture de la masse d'air à l'origine d'une bulle.

La rupture et la coalescence sont des événements simultanés qui sont reliés. Pour déterminer le rôle des solutés sur la rupture, un système fournissant seulement une rupture est requis. Dans cette thèse, deux techniques expérimentales sont développées permettant d'isoler la rupture de la coalescence.

La première technique consiste à produire un bulle d'air simple par la fuite d'air d'un tube capillaire simple immergé sous des conditions quasi-statiques. La fuite est observée à l'aide d'une technique acoustique passive et d'imagerie à haute vitesse. Les images montrent que la fuite produit un jet liquide formé indépendamment de l'addition d'agent moussant. En combinant l'analyse visuelle et acoustique, les résultats suggèrent que la dissipation du jet est associée à deux mécanismes, l'émission acoustique et la production de vagues de surface. Le taux de dissipation des deux mécanismes est caractérisé par leur ratio d'amortissement. Une augmentation de la concentration d'agent moussant mène à une diminution du ratio d'amortissement acoustique et à une augmentation de l'amortissement des vagues de surface. La deuxième technique expérimentale est un montage permettant de reproduire la rupture d'une masse d'air derrière une pale d'agitateur dans une cellule mécanique. Dans ce cas-ci, une bulle d'air simple est produite par la déformation mécanique d'une masse d'aire captive. Une première expérience a montré que la taille des bulles est fortement affectée par la présence d'agent moussant, mais faiblement par l'addition d'énergie mécanique et par le volume d'air captif. Une deuxième expérience a montré qu'une augmentation de la concentration d'agent moussant réduit initialement la taille des bulles jusqu'à l'atteinte d'un minimum pour ensuite l'augmenter. La notion de concentration de rupture critique (CRC, ou CBC pour "Critical Break-up Concentration") est introduite pour représenter la concentration permettant la taille de bulle minimum. Une dernière expérience a permis l'observation d'une diminution du temps requis pour la formation d'une bulle lorsqu'en présence d'agent moussant ou de sel. L'hypothèse est que la présence d'agent moussant et de sel accélère la rupture par l'addition d'énergie provenant du soluté.

Cette thèse fournie la preuve que la présence d'agent moussant réduit bien la taille des bulles formées lors de la rupture. Une explication proposée est que les variations de la tension superficielle produites par l'agent moussant jouent un rôle dans la formation et l'intensité des instabilités de l'interface (*i.e.* vagues de surface), celles-ci étant à l'origine de la taille des bulles à la rupture.

Acknowledgments

I would like to express my sincere gratitude to Prof. Jim Finch for accepting me as his 50th (also the last) PhD student. His kindness, understanding, and support, especially during some difficult times in my life, have been integral to the completion of this work. I very much appreciate the tremendous effort he spent on proof-reading and correcting this thesis and also the articles we have written together.

I would like to thank all my colleagues in the Mineral Processing Group at McGill for their kind friendship, especially Ray Langlois, Darryel Boucher, Frank Rosenblum, Prof. Kristian Waters, Dr. Adam Jordens, Ronghao Li and Dr. Mitra Mirnezami. Special thanks must be given to Ray Langlois who has provided tremendous help to the design of all my experimental set-ups. Additionally, the time we spent on building those wood projects in his private workshop is very memorable. I would also like to thank Dr. Randolph Pax for his help on designing the LabVIEW program.

Funding for this work was generously supported by Vale, Teck Resources, Xstrata Process Support, Barrick Gold, Shell Canada, SGS Lakefield Research, COREM and Flottec through the Chair in Mineral Processing under the Natural Sciences and Engineering Research Council of Canada (NSERC) Collaborative Research and Development (CRD) program. Financial support from the Brace Water Resources Fund under the McGill Engineering Doctoral Award (MEDA) program, and a Doctoral Research Scholarship from Fonds de recherche Nature et technologies (FQRNT) Quebec are also acknowledged.

I owe a big ‘Thank You’ to Xiaoqi Zhang. Thank you for your love and encouragement. Your support and accompany during the difficult time in my life have been the most prestigious gift I have ever received. I would also like to acknowledge your mom, Feng Xu, for her kind support during these years.

Finally, I would like to thank my late father Congjin Chu and my mother Xuehua Ni. Without you, I would never be where I am today. A special ‘Thank You’ to you, mom, your endurance and determination during the tough years have given me faith. It is your support that makes my PhD possible.

Contribution of Authors

Prof. James A. Finch, supervisor of my thesis research, is the co-author on all the manuscripts. Prof. Kristian E. Waters (Associate Professor, McGill University) contributed fruitful discussion to the work in which he appeared as a co-author. Ronghao Li (undergraduate student, McGill University) repeated some of the experiments and image analysis in Chapters 3 and 5. Dr. Randolph A. Pax (RAP Innovation & Development Pty Ltd) assisted in designing the data acquisition software for the work presented in Chapter 3 and Appendix 4. The candidate performed all the experiments, image analysis, and data analysis and prepared the first draft of each manuscript and revised them for final publication.

Table of Contents

List of Figures

List of Tables

CHAPTER 1 INTRODUCTION

1.1 Background

Break-up of an air mass to form a dispersion of bubbles in liquids is an important phenomenon in many engineering processes. Coupled with coalescence, break-up plays a critical role in determining bubble size that affects available interfacial area for such processes as heat and mass transfer, or, the interest in this thesis, collection of particles in flotation. Studies of coalescence-related phenomena have been well documented. In contrast, break-up has received less attention. In this work, break-up in different settings designed to mimic conditions in flotation was investigated. The specific interest was to determine whether solutes such as frothers and inorganic salts contribute to the break-up process, complementary to their known effects retarding coalescence. Some background to flotation is an appropriate start to the subject.

Flotation is a particle separation process that evolved in the mid-to-late 1800's and came to dominate the recovery of minerals. The principle lies with the differences in surface properties of minerals, whether the surface is hydrophobic or hydrophilic (Wills and Finch, 2016). Particles with hydrophobic surfaces can attach to gas bubbles to be levitated ("floated") usually to form a concentrate of the valuable mineral component in an ore, while the particles with hydrophilic surfaces remain in the pulp to be discharged as tailings. For brevity, reference will be to as hydrophobic or hydrophilic particles, it being understood to refer to their surface.

In the early days, the process was more bulk-oil flotation, the added oil forming oil/mineral agglomerates with air bubbles either entrained as a consequence of mixing, produced by cavitation, or as carbon dioxide from reaction between added acid (usually sulfuric) and carbonate minerals (Fuerstenau, 2007). Flotation as it is practiced today originated about a century ago in Australia with a patent granted to Minerals Separation Ltd. (Sulman et al., 1906). What distinguishes it from the old is that the new process involves only small quantities of specialty chemicals rather than just oil, and employs predominantly mechanically-produced air bubbles.

Albeit being described as “the greatest single metallurgical improvement of the modern era” (Mouat, 1996), flotation still remains poorly understood, in the sense that there is no fundamental model. The fact that it is an interaction via the surface of three phases, solids, air and liquid in the presence of surface active chemicals, helps explain the difficulty. Flotation has been visualized as a chemically-assisted physical process in which chemistry, ore, and machine interact, represented by Klimpel (1984) as a triangle. The prime function of the chemical variables is to control whether a particle is hydrophobic or hydrophilic; physical variables include particle size and composition which derive from the ore; while machine-derived factors refer to such factors as air rate and bubble size (Wills and Finch, 2016).

Bubble size plays the key role in the flotation of controlling the rate at which particles are collected, that is, the “flotation rate” (Ahmed and Jameson, 1985; Szatkowski, 1987; Yoon and Luttrell, 1989). A practical observation is that a large population of fine bubbles provides both many particle-bubble collision events and high transportation rate of the collected particles. There are also fundamental considerations. With large bubbles, fine particles with low inertial force closely follow the fluid streamlines and are deflected around the bubbles with consequent low collision probability resulting in low flotation rate. Reay and Ratcliff (1973) showed that collection efficiency strongly depended on the ratio of particle size to bubble size and concluded that bubble size should be as small as practical in order to maximize performance. Jameson et al. (1977) made a similar observation, concluding that bubbles less than 0.5 mm diameter are required to significantly increase collection efficiency of fine particles. Recognizing the need for bubbles to have sufficient buoyancy to rise, in practice the compromise bubble size is typically 0.5 to 2.5 mm (Finch and Dobby, 1991).

It is evident, therefore that production of fine bubble swarms is an important function of the flotation machine. However, water is not an easy medium in which to generate small bubbles because of the high surface energy (compared to most room temperature pure liquids) (Blander and Katz, 1975; Talanquer and Oxtoby, 1995). To overcome this obstacle, a chemical reagent known as a frother is typically introduced into the water.

Frothers are a class of surfactants active at the air-water interface. Most frothers are heteropolar compounds comprising a hydrophilic polar group and a hydrophobic hydrocarbon chain. For the industrially important frothers, the polar groups are usually hydroxyl (-OH) and ether linkages (-O-), and the hydrocarbon chains are of various lengths both straight chain and branched. It is postulated that the water molecules interact with the polar groups through H-bonding while there is practically no interaction with the non-polar groups (Wills and Finch, 2016). As a result, the frother molecules tend to accumulate at the air/water interface oriented with hydrophilic groups on the water side and the hydrophobic groups on the air side (Figure 1.1).

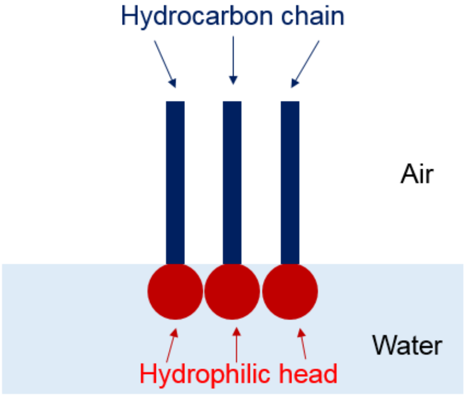

Figure 1.1 Orientation of frother molecules at the air/water interface

The quantity of frother added is typically just a few ppm, that is, a few grams per tonne of water, yet the effect is remarkable. Figure 1.2 illustrates an example of frother action in reducing the bubble size (Sauter mean diameter, D_{32}) in a 0.8 m^3 mechanical cell at gas superficial rate of 0.5 cm.s^{-1}. The results show bubble size decreasing progressively to a minimum size as frother concentration is increased. For a fixed volumetric input rate of air, this decrease in bubble size represents an increase in the number of bubbles, which in turn signifies an increase in the total surface area available for particle attachment. This marks the key function of frothers in affecting flotation performance.

Certain inorganic salts also act to reduce bubble size although in this case the concentration is high, 0.1 M and above. Sovechles and Waters (2015), investigating a series of inorganic salts (NaCl, KCl, Na_2SO_4, $CaCl_2$, $MgCl_2$, $MgSO_4$, $AlCl_3$, and $Al_2(SO_4)_3$)

using a laboratory-scale (5.5L) flotation cell, observed a correlation between bubble size and ionic strength. At least one operation, the Raglan concentrator (Xstrata Nickel), does not use frothers, the high inorganic salt content in the process water substituting for the role of the frother (Quinn et al., 2007).

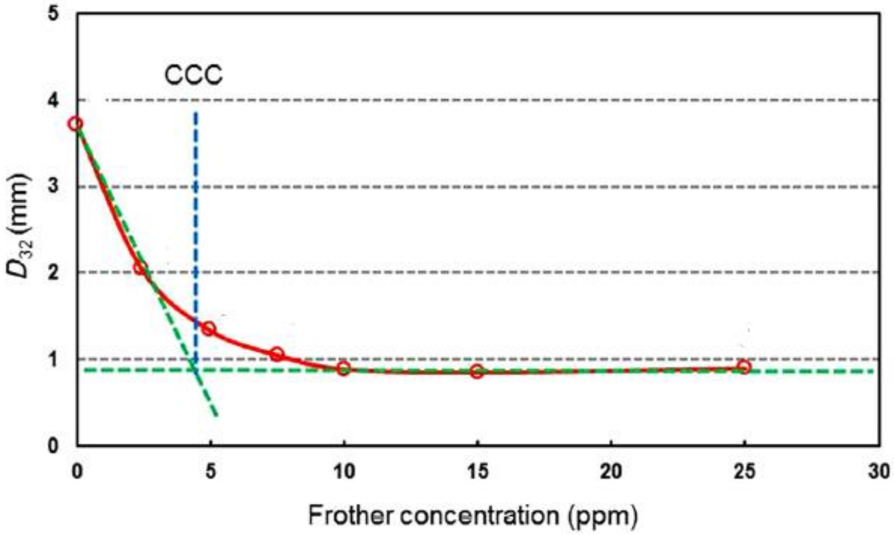

Figure 1.2 Frother action in reducing bubble size (0.8 m^3 mechanical cell at J_g = 0.5 cm▪s^{-1}). Included is measure of CCC (see text) (Adapted from Finch et al. (2008))

Given the key role of frothers (and salts) on small bubble production it is perhaps surprising that the action is not well understood, nor one that attracts much research. A common explanation is that the solutes hinder bubble coalescence (Harris, 1976), and this can certainly be demonstrated. For instance, Bournival and Ata (2014), using high speed cinematography to monitor the behaviour of two bubbles being brought together, showed the presence of frother increased the time required for coalescence. Likewise, Kracht and Finch (2009b), this time employing a passive acoustic technique to study interaction of bubbles formed at a capillary, showed that frothers retarded coalescence. The notion of coalescence suppression is evident in one way of quantifying the effect of frothers on bubble size reduction, namely the critical coalescence concentration (CCC) (a graphical method of estimation is included in Figure 1.2), introduced by Cho and Laskowski (2002). Observing that bubble size (specifically Sauter mean diameter) did not reduce further above a certain frother concentration, the CCC, they interpreted that this concentration corresponded to coalescence being fully suppressed. They hypothesized that the machine produces small bubbles and frother preserves them. The same CCC concept can be applied to salts (Sovechles and Waters (2015)).

The emphasis on coalescence prevention may be obscuring a role of frothers and salts on the initial break-up of the air mass. There is occasional speculation that frothers and salts may affect the break-up process (Acuña, 2007; Finch, 2006; Grau and Laskowski, 2006; Gupta and Yan, 2006). Supporting experimental evidence, however, is lacking. One reason is that break-up and coalescence events in flotation machines are intermingled making it difficult to identify the one in the presence of the other.

With this background, designing a way to examine break-up independent of coalescence in order to test the hypothesis that frothers and salts impact break-up was the prime motivation for the work reported in this thesis. Understanding the break-up process in bubble formation will provide an important addition to flotation theory.

1.2 Thesis objectives

The general objective is to determine the effect of frothers and inorganic salts on air mass break-up. Two experimental techniques were used. First, a quasi-static condition with single bubbles generated at a capillary and monitored by imaging and passive acoustic monitoring. Second, a novel set-up to generate single bubbles free of coalescence under turbulent conditions and monitored by imaging. The specific objectives of each experiment are as follows:

Experiment 1

1. establish a passive acoustic technique to monitor the acoustic signal emitted as a bubble breaks away from a capillary
2. use the established technique to determine the role of the solutes in the break-away process by:
    a. determining the damping behaviour of the oscillating bubble wall as the air bubble breaks away from the capillary
    b. determining the frequency of the sound emitted from the break-away event

Experiment 2

1. design an experimental set-up to isolate break-up from coalescence
2. determine the effect of the solutes on the break-up by:
    a. determining the relationship between the input mechanical energy, the initial volume of air mass, and solute concentration on the produced bubble size
    b. evaluating the apparent energy added by the solute to the mechanical energy required for the break-up

1.3 Thesis structure

This is a ‘manuscript-based’ thesis comprising eight chapters. The current chapter is a brief introduction to the subject. Chapter 2 presents the literature review. Chapters 3, 4, 5, and 6 contain manuscripts that have been published, namely:

> Chu, P., Pax, R., Li, R.H., Langlois, R., Finch, J.A., Using Sound to Study the Effect of Frothers on the Breakaway of Air Bubbles at an Underwater Capillary. Langmuir, 2017, doi:10.1021/acs.langmuir.7b00114.
>
> Chu, P., Waters, K.E., Finch, J.A., Break-up in formation of small bubbles: Break-up in a confined volume. Colloids and Surfaces A: Physicochemical and Engineering Aspects, 2016, 503, 88-93.
>
> Chu, P., Waters, K.E., Finch, J.A., Break-up in formation of small bubbles: Comparison between low and high frother concentrations. Minerals Engineering, 2016, 96–97, 15-19.
>
> Chu, P. Waters, K.E., Finch, J.A., Break-up in formation of small bubbles: An energy consideration. Canadian Metallurgical Quarterly, 2017, 56(1), 30-34.

Chapter 7 presents a unifying discussion and Chapter 8 provides conclusions, contributions to knowledge, and suggestions for future work.

Because this is a ‘manuscript-based’ thesis the reader should note that some aspects of the literature reviews are repeated.

References

Acuña, C.A., Nesset, J.E., Finch, J.A., 2007. Impact of frother on bubble production and behaviour in the pulp zone, In Proceedings of the Sixth International Copper-Cobre Conference, ed. de Villar, R., Nesset, J.E., Gomez, C.O., Strading, A.W. MetSoc CIM, Toronto, Ont., pp. 197-210.

Ahmed, N., Jameson, G.J., The effect of bubble size on the rate of flotation of fine particles. International Journal of Mineral Processing, 1985, 14(3), 195-215.

Blander, M., Katz, J.L., Bubble nucleation in liquids. AIChE Journal, 1975, 21(5), 833-848.

Bournival, G., Ata, S., Karakashev, S. I. and Jameson, G. J., An investigation of bubble coalescence and post-rupture oscillation in non-ionic surfactant solutions using high-speed cinematography. Journal of Colloid and Interface Science, 2014, 414, 50-58.

Cho, Y.S., Laskowski, J.S., Bubble coalescence and its effect on dynamic foam stability. The Canadian Journal of Chemical Engineering, 2002, 80(2), 299-305.

Finch, J.A., Dobby, G.S., Column flotation: A selected review. Part I. International Journal of Mineral Processing, 1991, 33(1), 343-354.

Finch, J.A., Gelinas, S., Moyo, P., Frother-related research at McGill University. Minerals Engineering, 2006, 19(6–8), 726-733.

Finch, J.A., Nesset, J.E., Acuña, C., Role of frother on bubble production and behaviour in flotation. Minerals Engineering, 2008, 21(12–14), 949-957.

Fuerstenau, D.W., 2007. A century of developments in the chemistry of flotation processing, In Froth Flotation: A Century of Innovation, ed. Maurice C. Fuerstenau, G.J., Roe-Hoan Yoon. SME, Littleton CO, USA pp. 3-64.

Grau, R.A., Laskowski, J.S., Role of Frothers in Bubble Generation and Coalescence in a Mechanical Flotation Cell. The Canadian Journal of Chemical Engineering, 2006, 84(2), 170-182.

Gupta, A., Yan, D.S., Mineral Processing design and operations: an introduction. 2006, Elsevier, Amsterdam.

Harris, C., Flotation machines. Flotation, A. M. Gaudin Memorial Volume, 1976, 2, 753-815.

Jameson, G.J., Nam, S., Moo Young, M., Physical factors affecting recovery rates in flotation. Minerals Science Engineering, 1977, 9(3), 103-118.

Klimpel, R.R., Use of chemical reagents in flotation. Chemical Engineering, 1984, 91(18), 75-79.

Kracht, W., Finch, J.A., Using sound to study bubble coalescence. Journal of Colloid and Interface Science, 2009, 332(1), 237-245.

Mouat, J., The development of the flotation process: technological change and the genesis of modern mining, 1898-1911. Australian Economic History Review, 1996, 36, 27.

Quinn, J.J., Kracht, W., Gomez, C.O., Gagnon, C., Finch, J.A., Comparing the effect of salts and frother (MIBC) on gas dispersion and froth properties. Minerals Engineering, 2007, 20(14), 1296-1302.

Reay, D., Ratcliff, G.A., Removal of fine particles from water by dispersed air flotation: Effects of bubble size and particle size on collection efficiency. The Canadian Journal of Chemical Engineering, 1973, 51(2), 178-185.

Sovechles, J.M., Waters, K.E., Effect of ionic strength on bubble coalescence in inorganic salt and seawater solutions. AIChE Journal, 2015, 61(8), 2489-2496.

Sulman, H.L., Kirkpatrick-Picard, H.F., Ballot, J., 1906. Ore concentration. Bristih Patent.

Szatkowski, M., Some comments on flotation kinetics. Chemical Engineering Science, 1987, 42(10), 2475-2478.

Talanquer, V., Oxtoby, D.W., Nucleation of bubbles in binary fluids. The Journal of Chemical Physics, 1995, 102(5), 2156-2164.

Wills, B.A., Finch, J.A., 2016. Chapter 12 - Froth Flotation, In Wills' Mineral Processing Technology (Eighth Edition), ed. Finch, B.A.W.A. Butterworth-Heinemann, Boston, pp. 265-380.

Yoon, R.H., Luttrell, G.H., The Effect of Bubble Size on Fine Particle Flotation. Mineral Processing and Extractive Metallurgy Review, 1989, 5(1-4), 101-122.

CHAPTER 2 LITERATURE REVIEW

Flotation is a process driven by swarms of fine bubbles. The generation of small bubbles is achieved by dispersing air via various mechanisms in the presence of solutes, namely surfactants (frothers) or certain inorganic salts. This chapter reviews three related topics, viz, break-up mechanisms, frother and inorganic salt solutes, and bubble acoustics, in order to provide the background necessary for this work.

2.1 Surface tension

The formation of air bubbles in water involves air/water interface-related phenomena. Consequently, it is usual to start with the fundamental property of an interface, that is, surface or interfacial tension (De Gennes et al., 2013).

Arguably, surface tension is one of the most important parameters when discussing the properties of an interface. It arises when there is a difference in intermolecular forces across an interface between two immiscible fluids. The consequence is a force per unit length or an energy per unit area which resists the creation of new interface (Israelachvili, 2011; Rowlinson and Widom, 2013). Surface tension is a material property which depends on the strength of intermolecular attraction forces, the size of the molecules, and the chemistry along the interface. As examples, low surface tensions are seen with air/oil interfaces, ~ 20 mN/m, because oil molecules offer some attraction for water molecules while for the air/water interface the surface tension is high, 72.8 mN/m, because in comparison air molecules being small and in low concentration offer less attraction for water molecules. The air/water surface tension is anomoulously high given the apparent simple nature of the water molecule because H-bonding increases the intramolecular attraction. The air/liquid mecury interfaces has the highest room temperature surface tension, ~ 500 mN/m, because of the high intramolecular attraction due to metallic bonding.

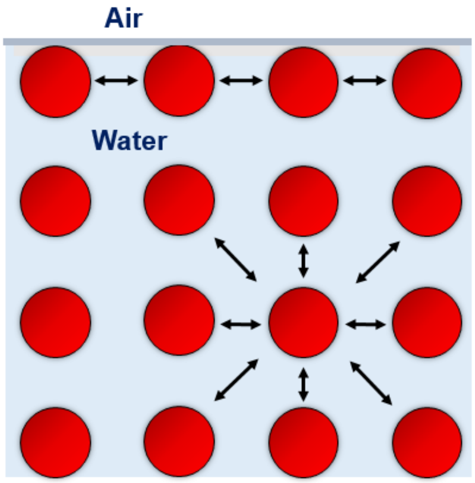

Figure 2.1 Interactions of water molecules at different locations: at the surface the water molecules experience a net force towards the bulk, giving rise to the tension in the surface

Surface tension is temperature dependent. When temperature is uniform along the interface this results in a uniform change in equilibrium surface tension. Commonly, an increase in temperature decreases surface tension because this increases molecular agitation and reduces intramolecular attraction. Temperature dependence of surface tension of the air/water interface is given in Figure 2.2.

Surface tension is also influenced by the chemistry along the interface. When water is ‘contaminated’ by adding surfactants such as frothers, the attraction between the water molecules is interrupted, causing a lowering of surface tension. Some authors argue that the reduction in surface tension is the cause of small bubble production but others point out deficiencies in this notion (Aldrich and Feng, 2000; Grau and Laskowski, 2006; Machon et al., 1997; Sweet et al., 1997).

Unless specified otherwise, surface tension referred to in the literature is usually the equilibrium value, i.e., the surface and solution are in thermodynamic equilibrium (Finch et al., 2008). When single bubbles are produced sufficiently slowly in pure liquids (i.e., attaining equilibrium is not an issue), for example at a capillary, the bubble size is predictable from the surface tension (Fritz, 1935). When solutes are present attaining equilibrium is an issue. Generating bubbles slowly at a capillary to test frother concentrations encountered industrially, Hernandez-Aguilar et al. (2006) found that bubble size, while reduced, was in general not predictable from the equilibrium surface tension. The reduction in size was also very much less than in the case of bubble swarms, which is part of the argument that (equilibrium) surface tension is not a large factor in control of bubble size in flotation machines. This is not to conclude that surface tension is not a factor rather that the equilibrium value is not. The thesis will introduce an alternative way of incorporating a surface tension-related effect into understanding the process of small bubble production.

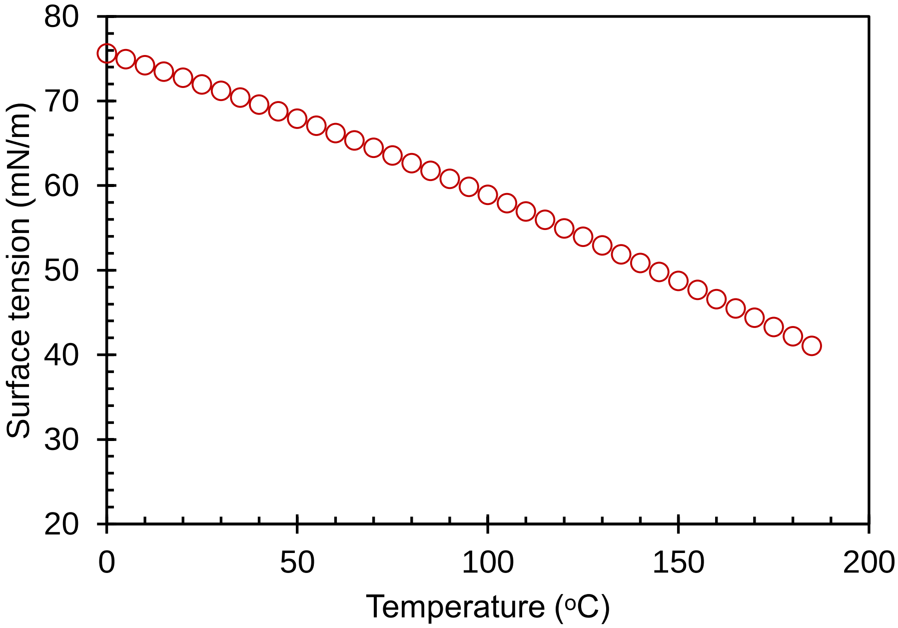

Figure 2.2 Temperature dependance of surface tension of an air/water interface (Data after Vargaftik et al. (1983))

Small bubble generation assisted by the presence frothers and salts is a physicochemical process. To understand the microscale phenomena of how solute chemistry affects surface tension to influence small bubble generation, one must also comprehend the macroscale physical conditions that initiate the formation process. Hence the next section considers air break-up mechanisms. Since most literature deals with break-up in surfactant-free systems this provides the starting point.

2.2 Break-up mechanisms

Air bubbles and liquid droplets are typically referred to as fluid particles. Both particles often deform similarly when exposed to turbulent conditions. As a result, much of the literature on break-up mechanisms does not distinguish explicitly, i.e., whether it is an air bubble or a droplet being considered. Due to this commonality, while the following refers to bubbles it uses perspectives from both bubble and droplet studies.

The break-up of air bubbles resulting in smaller air bubbles is one area of study in the formation of bubble swarms (Risso, 1998). To break a bubble must first deform. The deformation can occur in different ways depending on the liquid flow patterns around the bubble. In his seminal work 'Fundamentals of the Hydrodynamic Mechanism of Splitting in Dispersion Processes', Hinze (1955) identified three types of deformation: lenticular, cigar-shaped and bulgy, illustrated in Figure 2.3. For the lenticular case, the bubble becomes flattened and forms an oblate ellipsoid. As the deformation evolves a torus starts to form that eventually breaks into small bubbles upon further stretching. Cigar-shape deformation occurs when the bubble is first elongated and subsequently develops into a prolate ellipsoid followed by formation of a cylindrical thread that finally breaks into smaller bubbles. The bulgy case is where deformation takes place locally and sections of the bubble bodily separate.

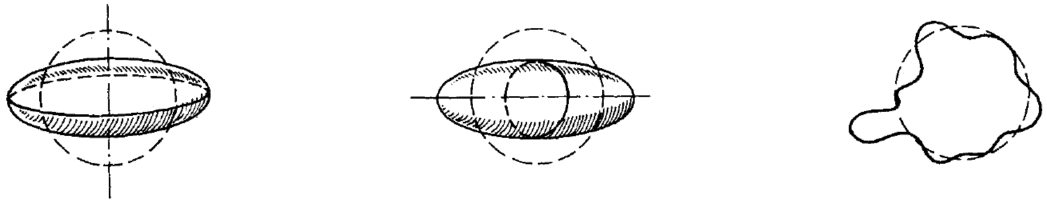

Type 1: lenticular Type 2: cigar-shaped Type 3: bulgy

Figure 2.3 Types of deformation (After Hinze (1955))

The deformation of air bubbles under turbulent conditions is affected by hydrodynamic stresses in the liquid phase (e.g., turbulent eddies) and surface stresses (e.g., surface tensions). The hydrodynamic stress tends to disrupt the bubble, whereas the surface stress attempts to restore the form and maintain a minimum surface area. It is the competition between the hydrodynamic stress and surface stress that determines whether break-up will occur (Liao and Lucas, 2009).

The first theory of bubble break-up in turbulent conditions was developed by Kolmogorov (1949) and Hinze (1955). They suggested that break-up is due to interactions with turbulent eddies that are of approximately the same size as the bubble. They argued that a bubble would break if the turbulent field is sufficiently strong to counterbalance the surface tension. Later known as the Kolmogorov-Hinze criterion, break-up occurs when the dimensionless critical Weber number (Equation 2.1) is exceeded. The Weber number defines the ratio of turbulence to surface tension forces:

$$We = \frac{\rho * < \delta u^2(d) > * \, d_e}{\sigma} \qquad \text{Equation 2.1}$$

where ρ is the liquid density, d_e the equivalent spherical diameter of the bubble, σ the surface tension, and $\delta u^2(d)$ the mean-square longitudinal velocity difference of the undisturbed flow over a distance d.

Following Kolmogorov and Hinze, many subsequent studies have examined bubble break-up in turbulent flows. Levich (1962) modified the Kolmogorov-Hinze criterion by including the density of the air. Zeitling (1972) approached the break-up problem by modeling the breakage efficiency of bubbles in a stirred tank. Coulaloglou and Tavlarides (1977) developed a phenomenological model that assumed break-up would only occur if the turbulent kinetic energy surpassed the surface energy of the bubble. Prince and Blanch (1990) examined the effect of eddy size on bubble break-up and concluded that the break-up was due to collision with eddies of length scale between 0.2 and one times the bubble diameter. They also concluded that eddies larger than this size are only responsible for transporting the bubbles, and those that are smaller only deform but do not break the bubble. In addition to the length scale, the impact of eddies of different energy has been considered. For instance, Luo and Svendsen (1996) postulated that the minimum energy to initiate break-up should be comparable to the increase in surface energy associated with the surface area increase as the bubble deforms in the break-up event.

Notably, while the bulk of the literature considers that the break-up process is controlled by the properties of the turbulent eddies (the length scale and the contained energy), there is another important phenomenon that also merits consideration. Risso (1998) extended the Kolmogorov-Hinze analysis to consider the impact of the stochastic succession of turbulent eddies. It was shown that the arrival time of the turbulent eddies during each cycle of bubble oscillation may either increase or decrease the bubble deformation; and if it increases, the bubble will break. This resonance-like mechanism means the system history is important.

Recently, Liao and Lucas (2009) reviewed break-up mechanisms and classified them into four main categories: (1) turbulent fluctuation and collision; (2) viscous shear stress; (3) shearing-off processes; (4) interfacial instability. In flotation machines bubbles are subjected to forces from multiple sources and therefore could break through any of these possibilities. The following briefly describes these four mechanisms.

2.2.1 Turbulent fluctuation and collision

As introduced, turbulence-induced break-up concerns the force balance between hydrodynamic stress in the liquid and surface stress of the bubble. Liao and Lucas (2009) identified five criteria:

a) Turbulent kinetic energy greater than a critical value
b) Velocity fluctuation around the bubble surface greater than a critical value
c) Turbulent kinetic energy of the colliding eddy greater than a critical value
d) Inertial force of the colliding eddy greater than the surface force of the smallest bubbles
e) Combination of c) and d)

Markedly, all the cases involve the concept of a critical value. The critical value can be taken as the surface energy of the bubble before break-up (Lee et al., 1987a, b; Martinez-Bazan et al., 1999a, b; Prince and Blanch, 1990), or the increase in the surface energy from before to after break-up (Luo and Svendsen, 1996; Wang et al., 2003; Zhao and Ge, 2007), or the mean value of the surface energy increase upon break-up resulting in daughter bubbles (Tsouris and Tavlarides, 1994).

2.2.2 Viscous shear force

The viscosity difference across the interface of a fluid particle (e.g*.,* an air bubble) creates the viscous shear effect. The effect is to distort the interface against the resistance by surface tension. The ratio between viscous shear force and surface tension defines a capillary number:

$$Ca = \frac{\upsilon \dot{\gamma} R_0}{\sigma} \qquad \text{Equation 2.2}$$

where υ is the viscosity of the liquid, $\dot{\gamma}$ the shear rate, R_0 the initial particle radius, and σ the surface tension.

Slightly different from the turbulence case, most studies of the viscous shear effect were performed in simple shear flows, and involved considerations of the capillary number and the viscosity ratio (or difference) between the fluids. For all viscosity ratios, the fluid particle shape will be nearly spherical provided that the capillary number is sufficiently small (Stone, 1994). Taylor (1932) demonstrated that the deformation of a fluid particle is linearly proportional to the increase in the capillary number, provided that the capillary number is much smaller than 1. Taylor (1934) and Grace (1982) suggested the critical capillary number not only depends on the viscosity ratio but also the flow type. de Bruijn (1989) constructed a curve, Figure 2.4, to fit Grace's data specifically for the case of drop break-up but the same applies to bubbles. In Figure 2.4 the sketches below the line indicate bubble shapes; sketches above the line illustrate the different break-up modes. As noted by Tucker and Moldenaers (2002), the understanding derived from the figure is twofold. One is that the break-up depends on viscosity ratio when the capillary number is slightly larger than the critical value. For a viscosity ratio much small than 1 break-up starts at the tip of the bubble. When the ratio is about 1 the bubble breaks through necking, this mechanism usually resulting in two large daughter bubbles and some smaller ones in between. The second understanding relates to when the capillary number is much larger than the critical value. Under this circumstance, the bubble is rapidly elongated into a cylindrical thread, which subsequently breaks into small fragments due to capillary-wave instability (i.e., Rayleigh instability).

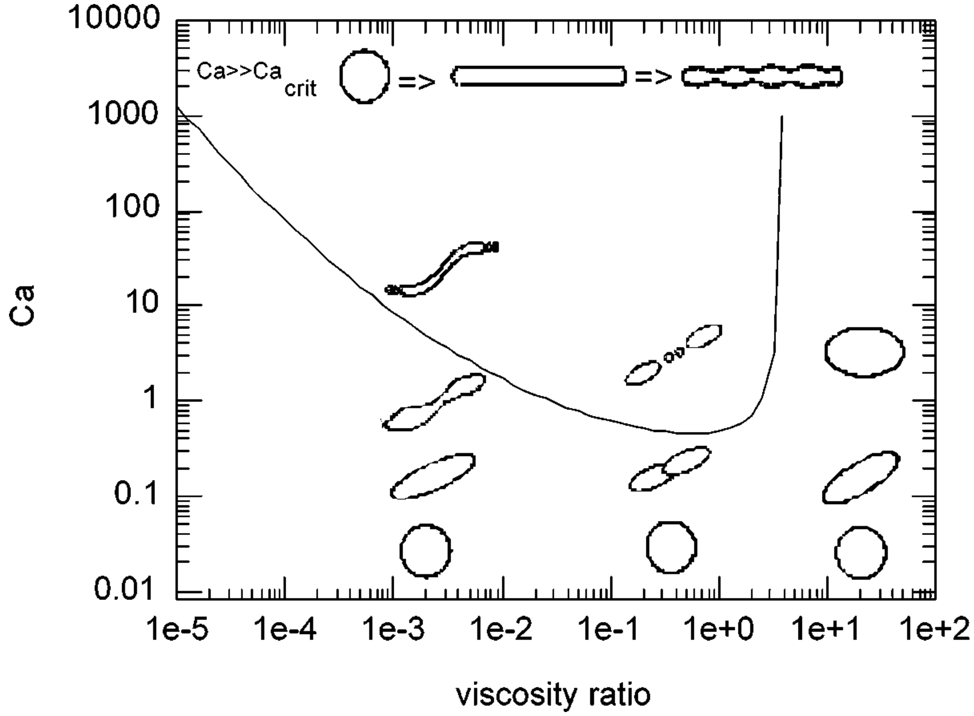

Figure 2.4 Critical capillary number in simple shear flows (After de Bruijn (1989))

2.2.3 Shearing-off mechanism

The shearing-off mechanism can be considered a special case of viscous shear break-up but for bubbles of large size, such as air slugs. Figure 2.5 shows an example of break-up induced by the shearing-off mechanism in a water column. The break-up process can be characterized as 'erosive breakage' in which a number of small bubbles are sheared off from a large bubble, e.g., a cap-shaped or slug bubble (Liao and Lucas, 2009). Fu and Ishii (2003) identified two cases for shearing-off. In the case of highly viscous flows, skirts are formed around the tails of the air slug. When the balance between viscous force and surface tension cannot be achieved due to high velocity or surface instability, the skirts become unsteady and will break into small bubbles. In a low viscous flow system, such as in an air/water system, the shearing-off is caused by the gas velocity profile inside the air slug. Gases inside the bubble move globally at the bubble velocity, except at the boundary near the air/water interface that has a velocity equal to the liquid film velocity. The gas in the thin boundary layer may penetrate into the liquid film and thus form small bubbles.

Figure 2.5 Break-up through shearing-off mechanism (After Fu and Ishii (2003))

2.2.4 Interfacial instability

In uncontaminated systems (e.g*.,* no frothers) interfacial instability is usually neglected because most of break-up situations are dominated by turbulent fluctuations (Liao and Lucas, 2009). However, it is noted that break-up can occur in the absence of net flow in the continuous phase, for example, a large air bubble rising in a quasi-static water system can break into several smaller bubbles. Under these circumstances, the break-up is the result of interfacial instabilities, during which the density difference between the two immiscible fluids dominates the surface tension.

What can be concluded from the above is that the mechanism of break-up is remarkably diversified. However, it is evident that all the mechanisms involve surface tension (or more precisely ‘equilibrium surface tension’). That modification of surface tension occurs when frothers are added or high salt concentration is present suggests such modification plays a role in break-up. Next, frothers and salts are considered.

2.3 Frothers and inorganic salts

2.3.1 Frother chemistry and frother classification

Frothers are a class of surfactants that are active at the air/water interface. They are widely used in flotation processes to provide the following functions (Klimpel and Isherwood, 1991):

1) Enhancing froth formation
2) Increasing the dispersion of air into small bubbles
3) Reducing bubble rise velocity
4) Retarding coalescence of bubbles

The structure of most frothers is hetero-polar. As depicted in Figure 1.1, the molecule consists a polar head group that is hydrophilic, and a non-polar hydrocarbon tail that is hydrophobic. When frothers are in water, their polar groups readily interact with water dipoles through H-bonding. A consequence of this interaction is the formation of a water layer around the air bubble, which serves to stabilize the system against coalescence (Kitchener and Cooper, 1959; Laskowski, 2004).

Laskowski (1993) classified frothers employed in the mineral industry into three main types: alcohols, polyglycols, and alkoxy substituted paraffins. Nowadays, however, only the first two are primarily used (Laskowski, 1998; Wills and Finch, 2016). This section thus only considers alcohol and polyglycol frothers.

The typical alcohol frother structure comprises a hydroxyl (OH) group and a hydrocarbon chain. The hydrocarbon chain usually contains 5 – 7 carbons, and can be either straight or branched. The common alcohol frother is MIBC, methyl isobutyl carbinol ($(CH_3)_2CHCH_2CH(OH)CH_3$)**,** which is a branched structure. Polyglycol frothers include polypropylene glycols (PPGs) ($H(OC_3H_6)_mOH$), PPG alkyl ethers ($C_nH_{2n+1}(OC_3H_6)_mOH$), and polyethylene glycol alkyl ethers ($C_nH_{2n+1}(OC_2H_4)_1OH$). The polyglycols provide great flexibility with varying molecular weight and chemical structure allowing control of the flotation process (Klimpel and Isherwood, 1991; Wills and Finch, 2016). Two familiar frothers from the polypropylene family are DF250 ($CH_3(PO)_4OH$), a PPG methyl ether, and F150 (or PPG425) ($H(PO)_7OH$), a PPG. In this work the frothers investigated were MIBC, DF250, and F150. Figure 2.6 shows their structures.

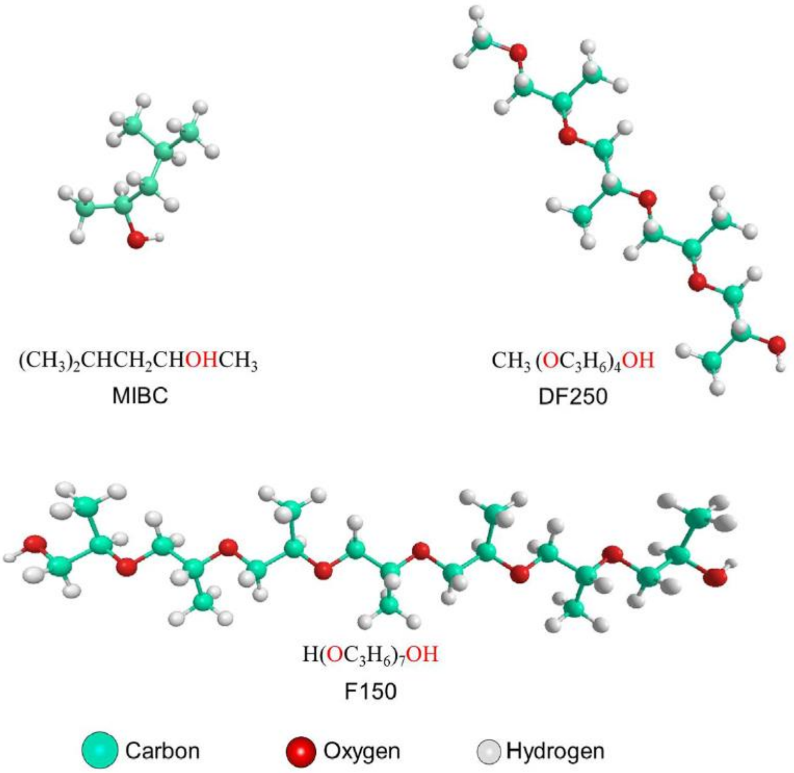

Figure 2.6 Molecular structures of MIBC, DF250, and F150 (Adapted from Wills and Finch (2016))

2.3.2 Frothers at the air/water interface

Frothers have remarkable effects on reducing bubble size especially given the small concentrations required, a few ppm (i.e., g/tonne of water). Though their precise action remains obscure, the fact that they are active at the air/water interface unquestionably plays a crucial role. While the literature on frother surface activity is scarce for the specific frothers studied here, it is believed that relevant information can be interpreted from other more studied surfactants.

As noted, the hydrogen-bonded network directs a force on the surface water molecules inwards to the bulk water which results in water's high surface tension (Hsieh et al., 2011). When surface active agents (surfactants), such as frothers, are present, interaction between the water molecules at the interface is interrupted, causing a lowering of surface tension. For a freshly formed interface in the presence of surfactants the equilibrium surface tension is not achieved instantaneously. Initially, the surface tension is close to that of the solvent alone. With time allowing for surfactant to arrive and adsorb, the surface tension will decay to the equilibrium value. This period of time can range from milliseconds to days depending on the surfactant type and concentration (Eastoe and Dalton, 2000). The surface tension during decay is the dynamic surface tension.

Surface tension is realized by two dynamic processes: adsorption of surfactant molecules at the interface, and their desorption from that interface (Danov et al., 1999). When the two occur are at the same rate, the equilibrium surface tension is achieved. Adsorption and desorption depend on the state of the interface. If the interface is abruptly disturbed, say by expansion, surfactant concentration at the interface will be reduced below the equilibrium value initiating adsorption. By analogy, if the interface is contracted surface concentration is increased above equilibrium and desorption is initiated. Figure 2.7 conveys these ideas.

Surfactant molecule adsorption is generally considered to occur in two stages (Figure 2.8): transfer from bulk to subsurface and transfer from subsurface to the interface (Chang and Franses, 1995; Danov et al., 1999; Defay and Petre, 1971; Eastoe and Dalton, 2000). The subsurface can be envisaged as an imaginary plane a few molecular diameters wide. It is the boundary between the domain in which only diffusion occurs (i.e., $0 < x < l$) and the region in which adsorption occurs. The surfactant concentration in the subsurface varies when a new interface is being formed. It first decreases as the surfactant molecules in the subsurface are adsorbed at the newly generated interface, and then increases as the surfactant molecules in the bulk start to diffuse to the subsurface. It is also noted that the domain in which only diffusion occurs (0 < x < l) is much larger than the thickness of the adsorption layer (i.e., x < 0).

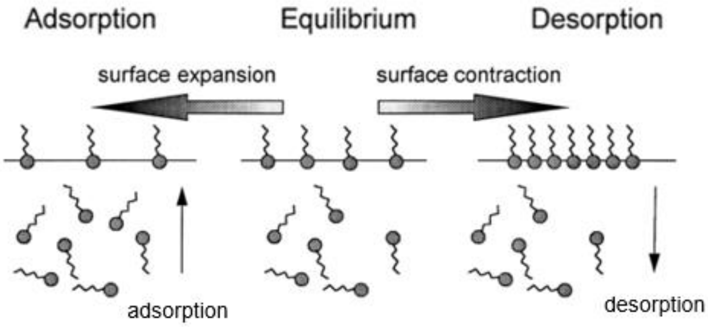

Figure 2.7 Adsorption and desorption caused by surface perturbation (Modified from Eastoe and Dalton (2000))

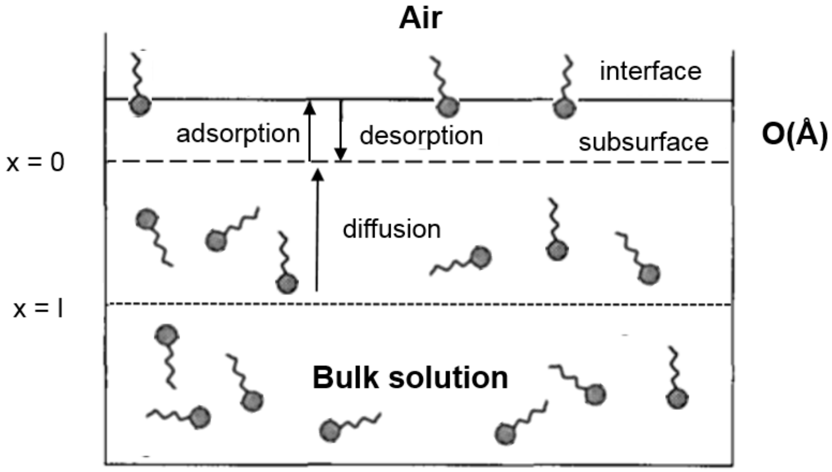

Figure 2.8 The dynamic adsorption process: 1) a diffusion region, 0 < x < l, and 2) adsorption region, x < 0. With sufficient time, desorption can also occur in 2). (Modified from Chang and Franses (1995))

2.3.3 Self-assembly

One of the characteristics of surfactants is that they can self-assemble to form a large variety of morphologically different aggregates known as micelles (McBain and Martin, 1914). The drive is that by forming these aggregates the free energy of the system is decreased (Israelachvili et al., 1976; Tanford, 1973). The concentration at which micelles start to form is referred to as the critical micelle concentration (CMC). Below the CMC, surfactant molecules are typically distributed in water as isolated molecules or monomers. Above the CMC, monomers and micelles exist in dynamic equilibrium (Dominguez et al., 1997).

The spontaneously formed micelles can take different structures such as spherical, globular, or rod-like, shown in Figure 2.9. The properties (e.g*.,* size and shape) of these structures is governed by small changes in multiple noncovalent interactions between the molecules. Some typical interactions of this type include coulombic, H-bonding, dipole or hydration (Romsted, 2012). Understanding this noncovalent interaction can be approached from two aspects, namely, free energy change, and molecular packing. The free energy change concept was proposed by Tanford (1973), and has been used to explain why micelles form in aqueous solutions, why they grow, and why they assume a given geometry. On the other hand, the molecular packing concept proposed by Israelachvili et al. (1976) suggests that a combination of molecular packing considerations and general thermodynamic principles can predict the size and shape of the micelles at equilibrium. According to Nagarajan (2002), the contributions of Tanford (1973) and Israelachvili et al. (1976) have provided significant insight.

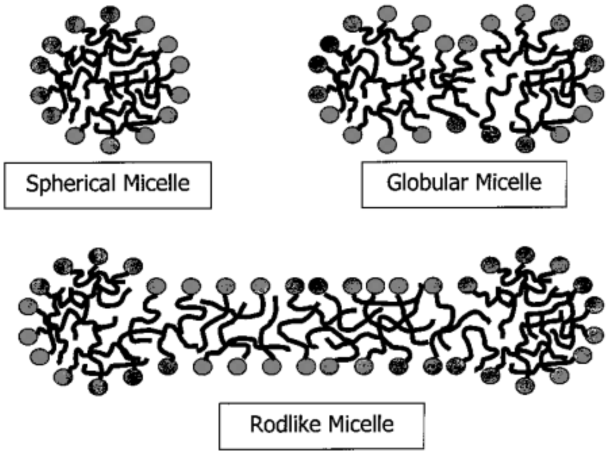

Figure 2.9 Schematic diagrams of surfactant aggregates in dilute aqueous solutions (After Nagarajan (2002))

Micelles have fluid structures on a mesoscopic scale (Chandler, 2005). Predicting the microstructure is an ongoing challenge, which has produced many theories (Meunier et al., 2012). Computer simulation is often employed to test and enhance the theories. Figure 2.10 demonstrates an example. The plot shows a hypothetical phase diagram for a three-component system of water, oil, and surfactant produced by Monte-Carlo simulation (Larson, 1989). The three sides of the phase diagram define binary systems expressed in weight percentage. Relevant to this study, the focus is the binary side of water-surfactant. It is fascinating that several distinct micelle structures can form depending on surfactant concentration. Other features of this phase diagram are discussed elsewhere (Holmberg et al., 2003; Laughlin, 1994).

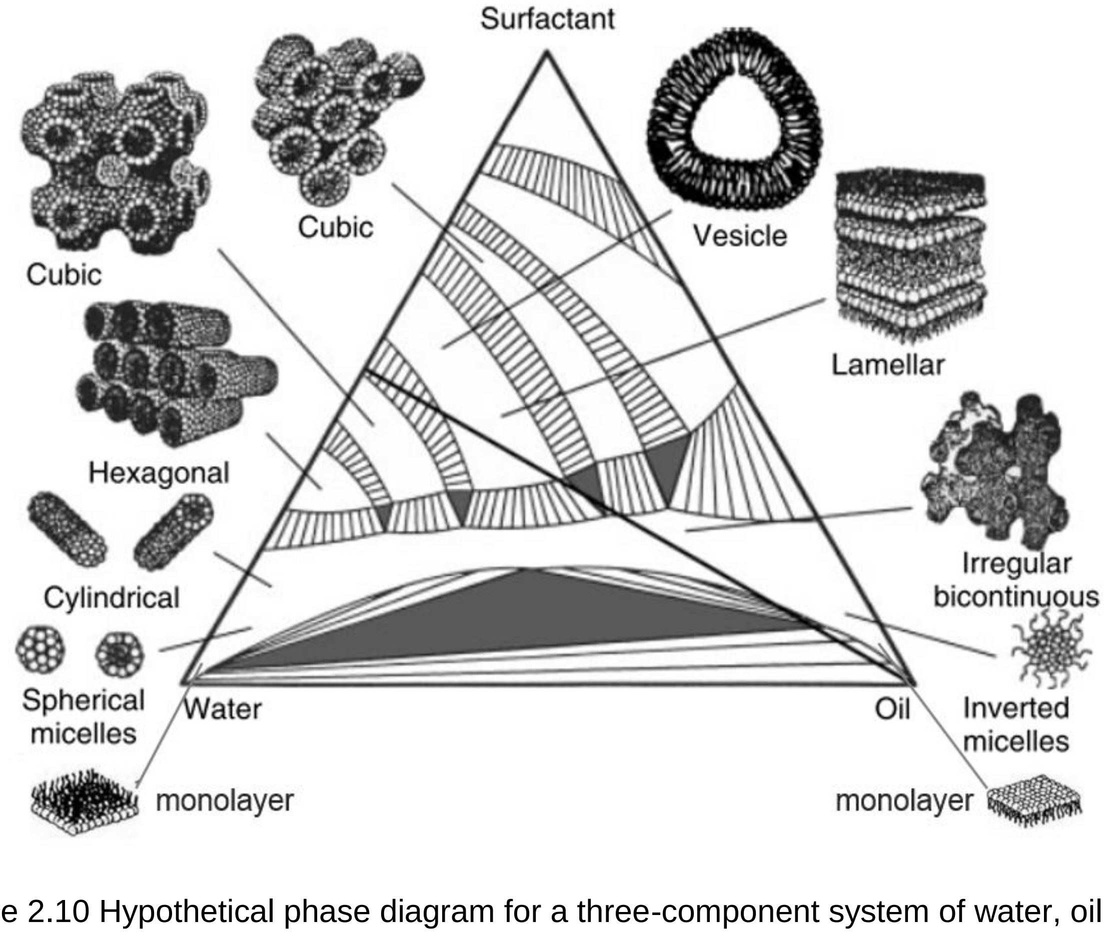

Figure 2.10 Hypothetical phase diagram for a three-component system of water, oil, and surfactant. Original diagram was by Larson (1989), the current is after the modified version in Romsted (2012)

It is speculated that structure of CMCs depends more on surfactant hydrocarbon chain length than on the nature of the head (Menger, 1979). Romsted (2012) suggested that surfactants with chains of fewer than eight carbons (that is the case for most alcohol frothers) may never reach sufficient concentration to form micelles. However, there are studies suggesting it is possible. For instance, Goetz and Lipowsky (1998) conducted computer modelling to simulate the aggregation behaviour of surfactant molecules with chains of only three to four carbons. They found that small aggregates can form provided that the local volume which the molecules occupy is small.

Incorporating the conclusion of Goetz and Lipowsky (1998), one can postulate that that frother molecules may spontaneously form small aggregates. In this case, they take the form of individual 'macro-surfactant molecules' that interact with the monomers in dynamic equilibrium, affecting the adsorption, desorption and diffusion processes that impinge on surface tension. An attempt to convey this notion is given in Figure 2.11, a modified version of Figure 2.10.

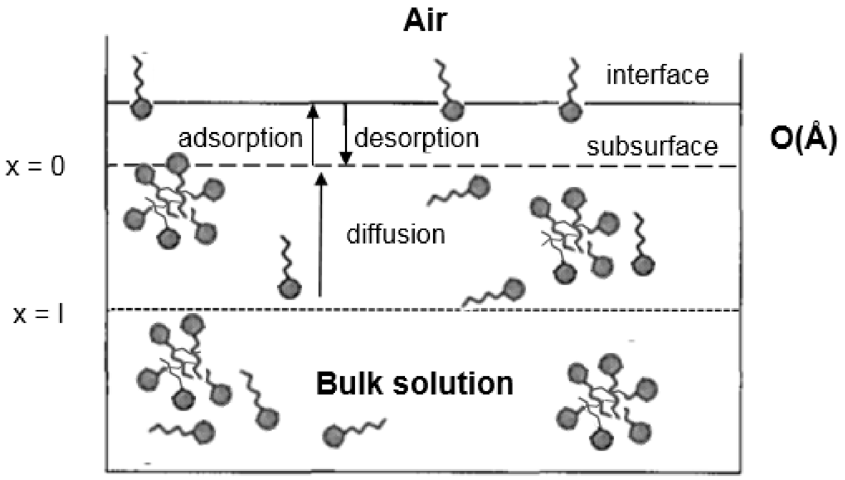

Figure 2.11 Dynamic adsorption in the presence of small aggregates. Modified from Chang and Franses (1995). Note that the structures of the small aggregates are for illustration purpose only

Applying the hypothetical phase diagram, Figure 2.10, it is possible that frother molecules can form layered or spherical structures. These spontaneously formed aggregates, similar to monomers, share a tendency to accumulate at the air/water interfaces. The literature suggests a few such arrangements: Figure 2.12 shows some examples. The most common is the monolayer assembly (Figure 2.12.a). It is the preferred arrangement at very low surfactant concentrations. At somewhat higher concentrations, Figure 2.12b introduces another possibility, a bilayer configuration (Figure 2.12.b) in which the head groups of some molecules interact with those of the molecules already adsorbed and oriented at the interface. It has been speculated that these layers can continue to grow as the concentration is further increased: Figure 2.12.c illustrates a three-layer configuration. Meguro et al. (1988) suggested that certain surfactants (e.g., sodium myristyl sulfate) can build up to ten layers in some circumstances. In addition to the layered structure, the increase in concentration can also lead to simultaneous formation of spherical aggregates. Once formed, these will randomly distribute along the interface, coexisting with the layered structures (Figure 2.12.d). Figure 2.12.e shows another possible arrangement which involves layered and spherical aggregates, but this time at a much higher concentration.

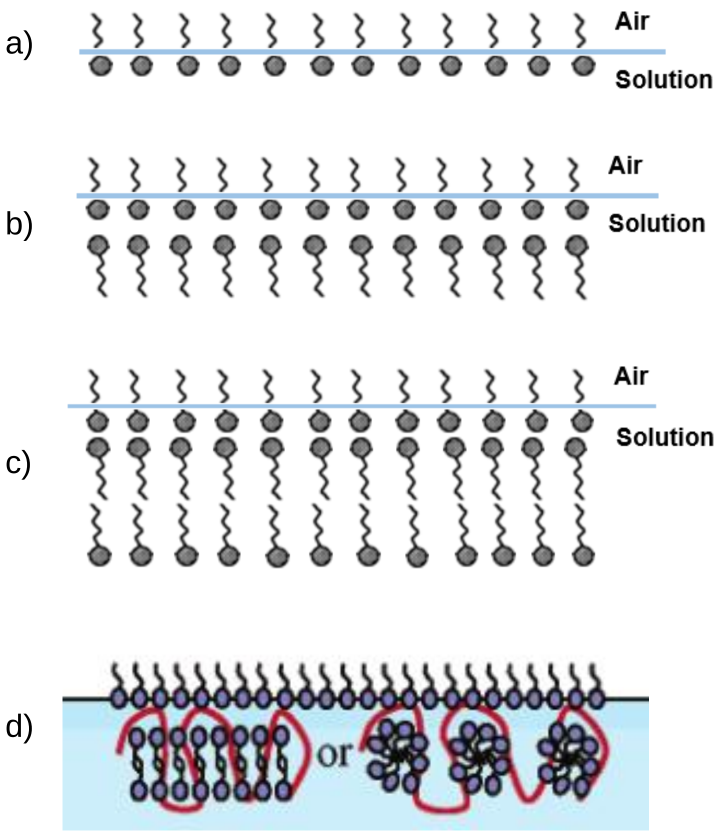

e)

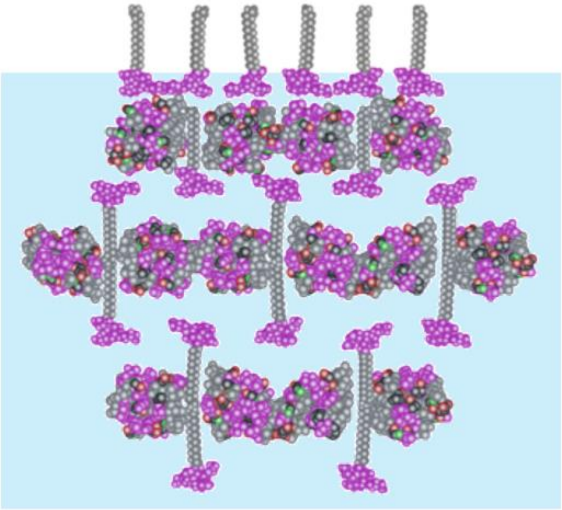

Figure 2.12 Possible arrangements in which surfactant molecules can accumulate at the interface corresponding to increasing concentration: a) a monolayer, b) a bilayer, c) a multiple layer configuration, modified from Meguro et al. (1988), d) a possible arrangement involving monolayer, bilayer and small spherical aggregates, adapted from Monteux et al. (2004), e) an extend case for c), adapted from Thomas and Penfold (2015)

Although the structures illustrated in Figure 2.12 are compiled from surfactants of different types, the intention is to acknowledge the possible existence of surfactants aggregates that might occur with frothers.

Self-assembly is a microscopic feature of surfactant molecules. The spontaneously formed aggregates may manifest themselves macroscopically through their effect on surface tension. What complicates the effect is that under certain circumstances such as in turbulent flotation systems, a uniform distribution (or concentration) of the aggregates and/or individual molecules (monomers) along the interface is almost impossible to achieve. The consequence of this difference in local interface concentration (or adsorption density) is the generation of surface tension gradients which may play a role in some surface properties. According to Marrucci (1969), such gradients can produce profound effects on the thinning behaviour of liquid films during break-up. Thus, the next section reviews some surface characteristics provoked by surface tension gradients.

2.3.4 Some surface tension-driven surface characteristics

Local differences in adsorption density result in surface tension gradients that produce a force and associated liquid flow known as Marangoni flow (Problestein, 1994). Acuña et al. (2008) developed a technique to reveal the surface flows on bubbles blown in frother solution. They showed that the surface of an air bubble (ca. 10 mm diameter) blown in polypropylene glycol and pentanol is perturbed and mobile. As illustated in Figure 2.13, the polyglycol gives a more 'roughened' surface than pentanol. The explanation is that the disturbed interface is the result of gravity-induced local variations in adsorption density resulting in Marangoni flow. This surface perturbation is reminiscent of the bulgy deformation recognized by Hinze (1955) and the interfacial instability categorized by Liao and Lucas (2009).

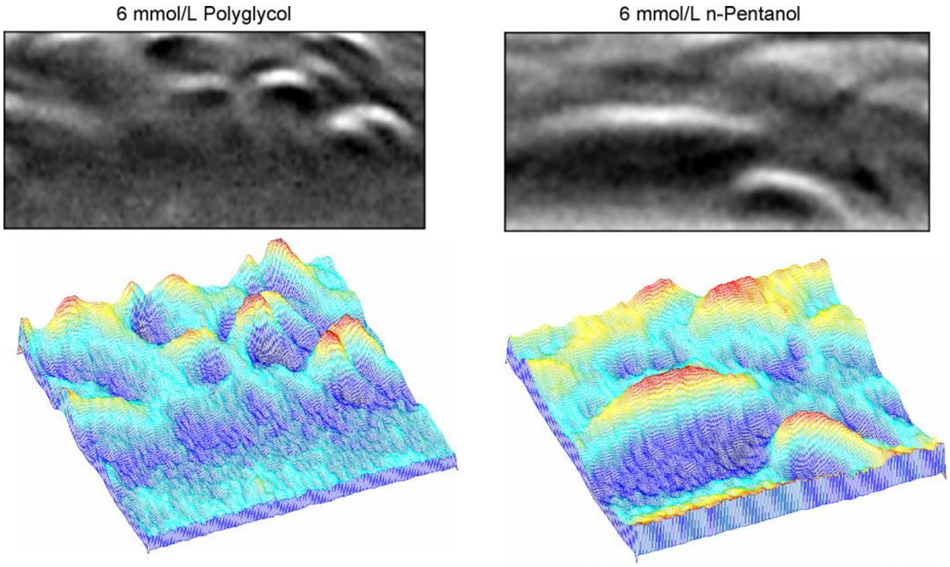

Figure 2.13 Close up of the surface of a bubble (ca. 10 mm dia.) blown in (top left) polyglycol and (top right) pentanol, and (below) the corresponding image intensity plots (note, scale is same in each case). After (Acuña et al., 2008)

The advent of surface tension gradients influences several characteristics of the interface, namely, surface elasticity, surface viscosity, and total stress. The next three sub-sections provide background on each of these characteristics.

2.3.4.1 Surface elasticity

The source of surface tension gradient of interest here is that from the redistribution of surfactant molecules (monomers and/or aggregates) at the interface during stretching. As the surface stretches the local concentration of surfactant decreases and therefore there is an increase in the local surface tension which opposes further stretching, i.e., it imparts film elasticity (Adamson, 1990). For a rising bubble in frother solutions, the force is manifested by the bubble resisting the deformation caused by the dynamic pressure across the rising bubble and remaining near spherical (Tan and Finch, 2016). Dukhin et al. (1998) proposed the following explanation: as water flows over the rising bubble surface, surfactant molecules are swept towards and concentrated at the trailing region of the bubble, causing an increasing surface tension towards the leading region of the bubble, which creates the surface tension-driven force that opposes the deformation.

Figure 2.14 illustrates this phenomenon. In the absence of frother (Figure 2.14.a) the downward liquid flow over the surface induces air circulation inside the bubble and the bubble surface is referred to as mobile. In the presence of frothers (Figure 2.14.b) the internal circulation is suppressed due to the generation of surface tension gradients and the bubble surface is said to be rigid (Clift et al., 2005; Finch, 2008).

The ability of surfactant to impart elasticity to liquid films is known as Gibbs elasticity (Rusanov and Krotov, 1979), defined as (Hofmeier et al., 1995):

$$E = 2\frac{d\sigma}{dlnA} = 2A\frac{d\sigma}{dc}\frac{dc}{dA} \qquad \text{Equation 2.3}$$

where σ is the surface tension, A the film area, c the concentration. The factor 2 allows for the fact that a liquid film has two liquid/air interfaces (it reduces to one if there is only one liquid/air interface, such as bubble deformation in a turbulent field).

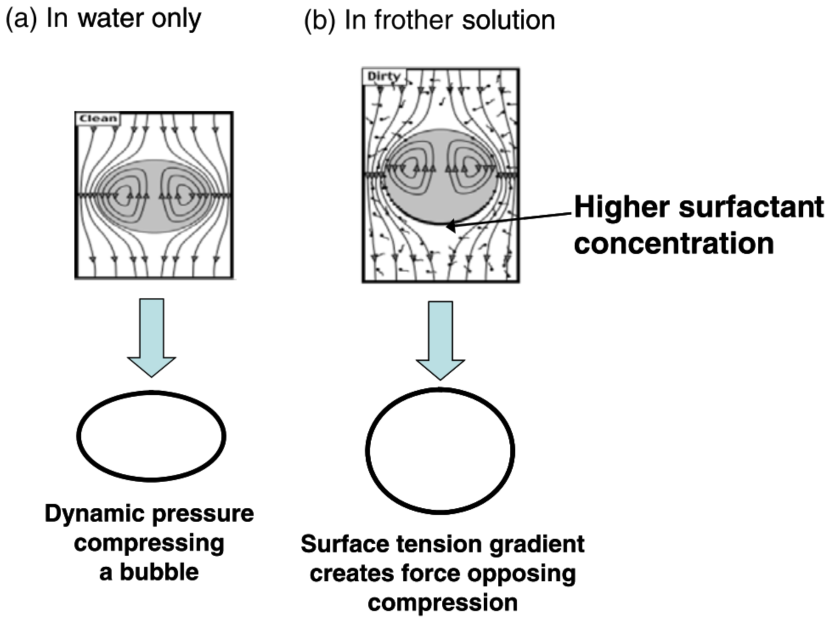

Figure 2.14 Deformation of a rising bubble in (a) water only, and resistance to deformation in (b) surfactant solution. Adapted from (Finch et al., 2008)

This elasticity provides two possible interpretations of the role of frothers in bubble production. One is that the coalescence process is delayed due to the restoring force; the other is that bubbles break if the surrounding turbulence is larger than the restoring force.

2.3.4.2 Surface viscosity

Surface tension gradients could be damped if diffusion and adsorption of surfactant from the neighbouring bulk liquid is sufficiently fast. This relaxation process is typically described as a surface having visco-elastic properties (Lucassen and Van Den Tempel, 1972). Depending on the rate of deformation, the effect could be purely elastic or purely visco-elastic. In the case of extremely slow deformation, equilibrium may be maintained and surface tension gradients vanish (Monroy et al., 1998). The relationship between surface tension gradient and deformation rate is characteristic of an intrinsic viscosity (Fruhner and Wantke, 1996) and the ratio between them defines the surface dilational viscosity (Dickinson, 1999):

$$\eta_d = \frac{d\sigma}{dlnA/dt}$$ Equation 2.4

2.3.4.3 Total stress

Elasticity and viscosity are usually combined in interpreting surface phenomena. Horozov et al. (1997) correlated the two with a total stress τ for a local deformation ε for system that contains surfactant:

$$\tau = E\varepsilon + \eta_d\dot{\varepsilon}$$ Equation 2.5

Surface tension gradients are suspected of playing a role in bubble break-up. Finch et al. (2008), based on Miller and Neogi (1985), proposed a break-up mechanism assuming that frothers produce local surface tension gradients that enhance surface instabilities. They argued wherever a frother molecule resides in a surface a force away from this point is generated. This produces local stress that can lead to a tearing action (Figure 2.15.a). In the case (Figure 2.15.b) involving multiple frother molecules, the opposing forces (or surface tension gradient stresses) promote the formation of a bulge that forms a bubble upon break-away.

While it is argued that frothers may promote break-up through this enhanced bulge mechanism it is also, and perhaps more commonly, argued that surfactants may act in the opposite direction to dampen the bulge (Hühnerfuss et al., 1985; Lemaire and Langevin, 1992; Lucassen, 1982). Miller and Neogi (1985) described the ‘calming’ effect of surfactants, and suggested that the difference in response may be the intensity of the disturbance: minor disturbance (minor deformation) and surfactants oppose growth of the deformation; major disturbance, as we might speculate exists in flotation machines, and surfactant makes the deformation grow.

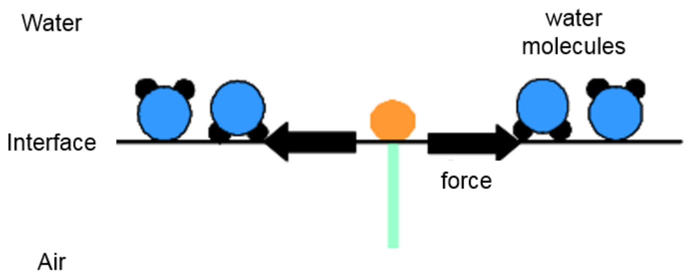

a. A frother molecule residing in the surface produces a force that leads to a 'tearing' action

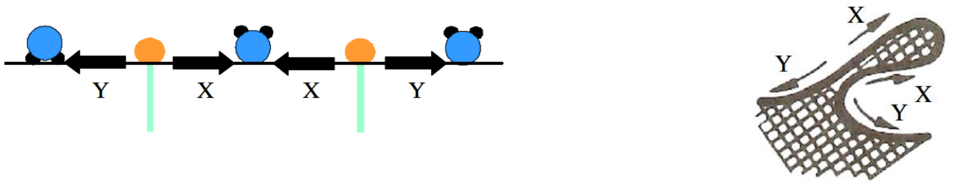

b. Tearing action involving the presence of two frother molecules

c. a liquid break-up model proposed by Miller and Neogi (1985)

Figure 2.15 Frother molecules induce local surface tension gradients that promote interfacial instabilities. Adapted from Finch et al. (2008)

As noted previously, certain inorganic salts can substitute for frothers in flotation systems, with at least one operation not employing frother at all (Quinn et al., 2007). These salts also alter surface tension and thus generate surface tension gradients. In the next section relevant background information on inorganic salts is reviewed.

2.3.5 Inorganic salts

Due to increasing scarcity of fresh water, many mining operations, such as shown in Table 2.1, have to use underground water (saline) or seawater as their process water source. The dissolved salts can affect a range of properties, including water structure, particle surface wettability, and colloidal interactions between bubbles and particles, which could result in either positive or negative impacts on mineral flotation (Wang and Peng, 2014).

One of the known effects of inorganic salts is that they reduce bubble size, a phenomenon that has been documented by many authors (Barigou and Greaves, 1992; Craig et al., 1993a; Quinn et al., 2007; Sovechles and Waters, 2015).

Table 2.1 Flotation operations using saline water (Drelich and Miller, 2012)

Project	**Company**	**Location**	**Water type**
Batu Hijau	Newmont	Indonesia	Sea and fresh water
Las Luces	Minera Las Cenizas	Chile	Sea water
Muchilla	Antofagasta	Chile	Sea water
KCGM	Barrack/Newmont	Australia	Saline
Mt Keith	BHP Billiton	Australia	Saline
Raglan	Xstrata	Canada	Saline
Esperanza	Antofagasta	Chile	Sea water

The common explanation of the effect of inorganic salts on reducing bubble size is related to their ability to prevent coalescence (Craig et al., 1993b; Hofmeier et al., 1995; Laskowski et al., 2003; Lessard and Zieminski, 1971). By bringing two bubbles together it can be readily shown that the presence of inorganic ions inhibits coalescence (Duineveld, 1998; Lessard and Zieminski, 1971; Sagert and Quinn, 1978; Tsang et al., 2004; Tsao and Koch, 1994). This observation has led to the common description of these inorganic salts as ‘coalescence inhibitors’. It has been postulated that the action of the salt ions is due to their ability to generate surface tension gradients which damp the formation of surface (capillary) waves that tend to destabilize the interface (Craig, 2004; Wang and Peng, 2014).

Inorganic salts affect surface tension of air/water interfaces through their perturbing effect on water structure (Enderby et al., 1973; Hancer et al., 2001; Tromp et al., 1992). The disturbance, similar to the case of surfactant, occurs in the network of the H-bonded water molecules. But in contrast to surfactants this time the action is more akin to application of high pressure (Leberman and Soper, 1995). Salt ions favour being fully hydrated and tend to deplete from the air/water interface into the bulk solution (i.e., they are negatively adsorbed), causing surface tension to increase (Craig, 2004).

The effect of salt ions on water structure depends on their relative affinity towards the air/water interface or towards the bulk solution (Bonner and Jumper, 1973). Ions that increase the fluidity of water are classified as 'structure breaking' ions. These ions are typically large inorganic ions, such as Cs^+ and I^-. On the other hand, small inorganic ions, such as Mg^{2+} and Cl^-, that increase the viscosity of the solution are referred to as 'structure making' ions (Hancer et al., 2001). On this basis, inorganic salts can also be classified as structure making salts or structure breaking salts. For instance, NaCl is classified as a structure making salt, and KCl a structure breaking salt.

The effect of salt ions on surface tension hence is also ion-specific. Noting surface tension generally increases with salt concentration, Pugh et al. (1997) compared inorganic salts through their rate of change in surface tension with concentration $(d(\Delta\sigma)/dc)$ (i.e., surface tension gradients). They found that flotation recovery of graphite particles was higher in solutions containing salts that can resulted in high surface tension gradients. The authors postulated that the improved recovery was attributed to an increase in bubble-particle collision probability. In fact this increase was due to a decrease in bubble size (Alexander et al., 2012). The correlation between surface tension gradient and the critical coalescence concentration (CCC), which is a measure of bubble size reduction ability, is examined in Table 2.2 using the CCC data of Sovechles and Waters (2015). It is observed that salts generating the larger surface tension gradients generally have smaller CCC. This can be taken as direct evidence that surface tension gradients play a role in small bubble formation in salt solutions.

Table 2.2 Effect of inorganic salts on surface tension gradient

Salt	$d(\Delta\sigma)/dc$, **mN/m**	**CCC (M)**
NaCl	1.55	0.224
KCl	1.60	0.252
Na_2SO_4	2.96	0.082
$CaCl_2$	3.22	0.091
$MgSO_4$	2.24	0.071

Bubble size distribution is ascribed to a combination of break-up and coalescence. Researchers, such as Walter and Blanch (1986) and Prince and Blanch (1990), have postulated that inorganic salts have negligible impact on break-up and that the reduction in bubble size is entirely due to their effect on coalescence prevention. However, a recent study by Kracht and Finch (2009a) has re-opened the question. In their set-up, depicted in Figure 2.16, the authors exposed mono-size bubbles to a turbulent field induced by an impeller. It was found that the presence of sodium chloride (0.4 M) not only reduced coalescence but, they surmised, also had an effect on break-up by noting the increased fraction of bubbles at about 90% (i.e., smaller than) the original volume. Finch et al. (2008) explained the effect of salts on break-up using the same mechanism illustrated in Figure 2.15. In this case, the surface tension gradient force is directed away from the water molecules but effectively the same tearing or bulge building effect is produced. This time the water molecules have taken on the role of frother molecules.

The unresolved debate evident in the literature urges further investigation on the action of frothers and inorganic salts in controlling bubble size. However, an obstacle is that break-up and coalescence are typically coupled (the case in Figure 2.16), making it difficult to distinguish which mechanism, break-up or coalescence inhibition, has been affected. Devising a set-up to isolate break-up from coalescence thus became one of the objectives of this thesis. Adapting the technique of Kracht and Finch (Figure 2.16) was a starting point, and interestingly they used acoustic monitoring to track events, an approach that also attracted attention for the present study. Accoridingly, the next section reviews bubble acoustics.

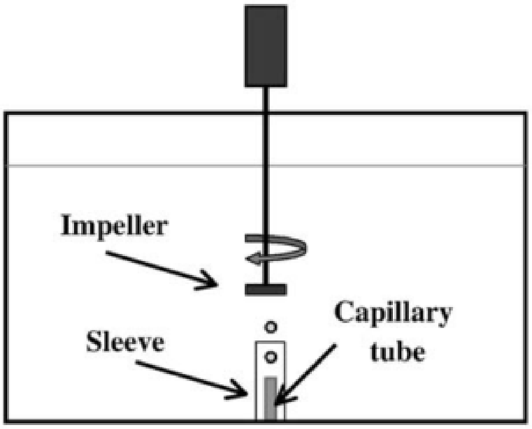

Figure 2.16 Experimental set-up of Kracht and Finch (2009a)

2.4 Bubble acoustics

2.4.1 The Minnaert relationship

Air bubbles pulsating in water behave as oscillators and emit sound (Leighton, 1994; Minnaert, 1933; Strasberg, 1956; Tulin, 1979). Minnaert (1933) studied bubble generation at a nozzle immersed in water, as depicted in Figure 2.17. He found that the sound was produced at the instant of bubble release, the new bubble being considered freely pulsating. On this basis he derived a model, named the Minnaert relationship, to correlate the frequency of the emitted sound with the size of the bubble formed:

$$f = \frac{1}{\pi d}\sqrt{\frac{3kP_0}{\rho}} \qquad \text{Equation 2.6}$$

where f is the sound frequency, d is the bubble diameter, k is the ratio of specific heats for the gas, P_0 is the liquid pressure and ρ is the liquid density.

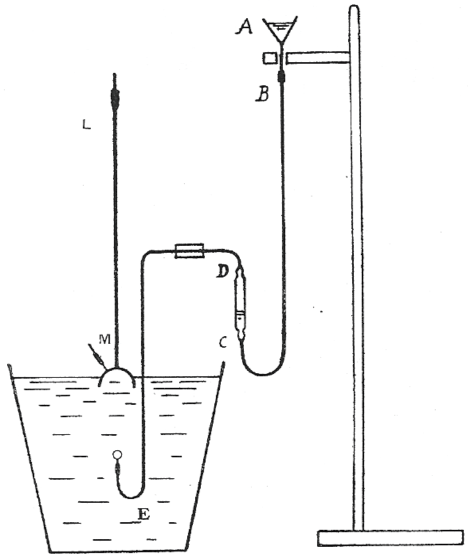

Figure 2.17 Experimental set-up used by Minnaert (1933)

Acoustic monitoring of bubble-emitted sound is a passive measurement, the sound being created by the formation process itself. Following Minnaert (1933), many authors have explored the possibility of using passive acoustic sensing to monitor processes involving bubbles. For instance: McComb and Ayyash (1980) studied the production, pulsation and damping of small air bubbles in dilute polymer solutions; Leighton (1987) conducted an experimental study of the sound emitted from different gas bubbles in a liquid; Pandit et al. (1992) developed an acoustic technique based on the Minnaert relationship to measure bubble size distribution in a tank; Al-Masry et al. (2006) investigated effect of antifoam agents on bubble characteristic in bubble columns using passive acoustic measurements; and, as noted, Kracht and Finch (2009b) used a sound approach to study bubble coalescence in frother solutions. Recently, Vanegas and Holtham (2010) reviewed the possibility of acoustic monitoring in flotation systems, and suggested that it could provide a potential non-intrusive, low cost and real-time online measurement technique.

Since bubble formation, regardless of break-up or coalescence considerations, always emits a sound that is related to the bubble size, acoustic monitoring of bubble formation could be a potential tool to characterize frothers or salts. An advantage of this acoustic approach is that it has the potential to work in three phase slurry systems which are opaque. Using the Minnaert relationship to predict bubble size requires the frequency spectrum of the emitted sound wave to be analyzed. Therefore, it is necessary to review, briefly, some characteristics of sound waves.

2.4.2 Sound waves; some basic facts

The sound wave produced during bubble formation in water is essentially a damped sinusoidal wave that travels through the water in all directions (Dawson, 2002). Figure 2.18 shows an example of such a wave from an air bubble leaving an underwater nozzle. It is evident from the synchronized high speed images of the bubble that the sound is produced at the instant the bubble left the nozzle (i.e., the second bubble image). This sound immediately started to decay and eventually died away after approximately 20 milliseconds. Leighton (1994) has shown that a spherical pulsating bubble, when subjected to low amplitude pulsation, can be treated as a harmonic oscillator. This oscillator emits spherical pressure waves as a single monopole source. But the bubble itself will be subject to damping.

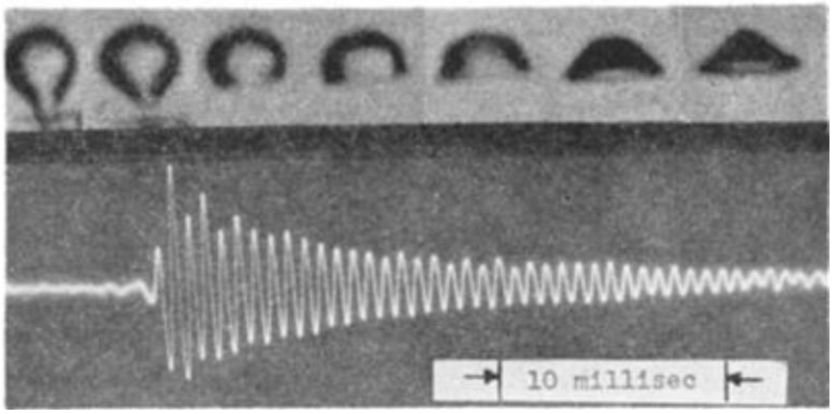

Figure 2.18 Oscillation of the sound pulse from an individual gas bubble leaving a nozzle, with synchronized high-speed photographs of the bubble itself. The horizontal location of each bubble picture is chosen so that each time the photograph was taken corresponds to the point on the graph below the center of the bubble. Adapted from (Strasberg, 1956)

Bubble pulsation treated as a harmonic oscillator can be represented as a mass-spring-damped system such as shown in Figure 2.19. This type of system can be described by the equation of motion based on Newton's second law. A force balance on this system typically yields Equation 2.7, in which the term on the left represents the total force exerted on the body, and the terms on the right the damping force and the elastic spring force, respectively.

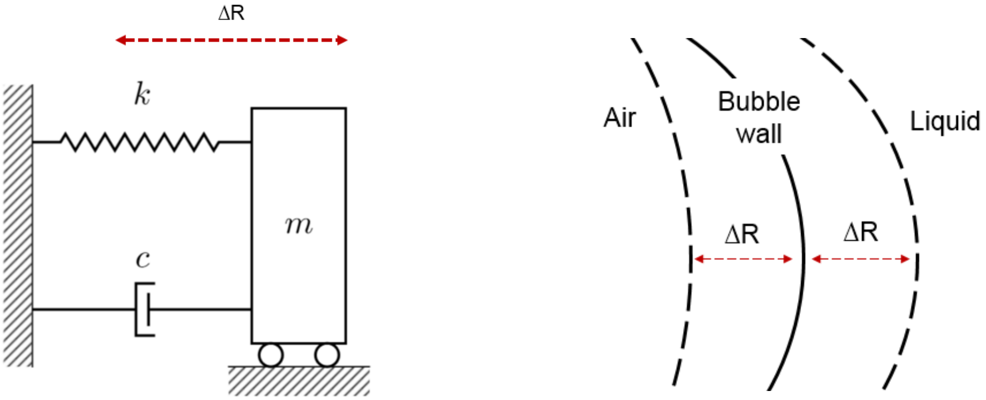

a) a spring-mass-damped system b) oscillation of an air bubble wall in a liquid

Figure 2.19 Oscillation of an air bubble wall as a spring-mass-damped system

$$m\ddot{x} = -c\dot{x} + -kx \qquad \text{Equation 2.7}$$

where m is mass in kilograms, k the spring constant in newtons per meter, c the damping coefficient in newton-seconds per meter or kilograms per second, and x the displacement in meters (or R the radius of the bubble in meters).

Study of wave motion usually involves descriptive parameters such as frequency and damping. In the case of harmonic oscillations, the natural (undamped) frequency of the system is defined by $\omega_0 = \sqrt{k/m}$, in radians per second, the critical damping coefficient, $c_c = 2\sqrt{km}$ or $c_c = 2m\omega_0$, and the dimensionless damping ratio, $\zeta = c/c_c$. Substituting these definitions into Equation 2.7 gives a new form of the second order equation:

$$\ddot{x} + 2\,\zeta\omega_0\dot{x} + {\omega_0}^2\,x = 0 \qquad \text{Equation 2.8}$$

The general solution to the second order differential equation usually takes the form of $x = e^{st}$. Substituting this into Equation 2.8 yields $s = \omega_0(-\zeta \pm i\sqrt{1-\zeta^2}\,)$. With this, the solution to the differential equation, i.e., Equation2.9, can be obtained, where C_1 and C_2 are constants to be determined by the initial conditions. The solution can also be written in a trigonometric form, shown in Equation 2.10, in which the damped frequency is defined by $\omega_d = \omega_0(\sqrt{1-\zeta^2}\,)$, with the phase shift φ in radians, and a constant C to be estimated by the initial conditions:

$$x(t) = C_1 e^{s_- t} + C_2 e^{s_+ t} \qquad \text{Equation 2.9}$$

$$x(t) = Ae^{-\zeta\omega_0 t}\cos(\omega_d t + \varphi) + C \qquad \text{Equation 2.10}$$

The solution to the second order equation (e.g*.,* Equation 2.10) suggests that the oscillation behavior of the system depends on the natural frequency ω_0 and the damping ratio ζ. Specifically, the qualitative behavior of the system depends on the state of the quadratic solution $s = \omega_0(-\zeta \pm i\sqrt{1-\zeta^2}\,)$. If there was only one solution, the case for $\zeta = 1$, the system is referred to as critically damped. In this case, the system tends to return its equilibrium position quickly without oscillating. When $\zeta > 1$, there are two real solutions, meaning the system is over-damped. An over-damped system still converges to its equilibrium state without oscillating but now takes a longer time than the critically damped system. The last possibility, when $0 < \zeta < 1$, generates two complex roots, which suggests the system is under-damped. Under this circumstance, the system will oscillate at the damped frequency ω_d, which is a function of the natural frequency ω_0 and the damping ratio ζ. Figure 2.20 illustrates an example showing the noted effect of damping ratio on the oscillation behaviour of a system.

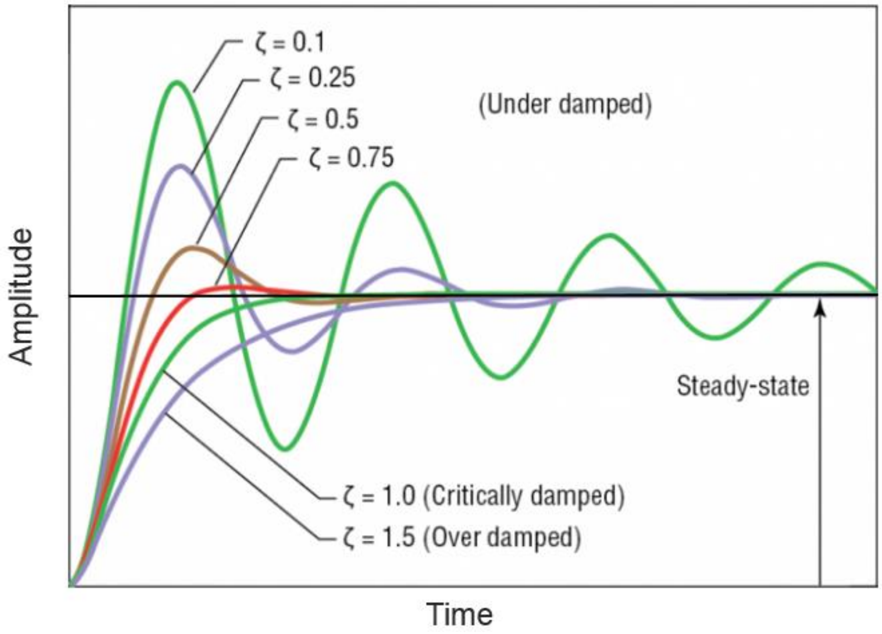

Figure 2.20 Example showing the effect of the damping ratio on the oscillation behaviour of a system

The damping ratio obtained from other techniques has also been employed as a descriptor in the study of bubble related phenomena. Ata (2008; 2009) used high speed imaging to monitor bubble coalescence between bubble pairs in surfactant solutions. The author described the oscillation of the resulting bubble with a damping ratio derived from analysis of its projected area, which is essentially an under-damped wave. That work showed the presence of surfactants affected the damping ratio of the oscillation of the resulting bubble, suggesting that the damping ratio is an effective descriptor that could be adopted in bubble related studies.

The sound wave emitted from a bubble formation event is an under-damped wave. In light of the work of Ata (2008; 2009), the intention in this thesis is to establish an acoustic approach to investigate the role of frothers and salts on bubble formation through break-up by determining their effect on the natural frequency and damping ratio of the sound emitted.

References

Acuña, C.A., Radman, J., Finch, J.A., Measurement of flow visualized on surface of bubble blown in air. Colloids and Surfaces A: Physicochemical and Engineering Aspects, 2008, 330(2–3), 112-115.

Adamson, A.W., Physical chemistry of surfaces. 5 ed. 1990, John Wiley & Sons, New York.

Al-Masry, W.A., Ali, E.M., Aqeel, Y.M., Effect of antifoam agents on bubble characteristics in bubble columns based on acoustic sound measurements. Chemical Engineering Science, 2006, 61(11), 3610-3622.

Aldrich, C., Feng, D., The effect of mothers on bubble size distributions in flotation pulp phases and surface froths. Minerals Engineering, 2000, 13(10–11), 1049-1057.

Alexander, S., Quinn, J., van der Spuy, J., Finch, J., 2012. Correlation of graphite flotation and gas holdup in saline solutions, In Water in Mineral Processing: Proceedings of the First International Symposium, SME, Englewood, pp. 41-50.

Ata, S., Coalescence of Bubbles Covered by Particles. Langmuir, 2008, 24(12), 6085-6091.

Ata, S., The detachment of particles from coalescing bubble pairs. Journal of Colloid and Interface Science, 2009, 338(2), 558-565.

Barigou, M., Greaves, M., Bubble-size distributions in a mechanically agitated gas—liquid contactor. Chemical Engineering Science, 1992, 47(8), 2009-2025.

Bonner, O.D., Jumper, C.F., Effect of ions on water structure. Infrared Physics, 1973, 13(3), 233-242.

Chandler, D., Interfaces and the driving force of hydrophobic assembly. Nature, 2005, 437(7059), 640-647.

Chang, C.-H., Franses, E.I., Adsorption dynamics of surfactants at the air/water interface: a critical review of mathematical models, data, and mechanisms. Colloids and Surfaces A: Physicochemical and Engineering Aspects, 1995, 100, 1-45.

Clift, R., Grace, J.R., Weber, M.E., Bubbles, drops, and particles. 2005, Courier Corporation.

Coulaloglou, C.A., Tavlarides, L.L., Description of interaction processes in agitated liquid-liquid dispersions. Chemical Engineering Science, 1977, 32(11), 1289-1297.

Craig, V.S.J., Bubble coalescence and specific-ion effects. Current Opinion in Colloid & Interface Science, 2004, 9(1–2), 178-184.

Craig, V.S.J., Ninham, B.W., Pashley, R.M., Effect of electrolytes on bubble coalescence. Nature, 1993a, 364(6435), 317-319.

Craig, V.S.J., Ninham, B.W., Pashley, R.M., The effect of electrolytes on bubble coalescence in water. Journal of Physical Chemistry, 1993b, 97(39), 10192-10197.

Danov, K.D., Kralchevsky, P.A., Ivanov, I.B., Equilibrium and dynamics of surfactant adsorption monolayers and thin liquid films. Surfactant science series, 1999, 303-418.

Dawson, P., The physics of the oscillating bubble made simple. European Journal of Radiology, 2002, 41(3), 176-178.

de Bruijn, R.A., 1989. Deformation and break-up of drops in simple shear flows. Eindhoven Univ. Technol., The Netherlands.

De Gennes, P.-G., Brochard-Wyart, F., Quéré, D., Capillarity and wetting phenomena: drops, bubbles, pearls, waves. 2013, Springer Science & Business Media.

Defay, R., Petre, G., Dynamic surface tension. Surface and Colloid Science, 1971, 3, 27.

Dickinson, E., Adsorbed protein layers at fluid interfaces: interactions, structure and surface rheology. Colloids and Surfaces B: Biointerfaces, 1999, 15(2), 161-176.

Dominguez, A., Fernandez, A., Gonzalez, N., Iglesias, E., Montenegro, L., Determination of Critical Micelle Concentration of Some Surfactants by Three Techniques. Journal of Chemical Education, 1997, 74(10), 1227.

Drelich, J., Miller, J.D., Induction time measurements for air bubbles on chalcopyrite, bornite, and gold in seawater. Water in Mineral Processing, 2012, 73-85.

Duineveld, P., 1998. Bouncing and coalescence of bubble pairs rising at high Reynolds number in pure water or aqueous surfactant solutions, In Fascination of Fluid Dynamics. Springer, pp. 409-439.

Dukhin, S.S., Miller, R., Loglio, G., 1998. Physico-chemical hydrodynamics of rising bubble, In Studies in Interface Science, eds. MÖbius, D., Miller, R. Elsevier, pp. 367-432.

Eastoe, J., Dalton, J.S., Dynamic surface tension and adsorption mechanisms of surfactants at the air–water interface. Advances in Colloid and Interface Science, 2000, 85(2-3), 103-144.

Enderby, J.E., Howells, W.S., Howe, R.A., The structure of aqueous solutions. Chemical Physics Letters, 1973, 21(1), 109-112.

Finch, J.A., Nesset, J.E., Acuña, C., Role of frother on bubble production and behaviour in flotation. Minerals Engineering, 2008, 21(12–14), 949-957.

Fritz, W., Berechnung des Maximalvolume von Dampfblasen. Phys. Z., 1935, 36, 379-388.

Fruhner, H., Wantke, K.D., A new oscillating bubble technique for measuring surface dilational properties. Colloids and Surfaces A: Physicochemical and Engineering Aspects, 1996, 114(0), 53-59.

Fu, X.Y., Ishii, M., Two-group interfacial area transport in vertical air–water flow: I. Mechanistic model. Nuclear Engineering and Design, 2003, 219(2), 143-168.

Goetz, R., Lipowsky, R., Computer simulations of bilayer membranes: Self-assembly and interfacial tension. The Journal of Chemical Physics, 1998, 108(17), 7397-7409.

Grace, H.P., Dispersion phenomena in high viscosity immiscible fluid systems and application of static mixers as dispersion devices in such systems. Chemical Engineering Communications, 1982, 14(3-6), 225-277.

Grau, R.A., Laskowski, J.S., Role of Frothers in Bubble Generation and Coalescence in a Mechanical Flotation Cell. The Canadian Journal of Chemical Engineering, 2006, 84(2), 170-182.

Hancer, M., Celik, M.S., Miller, J.D., The Significance of Interfacial Water Structure in Soluble Salt Flotation Systems. Journal of Colloid and Interface Science, 2001, 235(1), 150-161.

Hernandez-Aguilar, J.R., Cunningham, R., Finch, J.A., A test of the Tate equation to predict bubble size at an orifice in the presence of frother. International Journal of Mineral Processing, 2006, 79(2), 89-97.

Hinze, J.O., Fundamentals of the hydrodynamic mechanism of splitting in dispersion processes. AIChE Journal, 1955, 1(3), 289-295.

Hofmeier, U., Yaminsky, V.V., Christenson, H.K., Observations of Solute Effects on Bubble Formation. Journal of Colloid and Interface Science, 1995, 174(1), 199-210.

Holmberg, K., Jönsson, B., Kronberg, B., Lindman, B., 2003. Phase Behaviour of Concentrated Surfactant Systems, In Surfactants and Polymers in Aqueous Solution. John Wiley & Sons, pp. 67-96.

Horozov, T.S., Kralchevsky, P.A., Danov, K.D., Ivanov, I.B., Interfacial Rheology and Kinetics of Adsorption from Surfactant Solution. Journal of Dispersion Science and Technology, 1997, 18(6-7), 593-607.

Hsieh, C.-S., Campen, R.K., Vila Verde, A.C., Bolhuis, P., Nienhuys, H.-K., Bonn, M., Ultrafast Reorientation of Dangling OH Groups at the Air-Water Interface Using Femtosecond Vibrational Spectroscopy. Physical Review Letters, 2011, 107(11), 116102.

Hühnerfuss, H., Lange, P.A., Walter, W., Relaxation effects in monolayers and their contribution to water wave damping: I. Wave-induced phase shifts. Journal of Colloid and Interface Science, 1985, 108(2), 430-441.

Israelachvili, J.N., Intermolecular and surface forces: revised third edition. 2011, Academic press.

Israelachvili, J.N., Mitchell, D.J., Ninham, B.W., Theory of self-assembly of hydrocarbon amphiphiles into micelles and bilayers. Journal of the Chemical Society, Faraday Transactions 2: Molecular and Chemical Physics, 1976, 72(0), 1525-1568.

Kitchener, J.A., Cooper, C.F., Current concepts in the theory of foaming. Quarterly Reviews, Chemical Society, 1959, 13(1), 71-97.

Klimpel, R.R., Isherwood, S., Some industrial implications of changing frother chemical structure. International Journal of Mineral Processing, 1991, 33(1), 369-381.

Kolmogorov, A.N., On the disintegration of drops in a turbulent flow. Dokl. Akad. Nauk SSSR, 1949, 66, 825-828.

Kracht, W., Finch, J.A., Bubble break-up and the role of frother and salt. International Journal of Mineral Processing, 2009a, 92(3-4), 153-161.

Kracht, W., Finch, J.A., Using sound to study bubble coalescence. Journal of Colloid and Interface Science, 2009b, 332(1), 237-245.

Larson, R.G., Self-assembly of surfactant liquid crystalline phases by Monte Carlo simulation. The Journal of Chemical Physics, 1989, 91(4), 2479-2488.

Laskowski, J.S., Frothers and Flotation Froth. Mineral Processing and Extractive Metallurgy Review, 1993, 12(1), 61-89.

Laskowski, J.S., Frothers And Frothing. Frothing in Flotation II: Recent Advances in Coal Processing, 1998, 2, 1.

Laskowski, J.S., Testing flotation frothers. Fizykochemiczne Problemy Mineralurgii/Physicochemical Problems of Mineral Processing, 2004(38), 13-22.

Laskowski, J.S., Cho, Y.S., Ding, K., Effect of Frothers on Bubble Size and Foam Stability in Potash Ore Flotation Systems. The Canadian Journal of Chemical Engineering, 2003, 81(1), 63-69.

Laughlin, R.G., The aqueous phase behavior of surfactants. 1994, Academic Pr.

Leberman, R., Soper, A.K., Effect of high salt concentrations on water structure. Nature, 1995, 378(6555), 364-366.

Lee, C.-H., Erickson, L.E., Glasgow, L.A., Bubble Breakup and Coalescence in Turbulent Gas-Liquid Dispersions. Chemical Engineering Communications, 1987a, 59(1-6), 65-84.

Lee, C.-H., Erickson, L.E., Glasgow, L.A., Dynamics of Bubble Size Distribution in Turbulent Gas-Liquid Dispersions. Chemical Engineering Communications, 1987b, 61(1-6), 181-195.

Leighton, T.G., The Acoustic Bubble. Academic Press, 1994. ISBN 0-12-441920-8.

Leighton, T.G., Walton, A., An experimental study of the sound emitted from gas bubbles in a liquid. European Journal of Physics, 1987, 8, 7.

Lemaire, C., Langevin, D., Longitudinal surface waves at liquid interfaces: Measurement of monolayer viscoelasticity. Colloids and Surfaces, 1992, 65(2–3), 101-112.

Lessard, R.R., Zieminski, S.A., Bubble coalescence and gas transfer in aqueous electrolytic solutions. Industrial and Engineering Chemistry Fundamentals, 1971, 10(2), 260-269.

Levich, V.G., Physicochemical hydrodynamics. 1962, Prentice-Hall, Englewood Cliffs, N.J.

Liao, Y., Lucas, D., A literature review of theoretical models for drop and bubble breakup in turbulent dispersions. Chemical Engineering Science, 2009, 64(15), 3389-3406.

Lucassen, J., Effect of surface-active material on the damping of gravity waves: A reappraisal. Journal of Colloid and Interface Science, 1982, 85(1), 52-58.

Lucassen, J., Van Den Tempel, M., Dynamic measurements of dilational properties of a liquid interface. Chemical Engineering Science, 1972, 27(6), 1283-1291.

Luo, H., Svendsen, H.F., Theoretical model for drop and bubble breakup in turbulent dispersions. AIChE Journal, 1996, 42(5), 1225-1233.

Machon, V., Pacek, A.W., Nienow, A.W., Bubble Sizes in Electrolyte and Alcohol Solutions in a Turbulent Stirred Vessel. Chemical Engineering Research and Design, 1997, 75(3), 339-348.

Marrucci, G., A theory of coalescence. Chemical Engineering Science, 1969, 24(6), 975-985.

Martinez-Bazan, C., Montañés, J.L., Lasheras, J.C., On the breakup of an air bubble injected into a fully developed turbulent flow. Part 1. Breakup frequency. Journal of Fluid Mechanics, 1999a, 401, 157-182.

Martinez-Bazan, C., Montañés, J.L., Lasheras, J.C., On the breakup of an air bubble injected into a fully developed turbulent flow. Part 2. Size PDF of the resulting daughter bubbles. Journal of Fluid Mechanics, 1999b, 401, 183-207.

McBain, J.W., Martin, H.E., XCII.-Studies of the constitution of soap solutions: the alkalinity and degree of hydrolysis of soap solutions. Journal of the Chemical Society, Transactions, 1914, 105(0), 957-977.

McComb, W.D., Ayyash, S., The production, pulsation and damping of small air bubbles in dilute polymer solutions. Journal of Physics D: Applied Physics, 1980, 13(5), 773.

Meguro, K., Adachi, T., Fukunishi, R., Esumi, K., Formation of multiple adsorption layers of surfactants on particle surfaces. Langmuir, 1988, 4(5), 1160-1162.

Menger, F.M., The structure of micelles. Accounts of Chemical Research, 1979, 12(4), 111-117.

Meunier, J., Langevin, D., Boccara, N., Physics of Amphiphilic Layers: Proceedings of the Workshop, Les Houches, France February 10–19, 1987. 2012, Springer Science & Business Media.

Miller, C.A., Neogi, P., 1985. Interfacial phenomena: equilibrium and dynamic effects; CRC Press: Boca Raton, FL, 1985; pp 240−298.

Minnaert, M., On musical air-bubbles and the sounds of running water. Philosophical Magazine, 1933, 16, 235-248.

Monroy, F., Giermanska Kahn, J., Langevin, D., Dilational viscoelasticity of surfactant monolayers. Colloids and Surfaces A: Physicochemical and Engineering Aspects, 1998, 143(2-3), 251-260.

Monteux, C., Williams, C.E., Meunier, J., Anthony, O., Bergeron, V., Adsorption of Oppositely Charged Polyelectrolyte/Surfactant Complexes at the Air/Water Interface: Formation of Interfacial Gels. Langmuir, 2004, 20(1), 57-63.

Nagarajan, R., Molecular Packing Parameter and Surfactant Self-Assembly: The Neglected Role of the Surfactant Tail. Langmuir, 2002, 18(1), 31-38.

Pandit, A.B., Varley, J., Thorpe, R.B., Davidson, J.F., Measurement of bubble size distribution: an acoustic technique. Chemical Engineering Science, 1992, 47(5), 1079-1089.

Prince, M.J., Blanch, H.W., Bubble coalescence and break-up in air-sparged bubble columns. AIChE Journal, 1990, 36(10), 1485-1499.

Problestein, R., 1994. Physicochemical Hydrodynamics, An introduction. John Wiley & Sons New York.

Pugh, R.J., Weissenborn, P., Paulson, O., Flotation in inorganic electrolytes; the relationship between recover of hydrophobic particles, surface tension, bubble coalescence and gas solubility. International Journal of Mineral Processing, 1997, 51(1), 125-138.

Quinn, J.J., Kracht, W., Gomez, C.O., Gagnon, C., Finch, J.A., Comparing the effect of salts and frother (MIBC) on gas dispersion and froth properties. Minerals Engineering, 2007, 20(14), 1296-1302.

Risso, F.R., FABRE, J., Oscillations and breakup of a bubble immersed in a turbulent field. Journal of Fluid Mechanics, 1998, 372, 323-355.

Romsted, L.S., 2012. Introduction to Surfactant Self-Assembly, In Supramolecular Chemistry. John Wiley & Sons, Ltd.

Rowlinson, J.S., Widom, B., Molecular theory of capillarity. 2013, Courier Corporation.

Rusanov, A., Krotov, V., Gibbs elasticity of liquid films. Prog. Surf. Memb. Sci, 1979, 13, 415-524.

Sagert, N.H., Quinn, M.J., The coalescence of gas bubbles in dilute aqueous solutions. Chemical Engineering Science, 1978, 33(8), 1087-1095.

Sovechles, J.M., Waters, K.E., Effect of ionic strength on bubble coalescence in inorganic salt and seawater solutions. AIChE Journal, 2015, 61(8), 2489-2496.

Stone, H.A., Dynamics of Drop Deformation and Breakup in Viscous Fluids. Annu. Rev. Fluid Mech., 1994, 26(1), 65-102.

Strasberg, M., Gas Bubbles as Sources of Sound in Liquids. The Journal of the Acoustical Society of America, 1956, 28(1), 20-26.

Sweet, C., van Hoogstraten, J., H., M., , Laskowski, J.S., 1997. The effect of frothers on bubble size and frothability of aqueous solutions, In 2nd UBC-McGill Symposium Series on Fundemental in Mineral Processing, ed. Finch, J.A., Rao, S.R., Holubec, I. The Metallurgical Society of CIM, pp. 235-246.

Tan, Y.H., Finch, J.A., Frother structure–property relationship: Effect of alkyl chain length in alcohols and polyglycol ethers on bubble rise velocity. Minerals Engineering, 2016, 95, 14-20.

Tanford, C., The hydrophobic effect: formation of micelles and biological membranes. 1973, Wiley, New York.

Taylor, G.I., The Viscosity of a Fluid Containing Small Drops of Another Fluid. Proceedings of the Royal Society of London. Series A, 1932, 138(834), 41-48.

Taylor, G.I., The Formation of Emulsions in Definable Fields of Flow. Proceedings of the Royal Society of London. Series A, 1934, 146(858), 501-523.

Thomas, R.K., Penfold, J., Multilayering of Surfactant Systems at the Air–Dilute Aqueous Solution Interface. Langmuir, 2015, 31(27), 7440-7456.

Tromp, R.H., Neilson, G.W., Soper, A.K., Water structure in concentrated lithium chloride solutions. The Journal of Chemical Physics, 1992, 96(11), 8460-8469.

Tsang, Y.H., Koh, Y.-H., Koch, D.L., Bubble-size dependence of the critical electrolyte concentration for inhibition of coalescence. Journal of Colloid and Interface Science, 2004, 275(1), 290-297.

Tsao, H.K., Koch, D.L., Collisions of slightly deformable, high Reynolds number bubbles with short ‐ range repulsive forces. Physics of Fluids, 1994, 6(8), 2591-2605.

Tsouris, C., Tavlarides, L.L., Breakage and coalescence models for drops in turbulent dispersions. AIChE Journal, 1994, 40(3), 395-406.

Tucker, C.L., Moldenaers, P., Microstructural evolution in polymer blends. Annu. Rev. Fluid Mech., 2002, 34, 177-210.

Tulin, M.P., Mechanics of Underwater Noise. Pergamon Press, 1976.

Vanegas, C., Holtham, P.N., 2010. Possibilities for flotation acoustics monitoring-A review, In International Mineral Processing Congress 2010. Australasian Institute of Mining and Metallurgy, pp. 2457-2470.

Vargaftik, N.B., Volkov, B.N., Voljak, L.D., International Tables of the Surface Tension of Water. Journal of Physical and Chemical Reference Data, 1983, 12(3), 817-820.

Walter, J.F., Blanch, H.W., Bubble break-up in gas—liquid bioreactors: Break-up in turbulent flows. The Chemical Engineering Journal, 1986, 32(1), B7-B17.

Wang, B., Peng, Y., The effect of saline water on mineral flotation - A critical review. Minerals Engineering, 2014, 66-68, 13-24.

Wang, T., Wang, J., Jin, Y., A novel theoretical breakup kernel function for bubbles/droplets in a turbulent flow. Chemical Engineering Science, 2003, 58(20), 4629-4637.

Wills, B.A., Finch, J.A., 2016. Chapter 12 - Froth Flotation, In Wills' Mineral Processing Technology (Eighth Edition), ed. Finch, B.A.W.A. Butterworth-Heinemann, Boston, pp. 265-380.

Zeitling, M.A., Tavlarides, L.L., Fluid-fluid interactions and hydrodynamics. Can. J. Chem. Engng, 1972, 50, 207-215.

Zhao, H., Ge, W., A theoretical bubble breakup model for slurry beds or three-phase fluidized beds under high pressure. Chemical Engineering Science, 2007, 62(1–2), 109-115.

CHAPTER 3 USING SOUND TO STUDY THE EFFECT OF FROTHERS ON THE BREAK-UP OF AIR BUBBLES AT AN UNDERWATER CAPILLARY

3.1 Introduction

Bubbles are ubiquitous in nature and have found many significant industrial applications. One in particular is froth flotation. In flotation, hydrophobic particles are collected through attachment to air bubbles and carried (floated) to the overflow while hydrophilic particles remain in suspension and exit as an underflow. Usually the hydrophobic particles, natural or induced, comprise the valuable component and the overflow is the concentrate and the underflow the tailings. Bubbles clearly play the central role determining the available interfacial area for collecting and transporting the hydrophobic particles.

For a given volumetric air flowrate the smaller the bubbles the greater the interfacial area but the bubbles must have sufficient buoyancy to levitate the collected particles. A compromise size is ca. 1 mm diameter, with bubbles in practice ranging from ca. 0.5 to 2.5 mm (Finch and Dobby, 1991). It is, however, not easy to generate such size bubbles in pure water because the high surface tension drives bubbles to coalesce (Blander and Katz, 1975; Kitchener and Cooper, 1959; Talanquer and Oxtoby, 1995). To aid small bubble production surfactants known as frothers, are employed. The impact of these solutes on reducing bubble size is well known, but their action remains obscure (Finch et al., 2008). Reduction in surface tension has been speculated as the cause (Gupta and Yan, 2006; Napier-Munn and Wills, 2006) but others have pointed out the deficiencies of that notion (Aldrich and Feng, 2000; Grau and Laskowski, 2006; Machon et al., 1997; Sweet et al., 1997).

A common explanation of the role of frothers in reducing bubble size recognizes their ability to hinder coalescence, a phenomenon that can be readily demonstrated. For instance, in the work of Ata (2008) and Bournival et al. (2014) the authors used high speed cinematography to monitor the events when two bubbles each held at a capillary tip are brought together. It was demonstrated that coalescence was increasingly delayed as frother concentration was increased. In addition, the oscillation of the resultant bubble (i.e., after coalescence) could be characterised by a damping ratio derived by fitting the variation of the projected bubble area, and that the oscillation deceased as frother concentration was increased.

While noting that the bulk of the literature emphasizes the role of frothers in coalescence prevention, there are occasional references suggesting frothers may also have an impact on the other possible mechanism, namely, enhanced break-up (Acuña, 2007; Finch, 2006; Grau and Laskowski, 2006). The work of Kracht and Finch (2009a) is relevant in this regard. They investigated the role of frothers on break-up of a mono-size distribution of bubbles exposed to a turbulent field. In addition to suppressing coalescence, they surmised an effect on break-up by noting an increase in the fraction of bubbles at 90% of the original volume. Javor et al. (2013) adapted the same technique and came to a similar conclusion, their results indicating that the minimum observed bubble size was smaller with long chain frothers than with short chain frothers. A drawback of these experiments, however, is that both break-up and coalescence occur, which makes it difficult to distinguish which mechanism (i.e., coalescence and break-up) the frothers affect.

Break-up and coalescence are simultaneous events which are coupled. To isolate a possible role of frothers in break-up, an experimental procedure giving break-up only events is required. One straightforward approach is by releasing an air bubble at a capillary, an allied process perhaps better described as ‘break-away’. If done sufficiently slowly the volume of the detached bubble will be independent of the air volumetric flow, implying the bubble is formed at a quasi-static condition (Bolaños-Jiménez et al., 2008). Under this condition, an impact of frothers on the detached bubble can be ascribed to an impact on break-up.

The release of air bubbles in pure water under quasi-static conditions has been investigated by several authors, among the more recent Longuet-Higgins et al. (1991), Bolaños-Jiménez et al. (2008), and Keim (2011). By using high speed cinematography, these authors characterized detachment by describing the dynamics of the necking process, i.e., the evolution of the air bubble prior to break-away. Lin et al. (1994) studied the release of air bubbles in different pure liquids and concluded that surface tension controlled the size of the detached bubble. Hernandez-Aguilar et al. (2006) conducted a similar investigation but this time tested the influence of a frother in water. They found that the presence of frother decreased the detached bubble size but the impact was not readily predicted from surface tension data (or more precisely equilibrium surface tension). They found that the effect of the frother was compatible with the decrease in surface tension at high frother concentrations but not at low frother concentrations.

Another characteristic associated with the release of air bubbles at a capillary is the emission of acoustic signals. The first study of this kind was conducted by Minnaert (1933). He found that the sound was produced at the instant of bubble release, the new bubble being considered freely pulsating. On this basis he derived a model, now termed the Minnaert relationship (Equation 3.1), to correlate the frequency of the emitted sound to the size of the bubble formed:

$$f = \sqrt{3kP_0/\pi^2 d^2 \rho} \qquad \text{Equation 3.1}$$

where f is the sound frequency, d the bubble diameter, k the ratio of specific heats of the gas at constant pressure to that at constant volume, P_0 the liquid pressure, and ρ the liquid density.

Following Minnaert many authors subsequently used his acoustic approach, mostly accompanied with high speed cinematography, to study bubble related phenomena. For instance, Strasberg (1956) noted that bubble break-up or coalesce emits a decaying sinusoidal pulse of sound. Longuet-Higgins et al. (1991) studied the release of air bubbles at a capillary and observed formation of an axial jet directed upward into the bubble, and suspected this jet may play a part in stimulating the emission of sound. Leighton et al. (1991) observed high air rate through a capillary induced bubble coalescence in proximity to the capillary resulting in a characteristic acoustic signal. Exploiting this, Kracht and Finch (2009b) established an acoustic technique to study bubble coalescence in frother (and inorganic salt) solutions. They observed that the acoustic signal acts in response to the addition of frothers, and confirmed the presence of frothers delays the coalescence process.

Following on from Kracht and Finch (2009b), the objective of this work is to explore the possible use of a passive acoustic approach to determine the effects of frothers on bubble break-up at an underwater capillary. A prime motivation was that the acoustic technique provides a real-time and continuous measurement which could supplement high speed cinematography to better monitor the virtually instantaneous break-up process (at least in the order of milliseconds). In principle acoustic techniques could enable opaque systems such as slurries to be included in the study, to answer whether particles might play a role in break-up, which is another advantage over imaging techniques. By establishing a quasi-static condition with a constant and sufficiently low air flow rate, this chapter will examine several acoustic parameters pertinent to the break-up process, including the frequency and the damping ratio of the emitted sound. High speed cinematography will be employed to provide visuals, such as the size and the shape oscillation of the produced bubble, to correlate against the findings of the acoustic method.

3.2 Experimental

3.2.1 Apparatus

The experimental set-up (Figure 3.1.a) comprised a 21.5 cm (L) x 21.5 cm (W) x 16 cm (H) Plexiglas tank holding 2.5 L solutions into which air bubbles were generated through a glass capillary with internal diameter of 4 mm (Figure 3.1.c). A needle valve was used to regulate the air flow rate. A Fastec high speed camera (HiSpec5 8G Mono) equipped with a 60 mm macro lens (Nikon, AF Micro Nikon) was used to monitor the break-up process. Acoustic emissions were monitored using a hydrophone (Lab-40 hydrophone from LAB-core system) shown in Figure 3.1.b with a detectable frequency range 5 to 85000 Hz. Acquisition of the acoustic signal was achieved using a National Instrument data acquisition system (NI USB-6341, X SERIES DAQ). The entire set-up was placed on a super-cushioning foam slab (McMaster, 3/4" Thick Blue Polyurethane, 86195K35) to minimize extraneous vibrations that could corrupt the bubble release process.

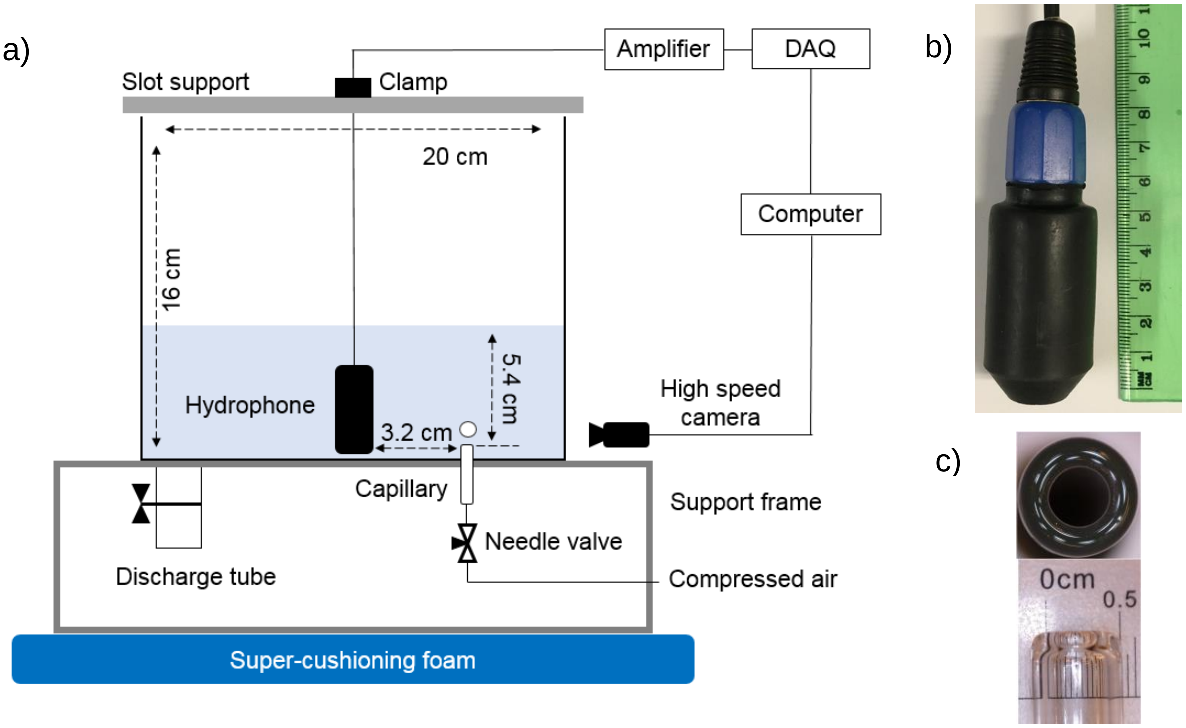

Figure 3.1 Experimental set-up

3.2.2 Frothers

All solutions were prepared in reverse osmosis (RO) water at room temperature of ~ 23°C. Two common polyglycol frothers (listed in Table 3.1), both non-volatile and soluble, were tested. The DF250 (American) with molecular weight (M.W.) 264 g/mol was purchased from Dow Chemicals, and F150 with M.W. 425 g/mol was provided by Flottec.

Table 3.1 Solutes tested

DF250[a] $CH_3(PO)_4OH$	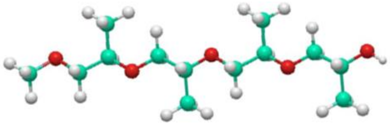
F150[a] $H(PO)_7OH$	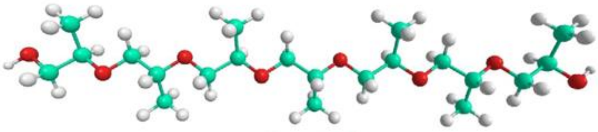
● Carbon	● Oxygen ○ Hydrogen

[a] PO is propylene oxide (propoxy) [-O-CH_2-CH_2-CH_2-]

3.2.3 Procedure

The experiment required significant effort to ensure reproducible acoustic signals. The response of the hydrophone was dependent on the distance from and orientation to the capillary. The hydrophone itself could be a disturbance if located too close to the sound source. On the other hand, if too far away, the acoustic signal was too weak and masked by background noise. By trial-and-error the positioning of the hydrophone is as shown in Figure 3.1.a. A slot support over the top of the tank allows the horizontal distance between the hydrophone and the capillary to be adjusted, and a clamp sliding through the slot allows the vertical distance and orientation of the hydrophone to be set. The clamp setting was marked and was fixed throughout the study. Since the hydrophone setting was crucial changing frother concentration was achieved by adding frother in small increments rather than using fresh solutions (hence the specification for non-volatile frothers as the experiment could last several hours).

To achieve the quasi-static condition for bubble production, a needle valve was used and after finding the opening required it was fixed for the tests. Always starting with 2.5 L RO water, after each addition of frother the solution was stirred for about 2 minutes to ensure uniform concentration. The measurements first started with high speed imaging during which at least four bubble pinch-offs were monitored. Acoustic recording followed, with each measurement lasting for 40 s, enough time to record a minimum of four bubble-associated acoustic emissions. After the target range of frother concentration had been covered, the tank was emptied by opening the discharge tube. The set-up was thoroughly rinsed with hot tap water for about five minutes, followed by another rinse with the RO water. Each test condition was repeated at least three times from which the mean and 95% confidence interval (CI) were calculated.

3.3 Data Analysis

3.3.1 Acoustic signals

Analysis of the acoustic signals was a three-step process performed in Matlab. An example is shown in Figure 3.2. In the first step the recorded data were digitized at 500 kHz followed by fast Fourier transformation (FFT) analysis. The purpose of FFT was not only to identify the frequency of the bubble-associated sound (as shown in Figure 3.2.b) but also that of the background noise (i.e., frequencies outside the highlighted box). The second step was removal of the noise using an eighth order Butterworth bandpass filter. In the last step (Figure 3.2.d), each bubble signal was modeled in the time domain with a sinusoidal decay function in the following form:

$$x(t) = Ae^{-\zeta\omega_0 t}\cos\left(\omega_0(\sqrt{1-\zeta^2})t + \varphi\right) + C \qquad \text{Equation 3.2}$$

where A is the amplitude, ω_0 the un-damped frequency, ζ the damping ratio, φ the phase angle, C a constant. The frequency and the damping ratio are the important metrics used in the study.

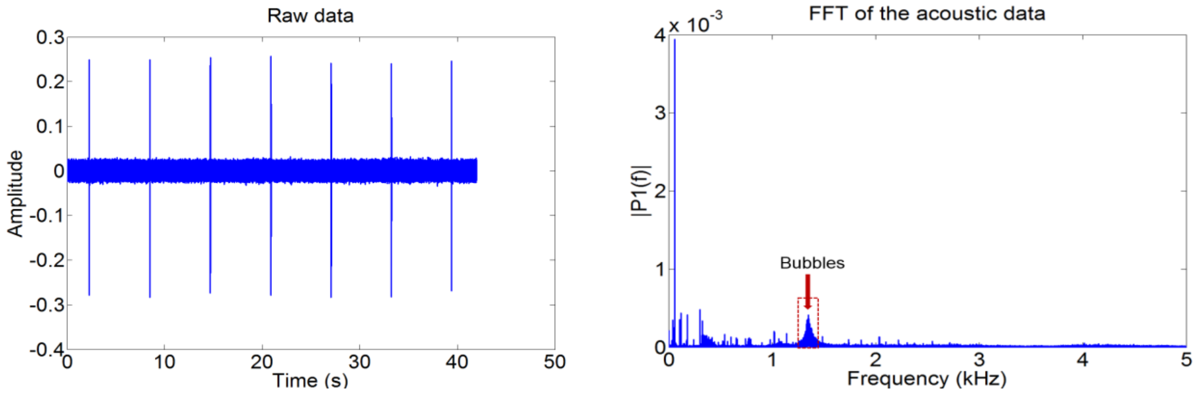

a) Raw data b) Fast Fourier transformation

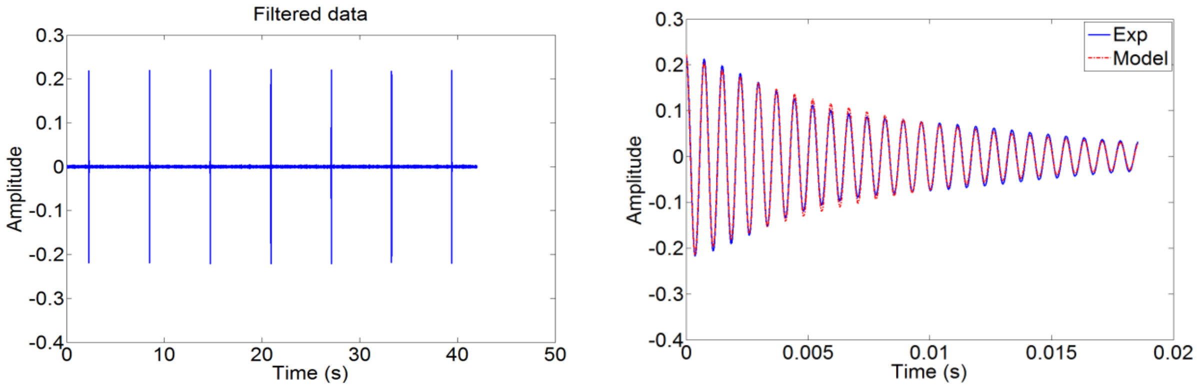

c) Filtered data d) Model fitting

Figure 3.2 Example showing the acoustic analysis procedure

3.3.2 Image processing

The images were processed with software ImageJ to obtain the sphere-volume equivalent diameter (D). Using the major (a) and minor (b) semi-axes of a fitted ellipse, this equivalent diameter was obtained using Equation 3.3. The aspect ratio (E) characterizing bubble shape was defined as the ratio of the semi-axes (b/a).

$$D = \sqrt[3]{(2a)^2 \times (2b)} \qquad \text{Equation 3.3}$$

3.4 Results

3.4.1 Visual

A feature of the break-away event is the creation of a liquid jet that shoots up into the bubble. Figure 3.3 shows an example in RO water. The sequence starts after the break of the neck (i.e., 0 ms) the jet being evident as the conical shape at the bottom of the bubble. At 0.50 ms, the jet has already reached its maximum height, 1.11 ± 0.02 mm (95% CI) and subsequently decays. The decay is fast, noting that the conical shape is only visible from 0.25 ms to 2.25 ms (i.e., ca. 2.00 ms). Over this period the bubble itself remains almost stationary (and even by the end of the sequence (4.25 ms) the top of the bubble has hardly changed location). As the sequence advances, the jet continues to decay and eventually transforms into a surface wave. This surface wave then acts as a perturbation to the bubble surface which propagates upward along the bubble surface as the bubble rises.

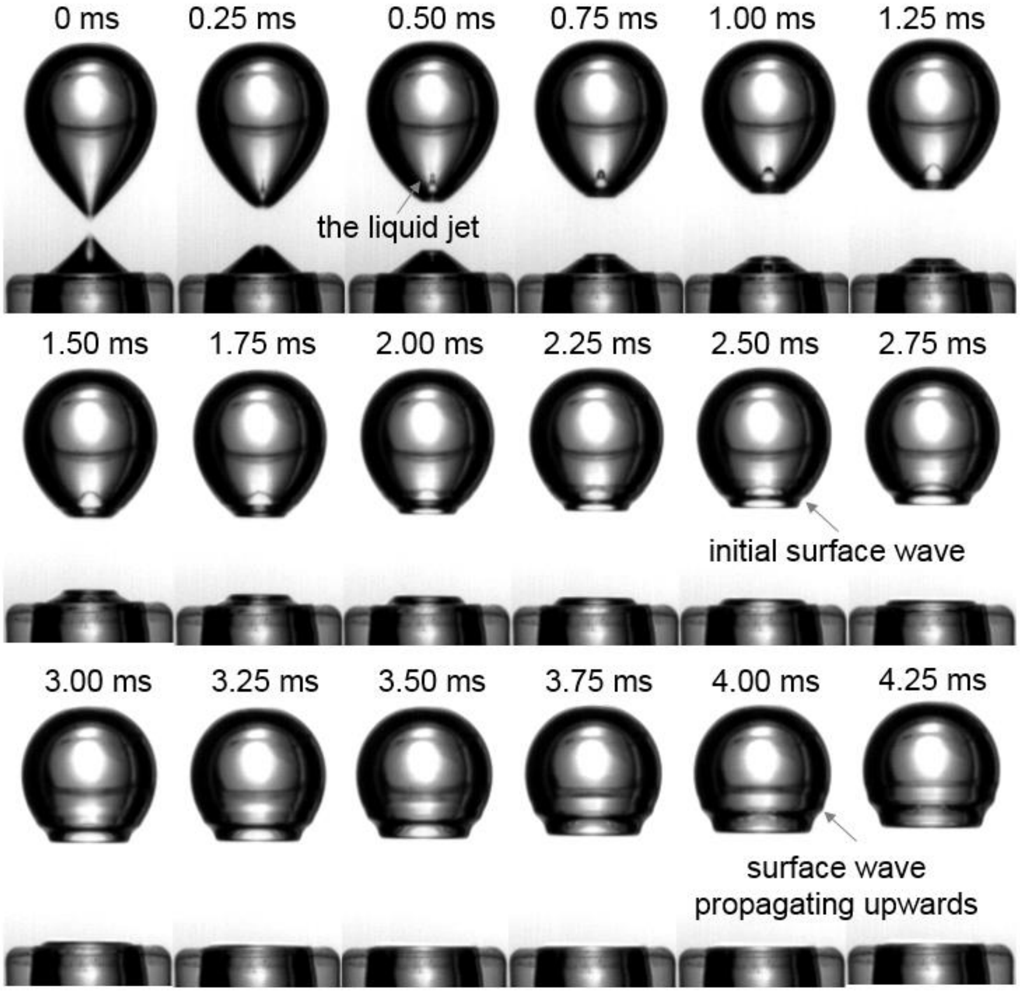

Figure 3.3 Formation of a liquid jet in RO water and subsequent surface wave. The outer diameter of the capillary (6.35 mm) serves as a scale bar.

Formation of the liquid jet appears to be independent of the presence of frother. Figure 3.4 shows some examples. The figure suggests that the liquid jets are essentially identical, all reaching the same maximum height (1.11 mm) at the same time (0.50 ms). If gravity is assumed to be the only force acting, the initial velocity of the jet can be estimated from Newton's kinematic equation, which gives ca. 148 mm/s.

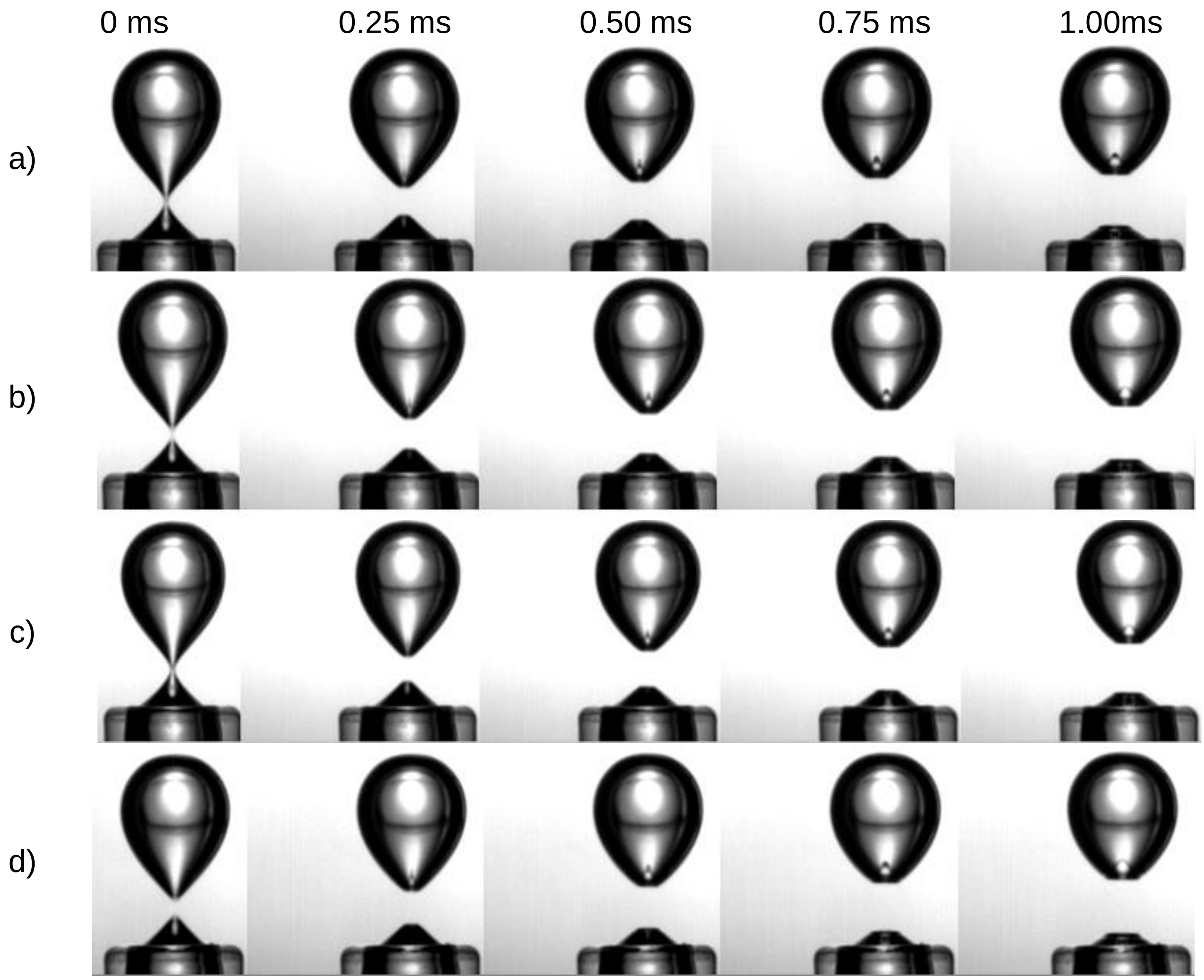

Figure 3.4 Formation of the liquid jet in F150 solution at: a) 2.3 μM, b) 24.3 μM, c) 144.4 μM, and in DF250 solution at d) 5.4 μM.

While the presence of frother does not seem to affect the formation or magnitude of the liquid jet, it does appear to produce an effect on the surface waves induced by the decay of the liquid jet. Figure 3.5 shows some observations in support of this claim. Each sequence starts with the bubble image at 3.00 ms after the initial break-away, and lasts for 0.75 ms to reveal development of the surface wave highlighted by the dashed circle. The choice of 3.00 ms as the start of the image sequence is because the surface wave is at about its most evident. Though refraction unavoidably exists, the range in frother concentration is too small to change the refractive index hence allowing comparison between frother concentrations. There are two prime observations of the effect of frother. One is that the size of the surface wave decreases as concentration is increased, as evident in the first image of each sequence. The other is that the rate of decay of the surface wave changes. In Figure 3.5.b at the low F150 concentration of 2.3 μM the surface wave is still visible at 3.75 ms, but at the same instant at the higher F150 concentration of 24.3 μM (Figure 3.5.c), it almost completely gone. Both observations suggest that an increase in frother concentration results in faster decay of the surface wave.

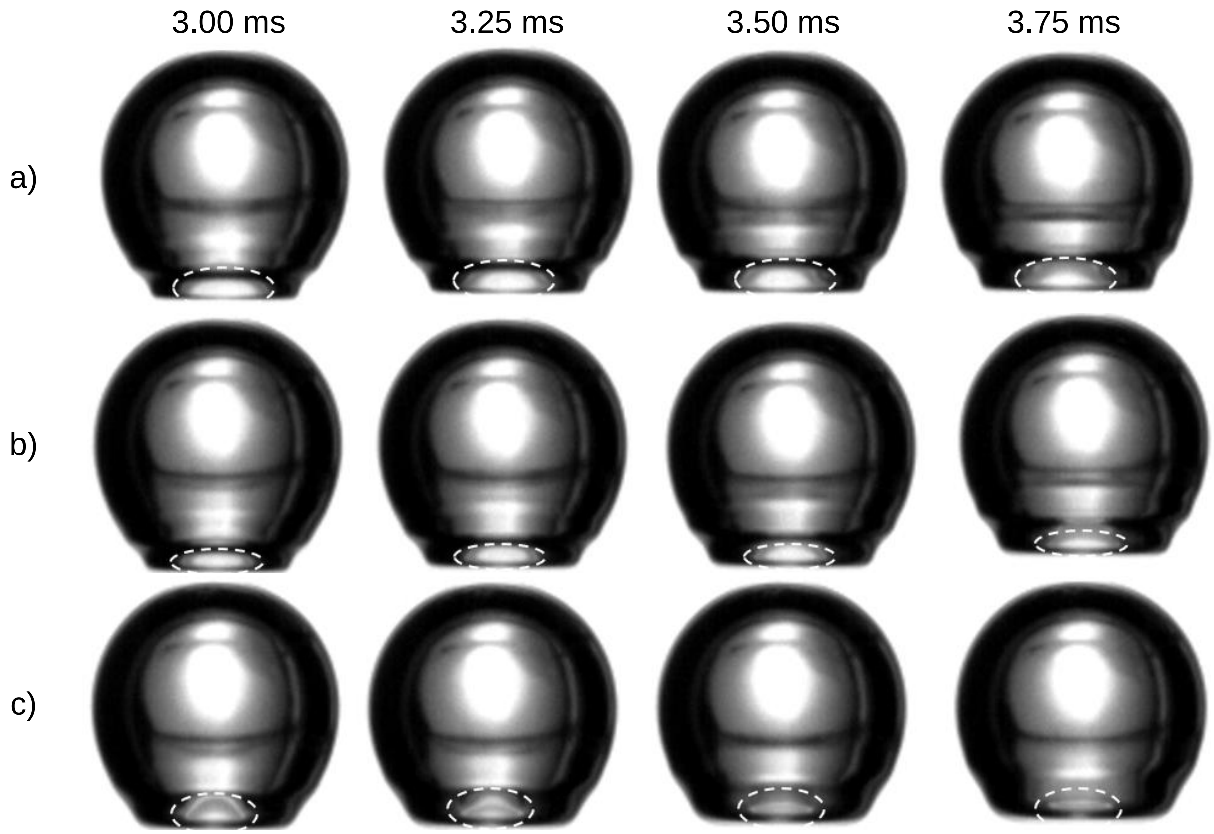

Figure 3.5 Dissipation of the surface wave in: a) RO water, b) F150 2.3 μM, and c) F150 24.3 μM

A consequence of surface waves of different size is manifest in the magnitude of surface oscillation as the bubble rises. Figure 3.6 shows sequences starting 8 ms after the break-away. It is evident that frother supresses the surface wave; comparing the final images (at 10 ms) shows a pronounced wave in RO water and essentially no wave at 71.8 μM F150. Along with suppressing the surface wave, frother also affected the bubble shape as captured by the aspect ratio, Figure 3.9 illustrating that the bubble tends to be spherical (aspect ratio approaches 1) when frother is present.

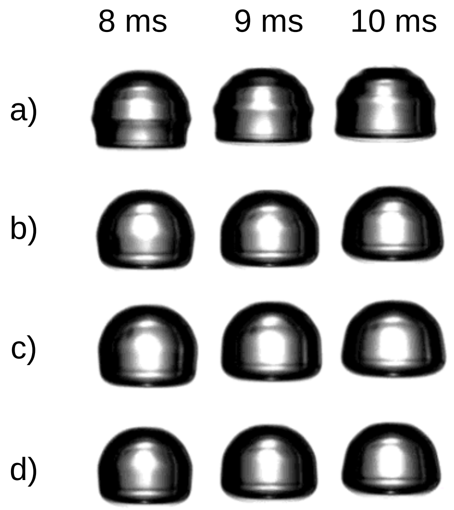

Figure 3.6 Sequence of air bubbles rising in: a) RO water, b) F150 at 7.8 μM, c) DF250 at 13.0 μM, and d) F150 at 71.8 μM. Images were taken 1 ms apart.

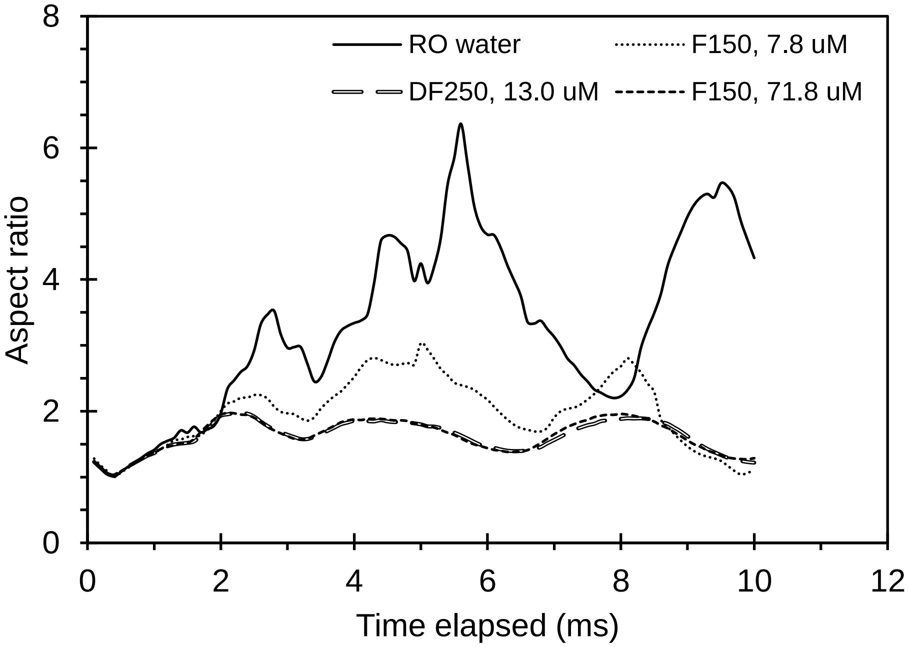

Figure 3.7 Aspect ratio in different solutions

3.4.2 Acoustic

The acoustic frequency obtained by fitting the sinusoidal decay function (Equation 3.2) is shown in Figure 3.8. Included in the Figure are bubble sizes estimated from the Minnaert relationship compared to those derived from imaging analysis. It is apparent that the acoustic frequency is hardly affected by the presence of the frothers until a certain concentration is reached when the frequency increases. For F150 this concentration is ca. 12.2 μM (5 ppm), and for DF250, ca. 26.4 μM (7 ppm).

Correspondingly, bubble size from the Minnaert relationship shows the same (but inverted) trend. This means there is initially little change in bubble size followed by a decreasing trend with increasing frother concentration, which aligns well with the imaging result. However, there is a consistent offset between the two trends, the imaging result being about 1.18 times bigger (a universal factor between all the paired data points). The Minnaert prediction can be argued as more accurate because it is directly based on the volume of the produced bubble which, in contrast, has to be estimated from the image. (It lies outside the current scope to establish the origin of the difference, which would require an independent measure such as the displaced-volume technique.)

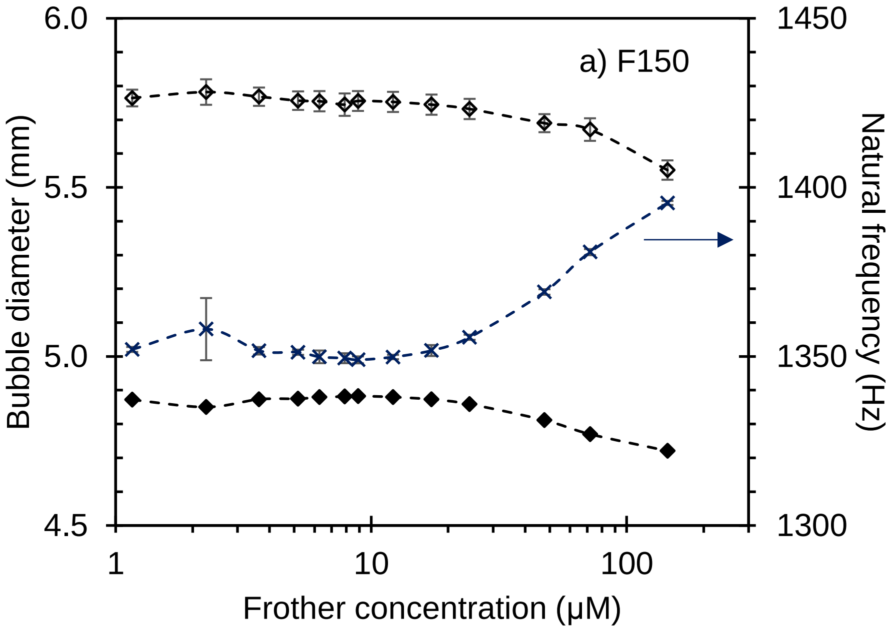

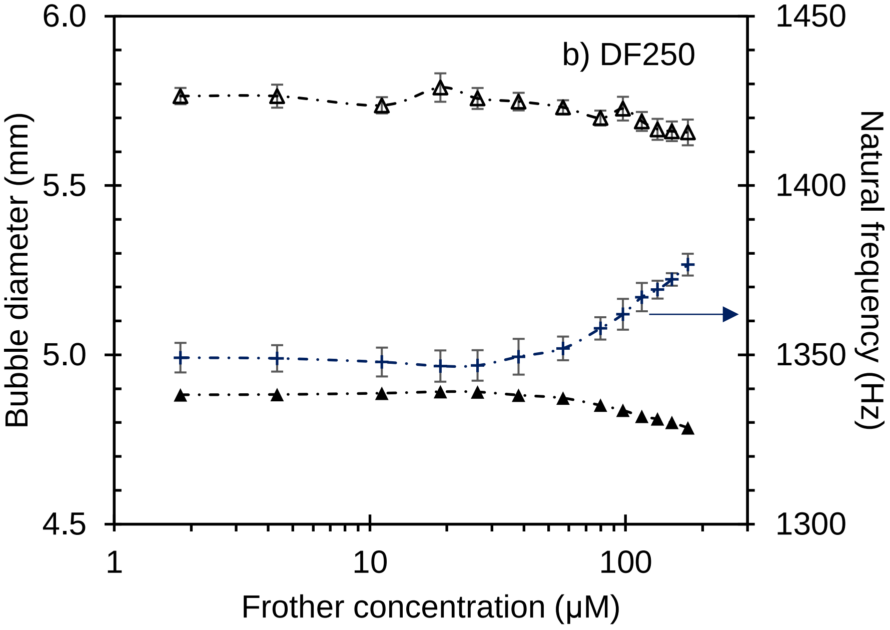

Figure 3.8 Acoustic frequency and bubble size compared to image-derived bubble size as a function of frother concentration in: a) F150 solution, b) DF250 solution. The open diamond and triangle symbols are imaging analysis results; the same but solid symbols are Minnaert relationship results using the acoustic frequency shown in crosses.

Along with frequency, the other important metric from acoustic analysis is the damping ratio. Figure 3.9 shows the normalized damping ratio (i.e., with respect to RO water) as a function of frother concentration. A general observation is that both frothers show an initial drop in the damping ratio followed by a plateau before a further decrease above a certain concentration. There are some differences in magnitude, however, the F150 producing a larger overall decrease in damping ratio than DF250; for example, the initial decrease is about 9% for DF250 and about 24% for F150.

Figure 3.10 shows the damping ratio versus the bubble size determined acoustically. For both frothers it can be seen that the damping ratio is generally associated with the bubble size, the smaller the bubble the lower the damping ratio.

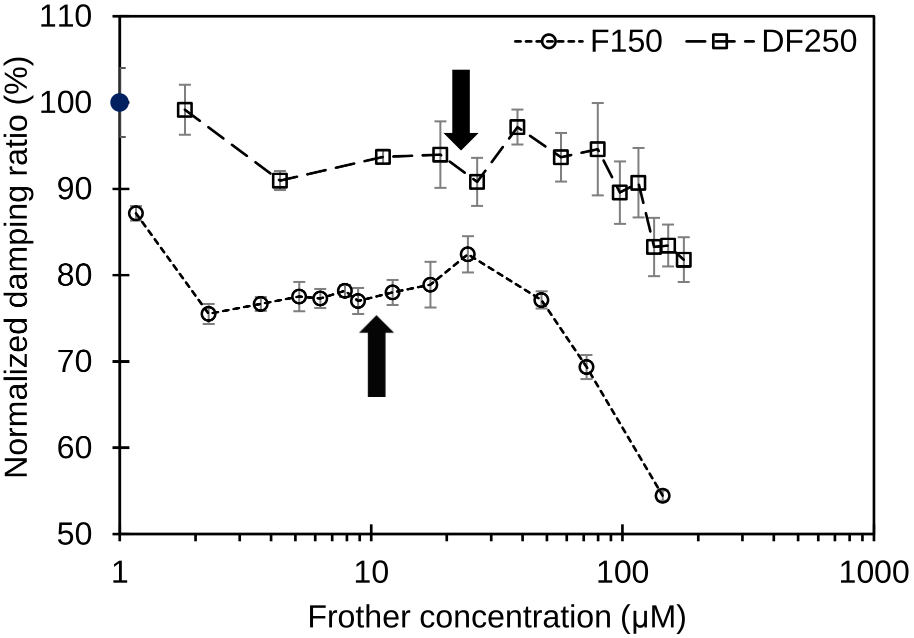

Figure 3.9 Normalized damping ratio (i.e., damping ratio relative to that of RO water) as a function of the frother concentration. The arrows indicate the concentration at which the frequency starts to significantly increase from Figure 3.8.

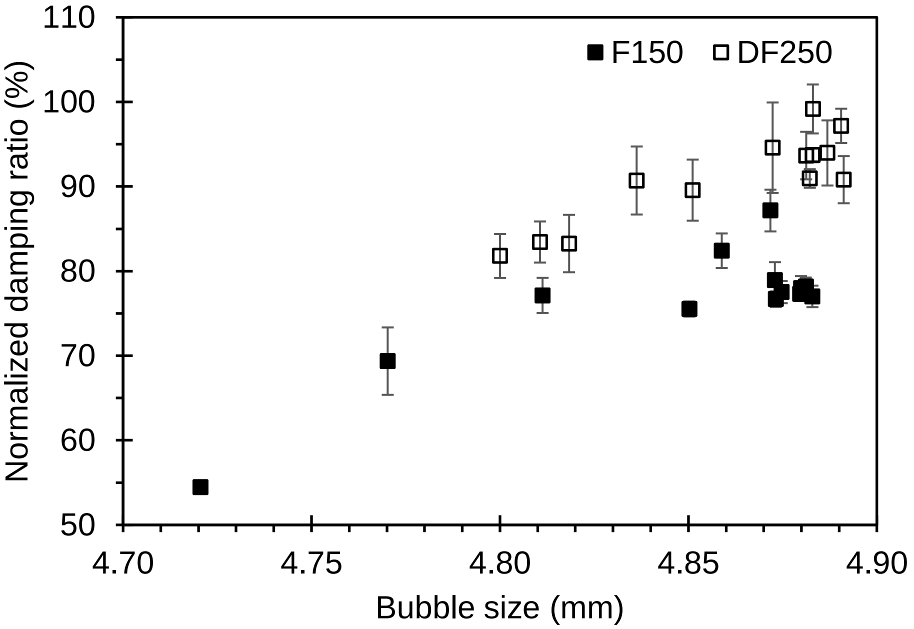

Figure 3.10 Normalized damping ratio as a function of bubble size predicted by the acoustic technique

3.5 Discussion

The experiment has exploited a passive acoustic technique to determine the effect of frothers on bubble break-away at a capillary, findings aimed to inform the impact of frothers on formation of bubbles by break-up of an air mass in flotation machines. The approach was augmented by image analysis. It is shown that the frequency and the damping ratio of the emitted acoustic signal do respond to the presence of frothers.

The acoustic signal was fitted with a sinusoidal decay function to estimate the frequency and damping ratio. From the frequency, bubble size was predicted using the Minnaert relationship. Albeit there was a consistent offset between the predicted and visually estimated size, both showed the same trend, initially little change followed by a decrease with increasing frother concentration. Over the tested frother concentrations, the variation in the bubble size (from the acoustic technique and imaging) is small (ca. 4% decrease from 0 to 144.4 μM for F150, and 2% from 0 to 175.1 μM for DF250). This is consistent with the observation of Hernandez-Aguilar et al. (2006). They further concluded that the impact of frother on reducing the bubble size cannot be explained solely by the decrease in equilibrium surface tension even under quasi-static conditions. One reason may be that equilibrium is still not attained, but there could be others. For instance, Blanchard and Syzdek (1977) proposed that the formation of a neck immediately before break-way can affect the air volume departing with the bubble hence altering the produced bubble size. Lin et al. (1994) postulated that the degree of wetting modifies the size of the neck. While F150 and DF250 are not expected to alter surface properties by adsorbing at the capillary (Hernandez-Aguilar et al., 2006), they will modify the air/water interface by H-bonding with water molecules (Gélinas et al., 2005) which may affect the degree of wetting and subsequently the size of the neck.

To achieve equilibrium as the growing bubble surface expands requires a uniform frother surface concentration and that can only be maintained if the adsorption rate keeps up. Arguing this is not the case, the corollary is that surface tension gradients exist. These gradients affect the dynamics at the bubble surface that influence the pressure gradients in the surrounding liquid. The hydrophone, essentially a sensitive pressure transducer, is able to detect these pressure changes. Since the surface tension gradients may either promote or dampen perturbations on the bubble surface (Miller and Neogi, 1985), this makes the damping ratio of the acoustic wave a potentially valuable measure.

The damping ratio describes the rate at which a system returns to its equilibrium state. For example, a system with a large damping ratio would achieve the equilibrium state faster because the system has a high energy dissipation rate. The current results show that the acoustic damping ratio, for both frothers, generally decreases as the frother concentration is increased, implying the acoustic wave energy dissipates at a lower rate when subjected to increasing frother concentration. Similar to the bubble size, the trend in the damping ratio cannot be explained by equilibrium surface tension. Figure 3.11 conveys this idea by noting the trends for the two frothers are not unified. More importantly, the question is how does the frother alter the acoustic damping ratio? The following proposes a mechanism.

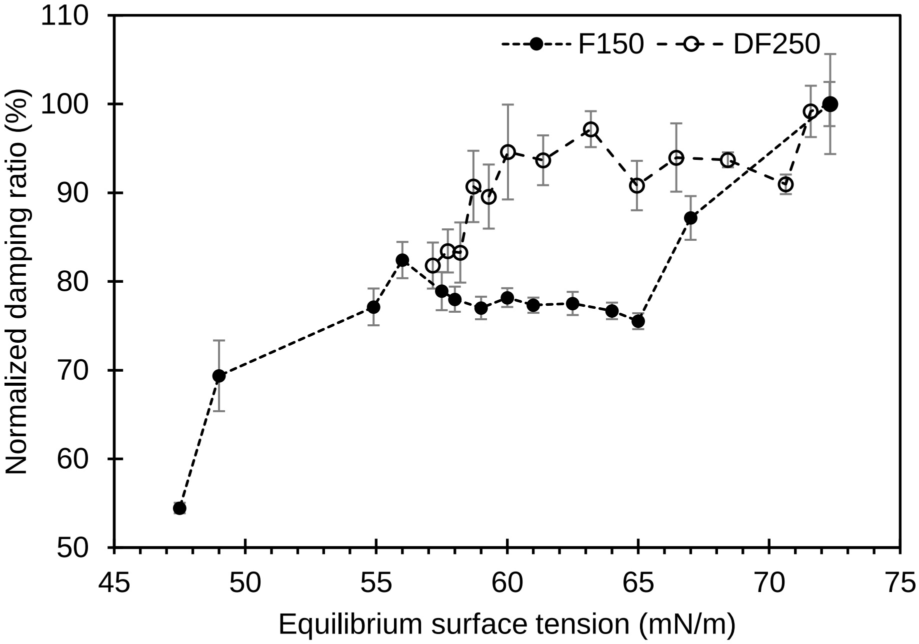

Figure 3. 11 Normalized damping ratio as a function of equilibrium surface tension. Surface tension data was adapted from Hernandez-Aguilar et al. (2006) for DF250 and Bournival and Ata (2014) for F150.

A bubble emerging from a capillary breaks away when its volume is maximum. Just prior to break-away, the bubble is held by a neck which rapidly thins as the volume grows.

During this thinning process, the liquid surrounding the neck moves inwards toward the axis of symmetry. At the instant of break-away an axial liquid jet forms which travels extremely fast upwards into the bubble to compensate for the inward liquid flow toward the axis. This liquid jet is postulated to play a role in the stimulating the acoustic emission (Leighton, 1994; Longuet-Higgins et al., 1991).

The liquid jet was found for all tested conditions. Interestingly, the initial velocity and maximum height of the jet seem to be independent of the addition of the frothers, consistent values of 148 mm/s and 1.11 mm, respectively, being recorded. Additionally, all the liquid jets reached the same maximum height at 0.5 ms after break-away, during which time the bubbles remained almost stationary. The presence of frother, however, does affect the subsequent processes as the liquid jet decays. From the high speed imaging results (Figure 3.5), it can be seen that the surface wave attributed to the decay of the liquid jet is damped by the addition of frother. A plausible explanation is the frothers produce surface tension gradients which act to suppress the surface wave, a known effect of surfactants (Davies and Vose, 1965). The current observation that damping of surface wave increases as frother concentration increases hints that this is through generation of surface tension gradients.

The liquid jet is thus associated with two mechanisms, acoustic emission and development of a surface wave (or capillary wave). Both mechanisms can be understood from an energy perspective. A freshly formed bubble can be considered as an isolated system that is excited by an external energy source. This energy takes the form of a liquid jet which is independent of the presence of frother (type or concentration). Once it rams the bubble, the bubble must act to dissipate the associated energy. From the observations here, the action seems to be related to the volume oscillation reflected in the acoustic emission, and the surface oscillation manifested as the capillary wave. Thermal dissipation is also possible but it is likely a small contributor that can be neglected (the temperature of the solution did not show any variation during the experiment).

Analogous to the acoustic wave, the capillary wave can also be envisaged as a damped system. The high speed imaging results (Figure 3.5) show that at higher frother concentration the capillary wave not only has a smaller size but also seems to dissipate more quickly, suggesting the system has a large damping ratio. The influence of this large damping ratio is more evident in the damping of the shape oscillation as the bubble starts to rise (i.e., Figure 3.6). This is consistent with the aforementioned work of Ata (2008) and Bournival et al. (2014) who also found the addition of frothers increases the damping ratio of the surface oscillation.

The opposite trends in damping of the two mechanisms with increasing addition of frother (i.e., damping decreases for the acoustic emission and increases for the capillary wave) can be explained by the law of conservation of energy. In the present case, the amount of energy associated with the liquid jet is always the same because the liquid jet always travels at the same initially velocity and reaches the same maximum height within the same timeframe. Thus when energy dissipation of the capillary wave accelerates, i.e., shows a larger damping ratio, that of the acoustic emission must correspondingly decrease, i.e., give a smaller damping ratio.

Figure 3.10 shows the acoustic damping ratio is associated with the bubble size. Without considering the effect of frother, the general observation is that a smaller bubble is usually allied with a smaller acoustic damping ratio. This corresponds to the experience that smaller bubbles tend to be more spherical implying their surface is less flexing. In other words, the capillary wave on the surface of a small bubble has a large damping ratio. Figure 3.10, therefore, offers support for the interpretation of the acoustic results.

The results also indicate that variation of the acoustic damping ratio depends on the frother type. Figures 3.9 and 3.10 show that F150 always contributes a larger decrease in the acoustic damping ratio than DF250, suggesting it has a more significant effect on increasing the damping ratio of the capillary wave; that is, F150 gives a smoother bubble surface as seen in Figure 3.8. The F150 having a longer chain than DF250 is considered more surface active producing larger surface tension gradients that are more efficient in suppressing the capillary wave (Chu et al., 2016).

3.6 Conclusions

A passive acoustic technique has been established to study the impact of frother on bubble break-away at a capillary. It was demonstrated that the acoustic frequency and acoustic damping ratio depend on frother type and concentration. The findings suggest that these two acoustic characteristics are associated with a liquid jet which initially excites the bubble then decays to form a surface wave. The presence of frother did not affect the initial energy of the jet but did increase its decay rate and dampen the surface wave. The frother action is interpreted as resulting from an effect on the magnitude of surface tension gradients. The acoustic damping ratio offers a new technique to study the role of frothers in bubble formation.

References

Acuña, C.A., Nesset, J.E., Finch, J.A., 2007. Impact of frother on bubble production and behaviour in the pulp zone, In Proceedings of the Sixth International Copper-Cobre Conference, ed. de Villar, R., Nesset, J.E., Gomez, C.O., Strading, A.W. MetSoc CIM, Toronto, Ont., pp. 197-210.

Aldrich, C., Feng, D., The effect of mothers on bubble size distributions in flotation pulp phases and surface froths. Minerals Engineering, 2000, 13(10–11), 1049-1057.

Ata, S., Coalescence of Bubbles Covered by Particles. Langmuir, 2008, 24(12), 6085-6091.

Blanchard, D., Syzdek, L., Production of air bubbles of a specified size. Chemical Engineering Science, 1977, 32(9), 1109-1112.

Blander, M., Katz, J.L., Bubble nucleation in liquids. AIChE Journal, 1975, 21(5), 833-848.

Bolaños-Jiménez, R., Sevilla, A., Martínez-Bazán, C., Gordillo, J.M., Axisymmetric bubble collapse in a quiescent liquid pool. II. Experimental study. Physics of Fluids, 2008, 20(11), 112104.

Bournival, G., Ata, S., Karakashev, S. I. and Jameson, G. J., An investigation of bubble coalescence and post-rupture oscillation in non-ionic surfactant solutions using high-speed cinematography. Journal of Colloid and Interface Science, 2014, 414, 50-58.

Chu, P., Waters, K.E., Finch, J.A., Break-up in formation of small bubbles: Comparison between low and high frother concentrations. Minerals Engineering, 2016, 96–97, 15-19.

Davies, J.T., Vose, R.W., On the Damping of Capillary Waves by Surface Films. Proceedings of the Royal Society of London. Series A. Mathematical and Physical Sciences, 1965, 286(1405), 218-234.

Finch, J.A., Dobby, G.S., Column flotation: A selected review. Part I. International Journal of Mineral Processing, 1991, 33(1), 343-354.

Finch, J.A., Gelinas, S., Moyo, P., Frother-related research at McGill University. Minerals Engineering, 2006, 19(6–8), 726-733.

Finch, J.A., Nesset, J.E., Acuña, C., Role of frother on bubble production and behaviour in flotation. Minerals Engineering, 2008, 21(12–14), 949-957.

Gélinas, S., Finch, J.A., Gouet-Kaplan, M., Comparative real-time characterization of frother bubble thin films. Journal of Colloid and Interface Science, 2005, 291(1), 187-191.

Grau, R.A., Laskowski, J.S., Role of Frothers in Bubble Generation and Coalescence in a Mechanical Flotation Cell. The Canadian Journal of Chemical Engineering, 2006, 84(2), 170-182.

Gupta, A., Yan, D.S., Mineral Processing design and operations: an introduction. 2006, Elsevier, Amsterdam.

Hernandez-Aguilar, J.R., Cunningham, R., Finch, J.A., A test of the Tate equation to predict bubble size at an orifice in the presence of frother. International Journal of Mineral Processing, 2006, 79(2), 89-97.

Javor, Z., Schreithofer, N., Comez, C.O., Finch, J.A., Heiskanen, K., 2013. Effect of scale dependent dynamic properties on bubble size, In Materials Science and Technology, Montreal.

Keim, N.C., Perturbed breakup of gas bubbles in water: Memory, gas flow, and coalescence. Physical Review E, 2011, 83(5), 056325.

Kitchener, J.A., Cooper, C.F., Current concepts in the theory of foaming. Quarterly Reviews, Chemical Society, 1959, 13(1), 71-97.

Kracht, W., Finch, J.A., Bubble break-up and the role of frother and salt. International Journal of Mineral Processing, 2009a, 92(3–4), 153-161.

Kracht, W., Finch, J.A., Using sound to study bubble coalescence. Journal of Colloid and Interface Science, 2009b, 332(1), 237-245.

Leighton, T.G., The Acoustic Bubble. Academic Press, 1994. ISBN 0-12-441920-8.

Leighton, T.G., Fagan, K.J., Field, J.E., Acoustic and photographic studies of injected bubbles. European Journal of Physics, 1991, 12(2), 77.

Lin, J.N., Banerji, S.K., Yasuda, H., Role of Interfacial Tension in the Formation and the Detachment of Air Bubbles. 1. A Single Hole on a Horizontal Plane Immersed in Water. Langmuir, 1994, 10(3), 936-942.

Longuet-Higgins, M.S., Kerman, B.R., Lunde, K., The release of air bubbles from an underwater nozzle. Journal of Fluid Mechanics, 1991, 230, 365-390.

Machon, V., Pacek, A.W., Nienow, A.W., Bubble Sizes in Electrolyte and Alcohol Solutions in a Turbulent Stirred Vessel. Chemical Engineering Research and Design, 1997, 75(3), 339-348.

Miller, C.A., Neogi, P., 1985. Interfacial phenomena: equilibrium and dynamic effects, pp. 240-298.

Napier-Munn, T., Wills, B.A., Wills' mineral processing technology: An introduction to the practical aspects of ore treatment and mineral recovery. 2006, Elsevier.

Strasberg, M., Gas Bubbles as Sources of Sound in Liquids. The Journal of the Acoustical Society of America, 1956, 28(1), 20-26.

Sweet, C., van Hoogstraten, J., H., M., Laskowski, J.S., 1997. The effect of frothers on bubble size and frothability of aqueous solutions, In 2nd UBC-McGill Symposium Series on Fundemental in Mineral Processing, ed. Finch, J.A., Rao, S.R., Holubec, I. The Metallurgical Society of CIM, pp. 235-246.

Talanquer, V., Oxtoby, D.W., Nucleation of bubbles in binary fluids. The Journal of Chemical Physics, 1995, 102(5), 2156-2164.

CONNECTING PARAGRAPH: CHAPTER 3 TO CHAPTER 4

Chapter 3 investigated the effect of frothers on bubble break-away in a quasi-static condition. With the use of the established acoustic technique and high speed cinematography, the study demonstrated that frothers do affect the break-away process. To make the case more analogous to flotation, a break-up process under turbulent conditions is targeted. This is the subject of Chapter 4.

CHAPTER 4 BREAK-UP IN FORMATION OF SMALL BUBBLES: BREAK-UP IN A CONFINED VOLUME

4.1 Introduction

Froth flotation is a process that separates valuable mineral particles from gangue minerals by attachment to air bubbles, a process that depends on differences in particle hydrophobicity. Small bubbles (ca. 1 mm) play a key role as they comprise the bubble swarms that provide the large interfacial area for collecting and transporting the selected mineral particles. The generation of fine bubbles can be viewed as a chemically assisted physical process where surfactants (frothers) are added to modify the bubble formation process. The effect of frothers on reducing bubble size is well known, but their detailed action remains obscure (Finch, 2008).

There are suggestions that frother action is related to surface tension reduction (Gupta and Yan, 2006), but experiments fail to support such a connection (Aldrich and Feng, 2000; Machon et al., 1997; Sweet et al., 1997). A common explanation is coalescence prevention (Harris, 1976; Pugh, 1996). On this basis, Cho and Laskowski (2002), noting that bubble size in a swarm reached a minimum at a particular concentration, argued that this concentration corresponded to complete suppression of coalescence and introduced the term critical coalescence concentration (CCC). By bringing two bubbles into contact it can be readily demonstrated that frother does retard coalescence (Bournival and Ata, 2014; Cho and Laskowski, 2002). There are occasional references that frothers also aid in the break-up of the air mass injected into the machine (Acuña, 2007; Finch, 2006; Grau and Laskowski, 2006; Gupta and Yan, 2006).

Understanding the role of frother in bubble formation is pertinent to flotation theory and practice. The purpose of this paper is to determine the possible effect of frother on the break-up process. To begin, we introduce some background relevant to this break-up hypothesis.

4.1.1 Frothers

Frothers are a class of surface-active agents or surfactants. They are simple hetero-polar compounds, such as alcohols and polyglycols, that comprise hydrophilic (polar) and hydrophobic (non-polar) groups. The polar groups typically contain hydroxyl (-OH), carbonyl (-C=O) and ether linkages (-O); the non-polar groups are hydrocarbon chains of various lengths both straight chain and branched. Through the polar groups the frother molecule H-bonds with water molecules to become hydrated while there is practically no interaction with the non-polar groups (Wills and Finch, 2016). As a result, the frother molecule tends to accumulate at the air/water interface orientated with hydrophilic groups on the water side and the hydrophobic group on the air side thus satisfying both properties of the molecule.

Frothers lower surface tension. In most industrial flotation systems, frother concentration is about 5 – 10 ppm (parts per million), which, comparing to the surface tension of water, 72.8 mN/m, would cause a reduction of, at most, about 7% (Pugh, 2007). The presence of frothers also affects perturbations at the air/water interface. Some authors (Acuña et al., 2008; Sarma and Chattopadhyay, 2001) observing waves on a bubble surface suggested that the presence of frothers promoted a surface tension gradient driven stress, which interplays with the mechanical stress to de-stabilize the interface.

Reference to surface tension usually implies the ‘equilibrium’ or ‘static’ value. However, the conditions in flotation are dynamic, especially around the impeller region where the air mass breaks up and where frother must act to influence bubble formation.

4.1.2 Break-up

The break-up of an air mass in a turbulent environment is a complex phenomenon. Prior to break-up the air/water interface must deform. The deformation can take different forms depending on the hydrodynamic forces associated with the liquid flow patterns around the interface. Hinze (1955) suggested that interfacial instability, shown in Figure 4.1, is one of the ways that can perturb the air/water interface. In this case, the deformation occurs locally resulting in parts of the air mass separating. This process appears to be relevant to air beak-up in mechanical flotation machines.

The rotor-stator device in a mechanical flotation machine is responsible for dispersing air into bubbles (Laskowski, 2001; Schubert, 1999). The rotation of the impellers induces mechanical suction that draws the incoming air to the downstream side of the impeller blades where air-loaded cavitation occurs. This air cavity deforms rapidly due to shear with the fluid flow around it. At the trailing edge, the air/water interface interacts with local turbulent eddies causing interfacial instabilities. These subsequently grow and eventually break away to form bubbles (Crozier and Klimpel, 1989; Grainger-Allen, 1969). Figure 4.2 shows an example of such a process and mirrors the break-up by interfacial instabilities described in Hinze (Figure 4.1). It is suggested that the downstream side of other objects (named as impeller elements), such as the stator wall, bars, fingers, are also regions where air-loaded cavitation might occur (Rodgers and Cooke, 2012; Schubert, 1999).

Bubble formation is not limited to break-up of an air mass. A minor phenomenon, which is not the interest of this work, is the degasification of microbubbles. In this case, the small bubbles are produced due to the degasification of dissolved air, which is caused by the pressure difference across the upstream and downstream sides of an impeller object.

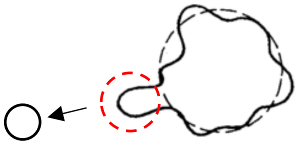

Figure 4.1 Disintegration of an air mass: Bulgy mechanism. Adapted from Hinze (1955)

Figure 4.2 Break-up of an air loaded cavitity behind an impeller object in a mechanical flotation machine. Adapted from Grainger-Allen (1969)

4.1.3 Role of frother on break-up

In recent work investigating a role of frother in break-up, Kracht and Finch (2009a) exposed a mono-size distribution of bubbles to a turbulent field generated by an impeller (Figure 4.3). It was observed that the presence of frother not only reduced coalescence but, they surmised, also had an effect on break-up by noting the increased fraction of bubbles at about 90% of (i.e., smaller than) the original volume. They developed a model relating uneven frother distribution on the stretching bubble prior to rupture to explain the effect of frother on bubble break-up. Javor et al. (2013) adopted the same technique and tested the effect of frother with different chain lengths. Their results indicate that with long chain frother the minimum bubble size created upon break-up of the air mass was smaller than with short chain frothers.

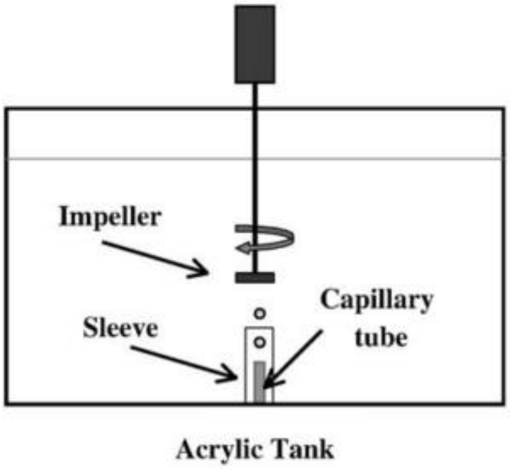

Figure 4.3 Experimental set-up of Kracht and Finch (2009a)

A drawback of the set-up in Figure 4.3 is that both break-up and coalescence can occur. The aim of the current work is to complement the work of Kracht and Finch (2009a) and Javor et al. (2013) by devising an experimental set-up to isolate break-up events from coalescence. In addition to frothers, the effect of the input mechanical energy and the volume of the air mass were also studied.

4.2 Experimental

4.2.1 Apparatus

The experimental set-up, shown in Figure 4.a, consists of four components: an 800 mL breaker with an inverted spoon (OD, 20 mm), a magnetic stirrer (Corning, PC-420D), a syringe pump (Fisher Scientific, 78-0100I) and a high speed camera (Fastec Imaging HiSpec5 8G Mono/Color).

Two stirring bars, 1 in. and 1.5 in., were used in this study and their rotational speed varied from 800 to 1100 RPM (revolutions per minute). There are two designs of spoon (same OD). One (Figure 4.c) has a solid handle and is used for experiments in the absence of frother. In this case, the air is injected through a tube directly into the spoon. The second design (Figure 4.d) has a hollow handle used for experiments with frother. This design allows the air mass to be continuously injected. The sealing of the air mass is by tightening a screw (not shown). Figure 4.b shows the initial state of a 2 mL air mass pocket.

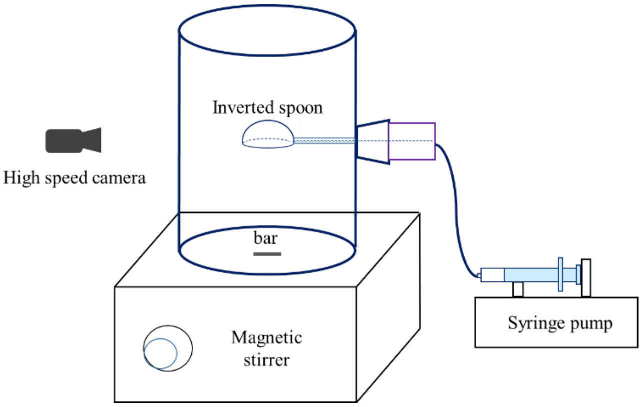

b) Initial state of an experiment

a) Set-up

c) Spoon with solid handle

d) Spoon with hollow handle

Figure 4.4 Apparatus

4.2.2 Procedure

The breaker was filled with 750 mL solution and placed on the magnetic stirrer. A known amount of air was injected. The stirrer was turned on to provide the mechanical energy. The rotation of the liquid causes a vortex that draws down air from the spoon forming a bulge. When sufficient energy input is reached, the bulge breaks away to form a bubble. To isolate break-up from coalescence, only the first bubble breaking away is considered. The digital high speed camera captured the bulging and breaking-away events. The image showing the newly formed bubble was processed (software ImageJ) to acquire the sphere-volume equivalent diameter, *d*, as depicted in Figure 4.5. This calculation uses the minor (a) and major (b) semi-axes of an ellipse to fit to the projected bubble area (Equation 4.1) and assumes the bubble to be symmetric about the minor axis.

$$\boldsymbol{d} = \sqrt[3]{(\boldsymbol{2a})^{2} \times (\boldsymbol{2b})} \qquad \text{Equation 4.1}$$

a) orignal image b) binary image c) image outline d) ellipse fitting

Figure 4.5 Image analysis procedure

4.2.3 Frothers tested

Using reverse osmosis (RO) water, frother solutions were prepared at room temperature (ca. 23 ^{o}C). Table 4.1 lists the frothers tested, one alcohol (MIBC) and two polyglycols. At least three replicate sets of experiments were conducted on each solution, each consisting of at least five bubble formation experiments. The experimental set-up was thoroughly rinsed with hot tap water followed by RO water between each set of experiments.

Table 4.1 Frothers and concentration range tested

Name	Formula	Molecular weight (g/mol)	Concentration range (mM)	Supplier
MIBC	$(CH_3)_2CHCH_2CH(OH)CH_3$	102.18	0 – 0.029	Aldrich
Dowfroth 250[a]	$CH_3(PO)_4OH$	264.35	0 – 0.026	Aldrich
Flottec 150	$H(PO)_7OH$	425	0 – 0.024	Flottec

[a] PO is propylene oxide (propoxy) [-O-CH_2-CH_2-CH_2-]

4.3 Results

Two types of results are shown: visual sequence of the bubble formation, and average bubble diameter.

4.3.1 Input mechanical energy

The variation of input mechanical energy was achieved by changing the size of the stirring bar (e.g*.,* torque) and the rotational speed (RPM). Figure 4.6 shows two sequences of images for bubble formation in RO water with 1 in. and 1.5 in. stirring bars, which indicates that bubble generation follows the sequence: formation of bulge, elongation of bulge, and bubble break-away. The 1.5 in. stirring bar created stronger turbulence than the 1 in bar, inducing significantly more distortion to the air/water interface and on average producing a larger bubble size.

The quantitative results are shown in Figure 4.7. For both stirring bars, the trend is similar, increasing RPM results in no significant impact on bubble size. Each stirring bar seems to create a unique bubble size: 1 in bar ca.1.23 mm and 1.5 in. bar ca*.* 1.72 mm. The large variation in results for 1.5 in. stirring bar (95% confidence interval on the mean) is likely due to the stronger turbulence.

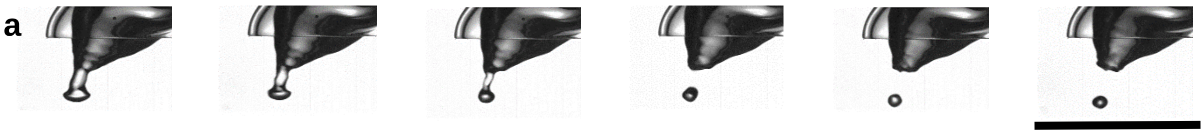

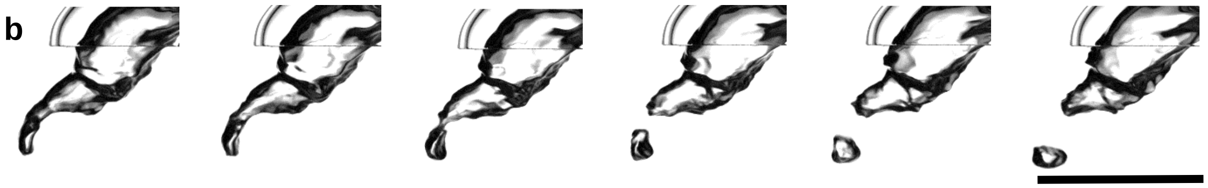

Figure 4.6 Sequence of images showing bubble formation (images 2 ms apart) in RO water at 900 RPM, 1.0 mL initial air (scale bar represents 20 mm): a) 1 in stirrer bar, b) 1.5 in stirrer bar

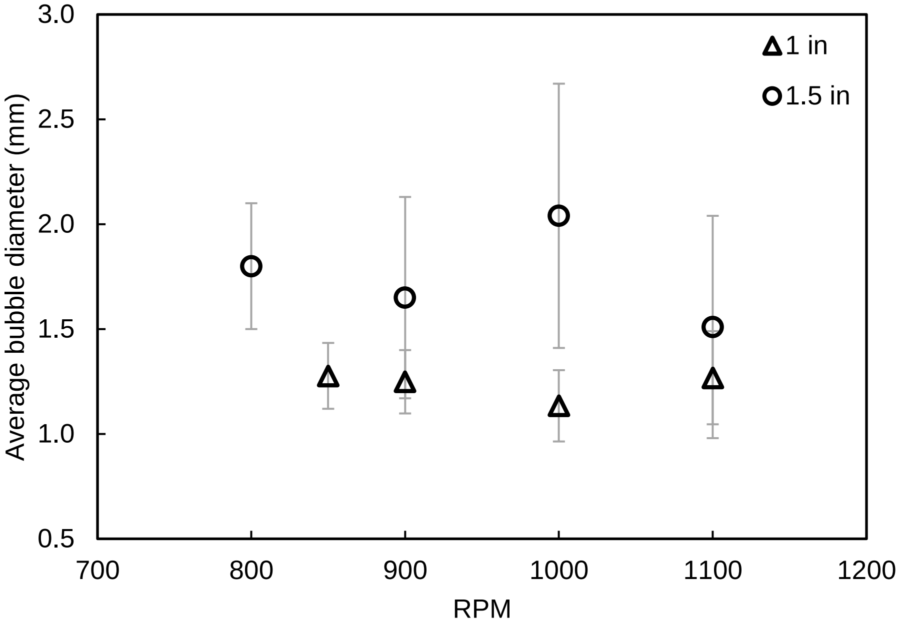

Figure 4.7 The effect of varying RPM: no frother, 1.0 mL initial air (bar is 95% C.I. on the mean)

4.3.2 Initial volume of the air mass

Figure 4.8 shows an example of bubble formation with a smaller initial air volume, 0.4 mL, with the 1.5 in. stirring bar at 900 RPM. The bubble formation sequence is similar, which remained the case when substituting the 1 in. stirring bar.

Similar to the effect of stirrer speed, Figure 4.9 suggests that the initial volume of the air mass is not a significant factor affecting the bubble size: The average bubble diameter remains essentially the same, apparently uniquely defined by the bar length, namely: 1 in. bar ca. 1.29 mm and 1.5 in. bar ca. 1.77 mm.

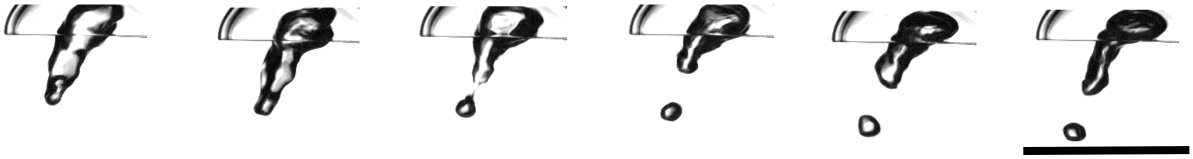

Figure 4.8 Sequence of images showing bubble formation in RO water: 0.4 mL air, 1.5 in. stirring bar rotating at 900 RPM (5 ms apart)

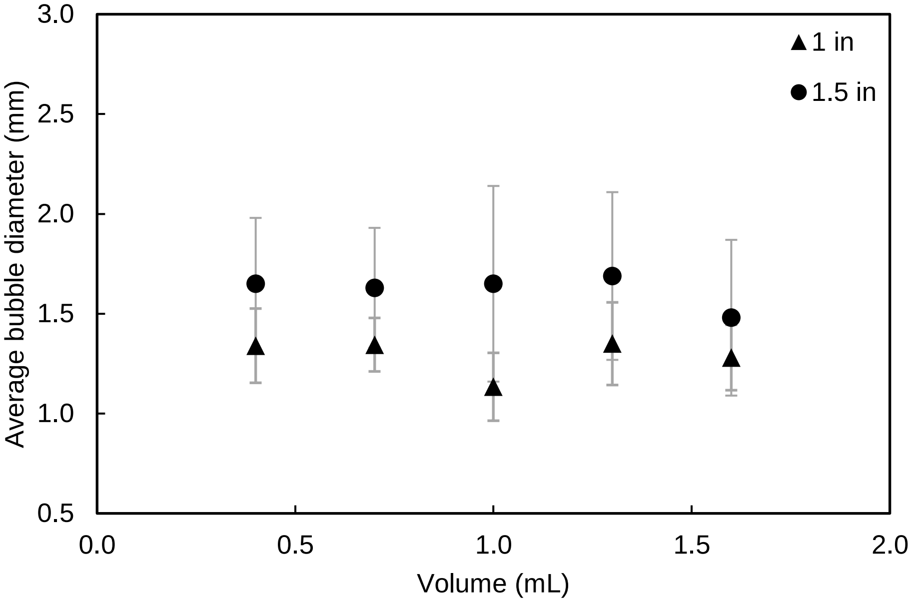

Figure 4.9 The effect of the initial air volume: 1 in. stirring bar rotating at 1000 RPM; 1.5 in. stirring bar rotating at 900 RPM

4.3.3 Frothers

The concentrations tested were chosen on the basis of common flotation practice (i.e. 5-10 ppm, but converted to molar basis). The spoon was that in Figure 4.3.c, agitation was by the 1.5 in. stirring bar at 900 RPM, and the initial air volume was 1.0 mL. Figure 4.10 shows bubble formation in the presence of 0.006 mM MIBC, which significantly altered the shape of the deformation bulge compared to RO water (Figure 4.5.b) and produced a smaller bubble.

Figure 4.10 Sequence of images showing bubble formation in MIBC solution at 0.006 mM (5 ms apart)

Figure 4.11 summarizes the result for all frothers tested. For the two polyglycol frothers, the bubble size gradually decreased with increasing concentration. The MIBC showed a different trend, initially decreasing sharply as concentration is increased then increasing above ca. 0.006 mM. Compared to the 1.90 mm bubble with zero frother (i.e*.*, RO water), the MIBC produced a minimum bubble diameter of ca*.* 1.12 mm, representing a 41% reduction, while for DF250 and F150, the smallest bubble reached was ca*.* 1.56 mm (18% reduction) and ca*.*1.34 mm (30%), respectively.

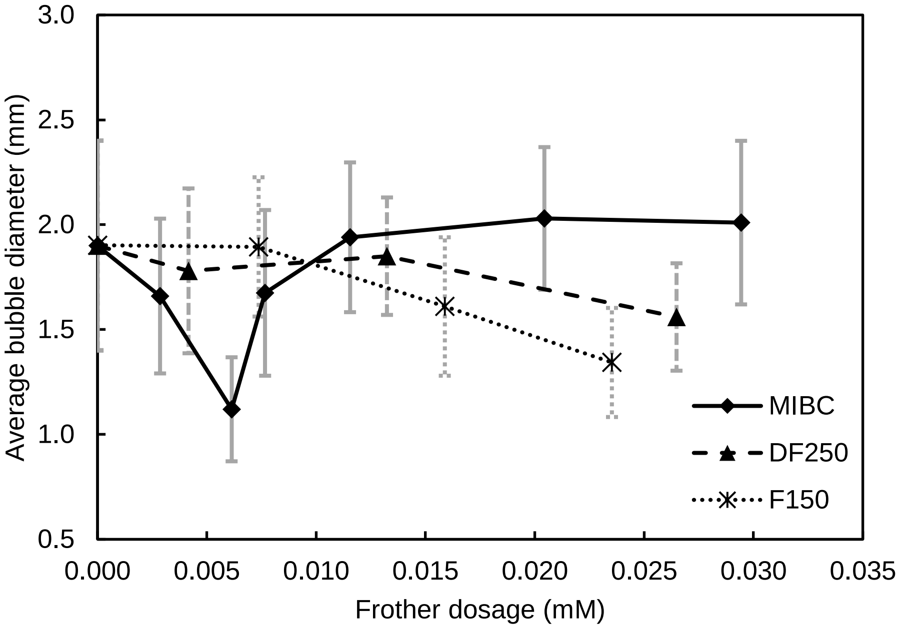

Figure 4.11 The effect of frothers: 1.5 in. stirring bar rotating at 900 RPM, 1.0 mL initial air

4.4 Discussion

The experimental technique simulates the break-up of the air mass in the cavity trailing the impeller of a mechanical flotation machine. In the absence of frother the results demonstrate that the size of bubble produced by break-up was affected by the size of the element (stirrer bar) producing the turbulence but not by the input mechanical energy for a given stirrer bar (i.e., stirrer speed), or the volume of the air mass. The effect of the size of the stirrer bar suggests an impact of geometry rather than mechanical energy, the counterpart in an industrial setting being the size of the impeller relative to the size of the cell. The lack of effect of input mechanical energy for a given stirrer size has its counterpoint in results for a pilot scale mechanical flotation machine that showed bubble size was little affected by impeller speed over a practical range (Amini and Bradshaw, 2013; Nesset, 2007). The lack of effect of initial air mass is perhaps surprising at it represents different energy input per unit mass which suggests an impact on bubble size. The counterpart in industrial flotation cells is an increase in air rate which in that case usually increases bubble size. The lack of air volume effect here may be related to the observed limited effect of mechanical energy input or the relatively small range of the tested air volume.

The above studies were antecedent to the main focus, the role of frother in break-up, but do indicate the important factors to hold constant in order to reveal the frother effect. In general, the presence of frother produced smaller bubbles compared to water alone. The results support those of Kracht and Finch (2009a) and Javor et al. (2013) but has removed the potential confounding effect of coalescence.

As a pure liquid (i.e., no solutes added), water is not an easy medium in which to generate small bubbles because of the high surface energy (compared to most room temperature pure liquids) (Blander and Katz, 1975; Talanquer and Oxtoby, 1995). The effect of frother can be viewed as an additional break-away energy to the mechanical energy. This additional energy, it is argued, derives from surface tension gradients that occur in the presence of frothers upon surface deformation.

Figure 4.12 illustrates a possible mechanism. The initial situation, that is, the undisturbed pocket of air, can be represented as a surface with frother uniformly distributed (Fig, 4.12.a). If, upon disturbance, the deformation rate of the air/interface is higher than the mass transfer rate of frother molecules to the interface, the local increase in surface area results in a local decrease in frother concentration (Figure 4.12.b). The decrease in frother concentration at the bulge means an increase in local surface tension compared to the neck of the bulge. The difference in surface tension creates a force directed towards the region of higher surface tension (Figure 4.12); or a surface tension-driven stress (Maldarelli and Jain, 1988). This stress is the source of the additional energy that promotes break away from the bulge. The additional energy means less mechanical energy is required and thus a bubble breaks away from the bulge before growing to the same extent as in the absence of frother; that is, a smaller bubble is formed.

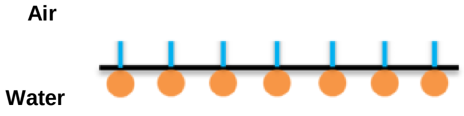

a) Initial situation: uniform distribution of frother on an undisturbed interface

b) Surface perturbation causes local decrease in frother concentration at the bulge with corresponding increase in surface tension

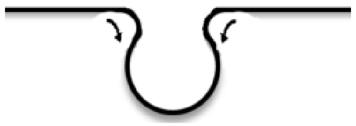

c) Stress driven by surface tension gradients adds to mechanical stress causing break-away

Figure 4.12 A possible mechanism explaining break-away in the presence of frothers

An argument based on generation of surface tension gradients means a dependence on the mass transfer rate of frother molecules to the air/water interface. Mass transfer rate will depend on molecule size, its interaction with water molecules, and the bulk concentration. If the mass transfer rate keeps up with the deformation rate of the interface, there will be no local concentration gradients along the interface and therefore no surface tension gradients. In such cases, the bubble size should not be affected. The result for MIBC, where the bubble size passes through a minimum and returns to the size in its absence (Figure 4.11), hints at this idea. Compared to the polyglycols, the MIBC molecule is smaller and has fewer hydrophilic sites to H-bond with water molecules (Table 4.1) and consequently is expected to have a higher mass transfer rate. Further investigation on this interpretation will be conducted.

The discussion above has some cross-over to the industrial setting. In a mechanical flotation machine bubble production is due to the break-up of the injected air mass behind the impeller elements (Grainger-Allen 1969; Harris 1976). The system turbulence deforms the air mass causing interfacial instabilities at the trailing edge. The presence of frother causes surface tension gradients which enhance the production of interfacial instabilities. For a given input rate of air, the more interfacial instabilities mean more and thus smaller bubbles will break off. A difference is that unlike the current experiment the air/water interface of the air mass behind the impeller elements is not in equilibrium with the solution; that is, the assumption of initial uniform frother distribution at the interface (Figure 4.12.a) is not the case. Nevertheless, it is plausible to argue that the random distribution of frother molecules in solution will generate the surface concentration variation depicted in Figure 4.12.b, at least for some bulges . The same argument will also mean some cases where frother is concentrated by chance at the neck of the bulge and the surface tension gradient will oppose break-away, but even if this is the majority of the cases it still means, on average, that frother assists break-away.

The latter possibility, that is, surfactants acting to dampen air/water interfacial instabilities, is perhaps the more common experience (Hühnerfuss et al., 1985; Lemaire and Langevin, 1992; Lucassen, 1982; Miller and Neogi, 1985). Which occurs, promotion or suppression of instabilities, may depend on the intensity of the disturbance: minor disturbance (minor deformation) and surface tension gradients oppose growth of the deformation; major disturbance, and the gradients make the deformation grow. The level of the turbulence in the current experimental set-up is evidently sufficient that surface tension gradients promote break-up, which can also be anticipated in mechanical flotation machines.

The viewpoint of our interpretation is based on surface tension gradients affecting surface deformation, but the literature lacks direct experimental evidence to support their presumed impact. It remains surprising that the process of small bubble production in presence of frothers, which is vital to industrial flotation, continues to defy an accepted explanation. Our speculation based on surface tension gradients invites other possibilities.

4.5 Conclusions

Break-up of an air mass trapped in a confined volume, mimicking bubble production in the cavity behind an impeller element in mechanical flotation machines, was investigated. It was demonstrated that break-up was affected by the presence of frothers but not by the input mechanical energy and the initial volume of the air mass. Break-up in the presence of frothers generally produces smaller bubble size compared to water alone. A mechanism based on frother-induced surface tension gradient-driven stresses that add to the mechanical stress to promote break-up is advanced. The mechanism is used to explain why for MIBC the size of bubble passes through a minimum as concentration is increased.

References

Acuña, C.A., Nesset, J.E., Finch, J.A., 2007. Impact of frother on bubble production and behaviour in the pulp zone, In Proceedings of the Sixth International Copper-Cobre Conference, ed. de Villar, R., Nesset, J.E., Gomez, C.O., Strading, A.W. MetSoc CIM, Toronto, Ont., pp. 197-210.

Acuña, C.A., Radman, J., Finch, J.A., Measurement of flow visualized on surface of bubble blown in air. Colloids and Surfaces A: Physicochemical and Engineering Aspects, 2008, 330(2–3), 112-115.

Aldrich, C., Feng, D., The effect of mothers on bubble size distributions in flotation pulp phases and surface froths. Minerals Engineering, 2000, 13(10–11), 1049-1057.

Amini, E., Bradshaw, D.J., Finch, J. A. and Brennan, M., Influence of turbulence kinetic energy on bubble size in different scale flotation cells. Minerals Engineering, 2013, 45, 146-150.

Blander, M., Katz, J.L., Bubble nucleation in liquids. AIChE Journal, 1975, 21(5), 833-848.

Bournival, G., Ata, S., Karakashev, S. I. and Jameson, G. J., An investigation of bubble coalescence and post-rupture oscillation in non-ionic surfactant solutions using high-speed cinematography. Journal of Colloid and Interface Science, 2014, 414, 50-58.

Cho, Y.S., Laskowski, J.S., Bubble coalescence and its effect on dynamic foam stability. The Canadian Journal of Chemical Engineering, 2002, 80(2), 299-305.

Crozier, R.D., Klimpel, R.R., Frothers: Plant Practice. Mineral Processing and Extractive Metallurgy Review, 1989, 5(1-4), 257-279.

Finch, J.A., Gelinas, S., Moyo, P., Frother-related research at McGill University. Minerals Engineering, 2006, 19(6–8), 726-733.

Finch, J.A., Nesset, J.E., Acuña, C. A., Role of frother on bubble production and behaviour in flotation. Minerals Engineering, 2008, 21(12–14), 949-957.

Grainger-Allen, T.J.N., Bubble Generation in Froth Flotation Machines. 1969, Warren Spring Laboratory.

Grau, R.A., Laskowski, J.S., Role of Frothers in Bubble Generation and Coalescence in a Mechanical Flotation Cell. The Canadian Journal of Chemical Engineering, 2006, 84(2), 170-182.

Gupta, A., Yan, D.S., Mineral Processing design and operations: an introduction. 2006, Elsevier, Amsterdam.

Harris, C., Flotation machines. Flotation, A. M. Gaudin Memorial Volume, 1976, 2, 753-815.

Hinze, J.O., Fundamentals of the hydrodynamic mechanism of splitting in dispersion processes. AIChE Journal, 1955, 1(3), 289-295.

Hühnerfuss, H., Lange, P.A., Walter, W., Relaxation effects in monolayers and their contribution to water wave damping: I. Wave-induced phase shifts. Journal of Colloid and Interface Science, 1985, 108(2), 430-441.

Javor, Z., Schreithofer, N., Comez, C.O., Finch, J.A., Heiskanen, K., 2013. Effect of scale dependent dynamic properties on bubble size, In Materials Science and Technology, Montreal.

Kracht, W., Finch, J.A., Bubble break-up and the role of frother and salt. International Journal of Mineral Processing, 2009, 92(3–4), 153-161.

Laskowski, J.S., 2001. Chapter 8 Flotation machines, In Developments in Mineral Processing. Elsevier, pp. 225-262.

Lemaire, C., Langevin, D., Longitudinal surface waves at liquid interfaces: Measurement of monolayer viscoelasticity. Colloids and Surfaces, 1992, 65(2–3), 101-112.

Lucassen, J., Effect of surface-active material on the damping of gravity waves: A reappraisal. Journal of Colloid and Interface Science, 1982, 85(1), 52-58.

Machon, V., Pacek, A.W., Nienow, A.W., Bubble Sizes in Electrolyte and Alcohol Solutions in a Turbulent Stirred Vessel. Chemical Engineering Research and Design, 1997, 75(3), 339-348.

Maldarelli, C., Jain, R.K., The hydrodynamic stability of thin films. 1988, Marcel Dekker, New York.

Miller, C.A., Neogi, P., 1985. Interfacial phenomena: equilibrium and dynamic effects, pp. 240-298.

Nesset, J.E., Finch, J.A., Comez, C.O., 2007. Operating variable affecting the bubble size in forced-air mechanical flotation machines, In AusIMM 9th Mill Operators' Conference, Fremantle, Australia, pp. 66-75.

Pugh, R.J., Foaming, foam films, antifoaming and defoaming. Advances in Colloid and Interface Science, 1996, 64(0), 67-142.

Pugh, R.J., 2007. The physics and chemistry of frothers, In Froth Flotation: A Century of Innovation, eds. Fuerstenau, M.C., Jameson, G.J., Yoon, R.H. Society for Mining, Metallurgy, and Exploration, pp. 259-282.

Rodgers, T.L., Cooke, M., Rotor–stator devices: The role of shear and the stator. Chemical Engineering Research and Design, 2012, 90(3), 323-327.

Sarma, T.K., Chattopadhyay, A., Simultaneous Measurement of Flowing Fluid Layer and Film Thickness of a Soap Bubble Using a UV−Visible Spectrophotometer. Langmuir, 2001, 17(21), 6399-6403.

Schubert, H., On the turbulence-controlled microprocesses in flotation machines. International Journal of Mineral Processing, 1999, 56(1–4), 257-276.

Sweet, C., van Hoogstraten, J., H., M., , Laskowski, J.S., 1997. The effect of frothers on bubble size and frothability of aqueous solutions, In 2nd UBC-McGill Symposium Series on Fundemental in Mineral Processing, ed. Finch, J.A., Rao, S.R., Holubec, I. The Metallurgical Society of CIM, pp. 235-246.

Talanquer, V., Oxtoby, D.W., Nucleation of bubbles in binary fluids. The Journal of Chemical Physics, 1995, 102(5), 2156-2164.

Wills, B.A., Finch, J.A., 2016. Chapter 12 - Froth Flotation, In Wills' Mineral Processing Technology (Eighth Edition), ed. Finch, B.A.W.A. Butterworth-Heinemann, Boston, pp. 265-380.

CONNECTING PARAGRAPH: CHAPTER 4 TO CHAPTER 5

Chapter 4 established an experimental technique to isolate break-up from coalescence in the formation of bubbles. The set-up mimics the break-up of the air-filled cavity behind an impeller blade in a mechanical cell. The study showed the break-up is affected by the presence of frothers, but weakly by the input mechanical energy and the initially trapped air volume. An argument based on frother introducing surface tension gradients was proposed to explain the findings. The generation of surface tension gradients assumes that frother concentration is not sufficient to maintain a uniform surface concentration. Based on this, a hypothesis is that with adequate frother concentration a uniform surface concentration can be maintained during incipient bubble formation. If so, at high enough frother concentration the effect of frother on decreasing bubble size should be lost. Chapter 5 tests this hypothesis.

CHAPTER 5 BREAK-UP IN FORMATION OF SMALL BUBBLES: COMPARISON BETWEEN LOW AND HIGH FROTHER CONCENTRATIONS

5.1 Introduction

Frothers in flotation help reduce bubble size. The concentrations required are remarkably small, just are a few ppm, that is, a few grams per tonne of water (Wills and Finch, 2016). However, the controlling mechanism is not well understood (Finch et al., 2008). The action of frother is often ascribed to surface tension reduction (Gupta and Yan, 2006), but experiments do not support such a connection, at least with the equilibrium (or static) surface tension (Aldrich and Feng, 2000; Grau and Laskowski, 2006; Machon et al., 1997; Sweet et al., 1997).

Generation of bubbles in a flotation machine is the result of two complementary mechanisms, namely, break-up and coalescence. Most literature on the role of frother is based on coalescence inhibition (Harris, 1976; Laskowski, 2003a). Cho and Laskowski (2002) introduced the term "critical coalescence concentration" (CCC) to describe the concentration when minimum bubble size in a swarm is reached. Table 5.1 lists the CCC95 (i.e., the concentration giving 95% reduction in bubble size relative to water alone) of some frothers under typical flotation conditions, confirming the low concentration required.

Table 5.1 – CCC95 of typical frothers, adapted from Nesset (2007)

Frother	Formula	CCC95 (ppm)	CCC95 (mM)
MIBC	$(CH_3)_2CHCH_2CH(OH)CH_3$	10.4	0.102
DF250[a]	$CH_3(PO)_4OH$	8.4	0.032
F150[a]	$H(PO)_7OH$	3.7	0.0087

[a] PO is propylene oxide (propoxy) [$-O-CH_2-CH_2-CH_2-$]

Experiments, such as bringing two bubbles together, have confirmed the role of frother in coalescence prevention (e.g., Bournival et al., 2014). There are occasional references that the frother also acts to promote break-up (Acuña, 2007; Finch et al., 2006; Grau and

Laskowski, 2006). Kracht and Finch (2009a) investigated the effect of frother on break-up by exposing mono-sized bubbles to a turbulent field generated by an impeller. They observed that frother not only reduced coalescence but also promoted break-up, noting that the fraction of bubbles within 90% of the original volume increased. Javor et al. (2013) adopted the same technique and tested the effect of frother with different chain lengths. Their conclusion was that with the long chain frothers the minimum bubble size on break-up is smaller than with the short chain frothers.

Coalescence and break-up generally take place simultaneously. To eliminate the impact of the former, Chu and Finch (2013; 2014) developed an experimental set-up and procedure to mimic single bubble formation at the break-up stage. The results revealed that the presence of frother produces smaller bubble sizes compared to water alone. They proposed an explanation based on the Marangoni effect, that frothers introduce a surface tension gradient-driven stress, which increases instabilities along the air/water interface: increasing the number of instabilities along the surface of a finite volume of air means that more small bubbles will break off.

The development of surface tension gradients may depend on two important processes. Stone and Leal (1990) conducted numerical simulation on the effects of surfactants on drop break-up. They suggested that the competition between convection of the surfactant, which lowers interfacial tension, and dilution of the surfactant due to rapid increase of interfacial area, determines the formation of the local instability. Based on this, one can postulate that in the case of air bubbles break-up in frother solution the formation of surface tension gradients could relate to the bulk frother concentration. If the bulk frother concentration is not sufficient to restore concentration uniformity at the air/water interface over the time involved in the break-up process, there will be surface tension gradients. The corollary is that sufficient frother concentration may equalize the competition between convention and dilution of the frother molecules at the interface, and hence damps surface tension gradients and does not contribute to bubble formation.

The purpose of this paper is to test the effect of increasing frother concentration on the bubble size formed at break-up. The hypothesis is that there may exist a critical bulk concentration above which surface tension gradients are lost such that the effect of frother on bubble size at break-up diminishes.

5.2 Experimental

5.2.1 Set-up

The experimental set-up adopted is that of Chu and Finch (2013; 2014). Figure 5.1.a shows the main components: an 800 mL beaker with a custom-made glass spoon to accommodate a known volume of air (the ‘air pocket’); a magnetic stirrer (Corning, PC-420D); and a syringe pump (Fisher Scientific, 78-0100I). The spoon, with an inner diameter of 20 mm, is connected to the syringe pump through a hollow handle and plastic tubing. Figure 5.1.b shows the initial state of a 2 mL-air pocket.

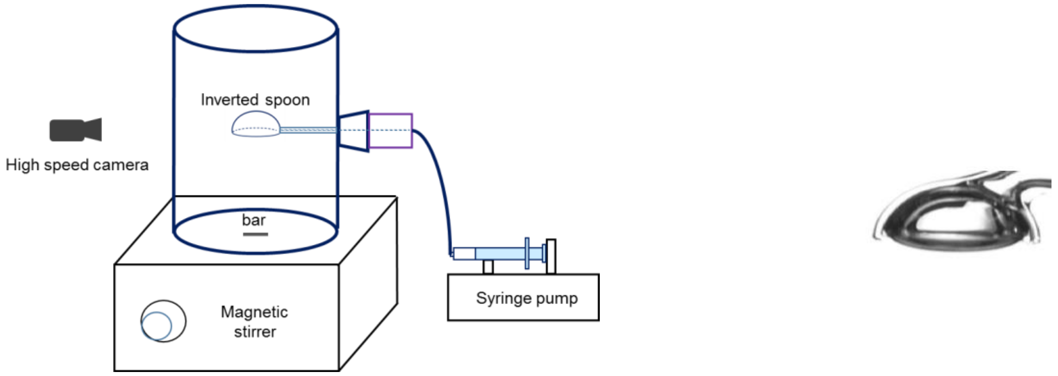

a) Set-up b) Initiate state of 2 mL-air pocket

Figure 5.2 Apparatus

5.2.2 Frothers

Table 5.2 gives the frothers tested. Reverse osmosis (RO) water was used to prepare 4L of frother solution at room temperature (ca. 23^{o}C). At least three separate sets of experiments were conducted on each solution, each consisting of six bubble formation experiments. The apparatus was thoroughly rinsed with hot tap water followed by RO water between each set of the experiments.

Table 5.2 – Frothers tested

Name	Formula	Molecular weight (g/mol)	Supplier
MIBC	$(CH_3)_2CHCH_2CH(OH)CH_3$	102.18	Sigma -Aldrich
Dowfroth 250[a]	$CH_3(PO)_4OH$	264.35	Sigma -Aldrich
F150	$H(PO)_7OH$	425	Flottec
F160-13	polyethylene and polypropylene ethers	250	Flottec

[a] PO is propylene oxide (propoxy) [$-O-CH_2-CH_2-CH_2-$]

5.2.3 Procedures

The volume of each tested solution was kept constant as 750 mL, and a 1.5 in. magnetic stirrer rotating at 900 RPM provided the agitation. Rotation of the liquid causes a vortex that draws down air from the pocket forming a bulge. With sufficient energy input the bulge breaks away to form a bubble. The bulging and break-away events were recorded with a digital high-speed camera (Fastec Imaging HiSpec5 8G Mono/Color). The image of the newly formed bubble is processed (software ImageJ) to acquire the sphere-volume equivalent diameter (Figure 5.2). Using the major (b) and minor (a) semi-axes of an ellipse fitted to the projected bubble area and assuming the bubble is symmetric about the minor axis, the diameter, *d*, is given by:

$$\boldsymbol{d} = \sqrt[3]{(2\boldsymbol{a})^2\times(2\boldsymbol{b})} \qquad \text{Equation 5.1}$$

a) original image b) binary image c) image outline d) ellipse fitting

Figure 5.2 Image analysis procedure

5.3 Results

5.3.1 Visual

A typical bubble formation sequence in RO water is shown in Figure 5.3.a. It was observed that the induced mechanical energy deforms the air pocket with bubble production following the sequence: formation of bulge, elongation of bulge, and bubble break-away.

Figure 5.3.b shows an example of bubble formation in the presence of frother. A dosage of only 0.6 ppm (0.006 mM) MIBC noticeably alters the shape of the bulge compared to RO water and produces a finer bubble size. In the presence of frother, bubble formation also seems to occur faster, the bubble appearing by image 4 (Figure 5.3.b) compared with image 6 (Figure 5.3.a). (Figure 5.3.b also shows a second bubble forming but only the first is considered in such cases to avoid possible effects due to subsequent coalescence.)

Figure 5.3.c shows a sequence of bubble formation with MIBC at increased frother concentration, 2.88 ppm (0.028 mM). At this concentration (ca. 380% increase) the bulge formation process becomes similar to that in RO water, and consequently produces a larger size bubble compared with 0.6 ppm MIBC.

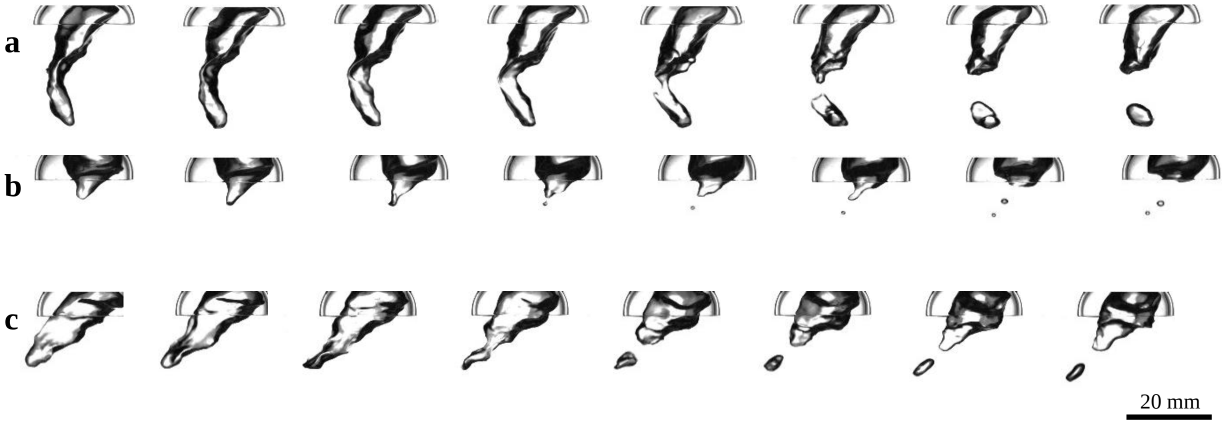

Figure 5.3 Bubble formation sequence (5 ms apart) in: a) RO water, b) 0.006 mM MIBC, c) 0.028 mM MIBC

Bubble formation generally followed the described three-stage sequence. However, there are occasions where a bubble forms in a different manner. Figure 5. 4 shows such an example for MIBC solution at 0.006 mM. In this case, the air/water interface is perturbed at a point location, generating a smaller bulge than typical and subsequently a smaller bubble. This phenomenon was only observed in the presence of frother, and more frequently at ‘low’ concentrations.

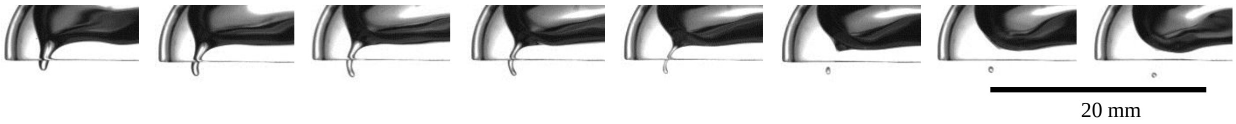

Figure 5.4 An occasional observation: a small bulge in MIBC solution at 0.006 mM

5.3.2 Quantitative

The effect of increasing frother concentration on the average bubble diameter is shown in Figure 5.5. The error bars denote the 95% confidence interval on the mean (95% CI) for typically 18 measurements. For all four frothers tested, a general trend is observed: with increase in frother concentration, bubble size reduces to a minimum, and then reverses. This minimum is interpreted as a critical break-up concentration (CBC), which describes the most effective concentration for producing the smallest bubble at break-up. The minimum bubble diameter and corresponding concentration (CBC) are: MIBC ca. 1.12 mm (± 0.25 mm at 95% C.I.) at ca. 0.006 mM; F160-13 ca. 1.20 mm (± 0.26 mm) at 0.004 mM; DF250 ca. 1.56 mm (± 0.26 mm) at 0.038 mM; and F150 ca. 1.34 mm (± 0.26 mm) at 0.024 mM.

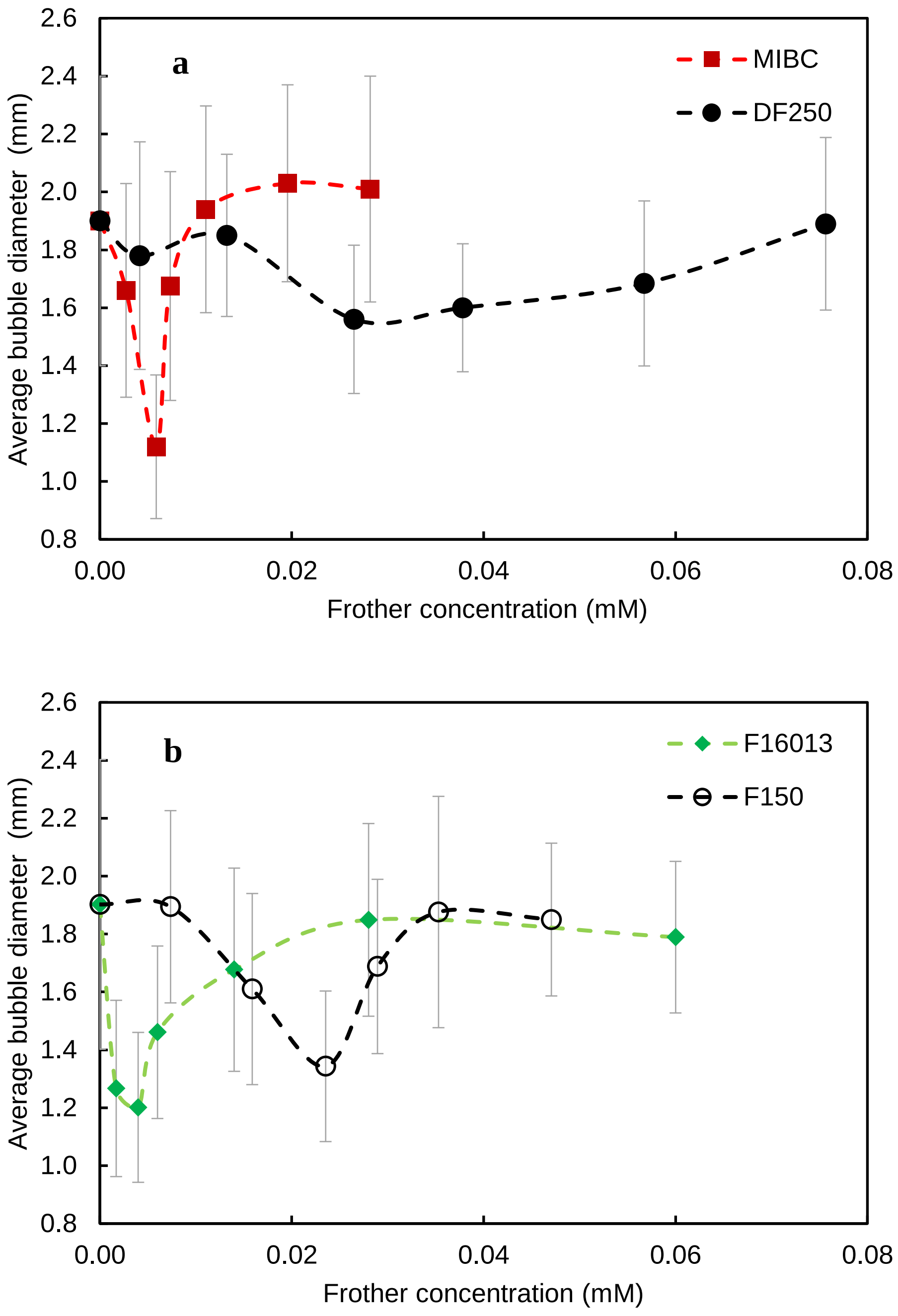

Figure 5.5 Effect of frother concentration on average bubble diameter

5.4 Discussion

Four frothers were investigated to determine the effect of increasing concentration on bubble size through break-up. The common trend is first a decrease in size compared to water alone followed by an increase. A critical break-up concentration is introduced referring to the concentration giving the minimum size.

The results support the hypothesis that it is through surface tension gradients that frother induces small bubbles through break-up. The process is stochastic. The surface tension gradient must increase towards the tip of the bulge for break-away forces to be enhanced. This in turn means the frother molecules must be more concentrated at the neck of the bulge than at the tip (Chu, 2013, 2014; Miller and Neogi, 1985). This arrangement will occur some of the time by chance, at other times the arrangement might be such as to oppose bulging. The damping of air/water interfacial instabilities by surfactants is well documented (Hühnerfuss et al., 1985; Lemaire and Langevin, 1992; Lucassen, 1982; Miller and Neogi, 1985). This randomness in the distribution of frother molecules around the bulge contributes to the scatter in bubble size (Figure 5.7). Only by taking more bubbles can this uncertainty be reduced. The procedure gave a minimum of 18 bubbles, but this is far short of the number involved in bubble swarms, as used to determine critical coalescence concentration, which gives high precision of the mean bubble size.

The effect of frother concentration can be understood here in the context of a finite-volume air bubble: with low frother bulk concentration, the mass transfer rate (e.g., convection) of the frother molecules to the air/water interface is low such that it lags the deformation rate (bulging represents increase of interfacial area) of the interface. The resulting non-uniform frother (molecule) distribution along the deforming air/water interface produces surface tension gradient-driven stresses. These forces enhance the disruption of the air/water interface initiated by the mechanical turbulence and result in more, smaller interfacial instabilities, which then break away to form smaller bubbles. If, on the other hand, there is a sufficiently large concentration of frother, the mass transfer rate will be high enough to maintain more uniform surface concentration, implying that surface tension gradient-driven stresses will be diminished, and consequently the effect of frother on producing a smaller bubble will diminish. This appears to correspond to the current situation where the CBC identifies the transition.

The argument needs to consider the effect of frother type as this affects mass transfer rate. The shorter the hydrocarbon chain generally the higher the mass transfer rate

(Walter and Blanch, 1986). Comparing a short and long chain frother, the former is, therefore, likely to replenish faster at the interface. It is notable that MIBC, with the shortest chain length, gave a lower CBC than F150, the longest chain frother. Chain length also influences surface activity, for example, controlling the rate of decrease in surface tension with concentration. The longer chain frothers are generally more surface active and might, therefore, be expected to produce larger surface tension gradients that could result in enhanced break away forces and thus smaller bubbles. The results show that, if anything, the longer chain frothers produce larger bubbles, but statistically the differences from MIBC are not significant. At present, however, there is insufficient variation in frother type, for example, a systematic study of chain length for a homologous series, to pursue interpretations further.

The concept of CBC is another potential characterization of frothers along with CCC. Table 5.4 lists CBC for this work and CCC95 for MIBC, DF250 and F150 given by Nesset et al*.* (2007). An observation is that the trends go in opposite directions, that frothers with lower CBC have higher CCC. Nesset et al*.* (2007) using CCC as the criterion gave the order of ‘strength’ of the frothers F150 > DF250 > MIBC. Using the same analogy, we can rank the ‘break-up strength’ as MIBC < DF250 < F150. Part of the difference may be that CBC is based on single bubbles, while CCC refers to bubble swarms; the concentration experienced by individual bubbles forming in a swarm is difficult to estimate.

Table 5.4 Comparison of CBC and CCC95[a]

	mM		ppm	
	CBC	CCC95	CBC	CCC95
MIBC	0.006	0.102	0.6	10.4
DF250	0.026	0.032	7	8.35
F150	0.024	0.0087	10	3.74

[a] CCC95 data from Nesset et al. (2007)

This different trend is also indicated in the classic two-bubble coalescence study of Bournival et al*.* (2014). They found that coalescence prevention occurred with as little as 0.0009 mM PPG425 (equivalent to F150) but required 0.1 mM MIBC. These differences suggest that short chain frothers like MIBC, while effective at producing small bubbles at low concentration need high concentration to preserve them against coalescence and thus coalescence is the dominant factor in giving the minimum bubble size. For frother with long hydrocarbon chain (e.g., F150) coalescence prevention appears to occur at lower concentrations than required to reduce bubble size at formation, which again suggests coalescence dominates the minimum size of bubble seen in swarms.

5.5 Conclusions

This work demonstrated the effect of increasing frother concentration on bubble size produced by break-up. It shows that the bubble size initially deceases with increase in frother concentration, then increases. A critical break-up concentration for the four frothers tested was identified. The findings support the hypothesis that high frother concentration can dampen the surface tension gradients believed to promote break-up.

References

Acuña, C.A., Nesset, J.E., Finch, J.A., 2007. Impact of frother on bubble production and behaviour in the pulp zone, In Proceedings of the Sixth International Copper-Cobre Conference, ed. de Villar, R., Nesset, J.E., Gomez, C.O., Strading, A.W. MetSoc CIM, Toronto, Ont.

Aldrich, C., Feng, D., The effect of mothers on bubble size distributions in flotation pulp phases and surface froths. Minerals Engineering, 2000, 13(10–11), 1049-1057.

Bournival, G., Ata, S., Karakashev, S.I., Jameson, G.J., An investigation of bubble coalescence and post-rupture oscillation in non-ionic surfactant solutions using high-speed cinematography. Journal of Colloid and Interface Science, 2014, 414, 50-58.

Cho, Y.S., Laskowski, J.S., Bubble coalescence and its effect on dynamic foam stability. The Canadian Journal of Chemical Engineering, 2002, 80(2), 299-305.

Chu, P., Finch, J.A., 2013. Frother and breakup in formation of small bubbles, In Materials Science & Technology. CIM, Montreal, pp. 2034-2043.

Chu, P., Finch, J.A., 2014. Break-up in formation of small bubbles: Salts and frothers, In XXVII International Mineral Processing Congress, ed. J., Y. Gecamin, Santiago, Chile, pp. 312-321.

Finch, J.A., Gelinas, S., Moyo, P., Frother-related research at McGill University. Minerals Engineering, 2006, 19(6–8), 726-733.

Finch, J.A., Nesset, J.E., Acuña, C., Role of frother on bubble production and behaviour in flotation. Minerals Engineering, 2008, 21(12–14), 949-957.

Grau, R.A., Laskowski, J.S., Role of Frothers in Bubble Generation and Coalescence in a Mechanical Flotation Cell. The Canadian Journal of Chemical Engineering, 2006, 84(2), 170-182.

Gupta, A., Yan, D.S., Mineral Processing design and operations: an introduction. 2006, Elsevier, Amsterdam.

Harris, C., Flotation machines. Flotation, A. M. Gaudin Memorial Volume, 1976, 2, 753-815.

Hühnerfuss, H., Lange, P.A., Walter, W., Relaxation effects in monolayers and their contribution to water wave damping: I. Wave-induced phase shifts. Journal of Colloid and Interface Science, 1985, 108(2), 430-441.

Javor, Z., Schreithofer, N., Comez, C.O., Finch, J.A., Heiskanen, K., 2013. Effect of scale dependent dynamic properties on bubble size, In Materials Science and Technology, Montreal.

Kracht, W., Finch, J.A., Bubble break-up and the role of frother and salt. International Journal of Mineral Processing, 2009, 92(3–4), 153-161.

Laskowski, J.S., 2003. Fundamental properties of flotation frothers, In XXIInd International Mineral Processing Congress, ed. Lorenzen, L., Bradshaw, D.J., South Africa, pp. 788-797.

Lemaire, C., Langevin, D., Longitudinal surface waves at liquid interfaces: Measurement of monolayer viscoelasticity. Colloids and Surfaces, 1992, 65(2–3), 101-112.

Lucassen, J., Effect of surface-active material on the damping of gravity waves: A reappraisal. Journal of Colloid and Interface Science, 1982, 85(1), 52-58.

Machon, V., Pacek, A.W., Nienow, A.W., Bubble Sizes in Electrolyte and Alcohol Solutions in a Turbulent Stirred Vessel. Chemical Engineering Research and Design, 1997, 75(3), 339-348.

Miller, C.A., Neogi, P., 1985. Interfacial phenomena: equilibrium and dynamic effects, pp. 240-298.

Nesset, J.E., Finch, J.A., Comez, C.O., 2007. Operating variable affecting the bubble size in forced-air mechanical flotation machines, In AusIMM 9th Mill Operators' Conference, Fremantle, Australia, pp. 66-75.

Stone, H., Leal, L., The effects of surfactants on drop deformation and breakup. Journal of Fluid Mechanics, 1990, 220, 161-186.

Sweet, C., van Hoogstraten, J., H., M., , Laskowski, J.S., 1997. The effect of frothers on bubble size and frothability of aqueous solutions, In 2nd UBC-McGill Symposium Series on Fundemental in Mineral Processing, ed. Finch, J.A., Rao, S.R., Holubec, I. The Metallurgical Society of CIM, pp. 235-246.

Walter, J.F., Blanch, H.W., Bubble break-up in gas—liquid bioreactors: Break-up in turbulent flows. The Chemical Engineering Journal, 1986, 32(1), B7-B17.

Wills, B.A., Finch, J.A., 2016. Chapter 12 - Froth Flotation, In Wills' Mineral Processing Technology (Eighth Edition), ed. Finch, B.A.W.A. Butterworth-Heinemann, Boston, pp. 265-380.

CONNECTING PARAGRAPH: CHAPTER 5 TO CHAPTER 6

Evidence from Chapters 4 and 5 confirmed that frothers also affect the break-up process in turbulent conditions. Chapter 5 identified a critical break-up concentration (CBC), suggesting the effect of frother is possibly manifest through a surface tension gradient-related phenomenon. Bubble size reduction stimulated by the presence of frother can be considered as an increase in surface energy. This lead to the thinking that frothers may add an apparent energy to the mechanical energy required for break-up. In other words, frothers will accelerate the break-up process. Chapter 6 tests this hypothesis. In addition to frothers, inorganics salts were also studied.

CHAPTER 6 BREAK-UP IN FORMATION OF SMALL BUBBLES: AN ENERGY CONSIDERATION

6.1 Introduction

Small bubbles (ca. 1 mm) are vital to the flotation process since they provide large interfacial area for collecting and transporting particles. The creation of these bubbles is typically accomplished by addition of frother, but sometimes the presence of high inorganic salt content in the water can substitute for the role of frother. Although these solutes' action is related to modification of the air/water interface (Rao and Leja, 2004), the mechanism by which they control small bubble production is not fully understood (Finch et al., 2008). A possible mechanism is inhibition of coalescence (Harris, 1982; Laskowski, 2003a). By bringing two bubbles into contact, it can be readily demonstrated that frothers and salts retard coalescence (Cho and Laskowski, 2002; Craig et al., 1993b). Another possibility is that the solutes aid in small bubble formation at the initial air break-up stage (Acuña, 2007; Finch et al., 2006; Grau and Laskowski, 2006; Gupta and Yan, 2006). This possibility has not been experimentally explored.

For break-up the air mass must first undergo deformation caused by turbulence in the water. Hinze (1955) identified three types of deformation based on different flow patterns around the air mass. The first is when the air mass is flattened, forming an oblate ellipsoid (Figure 6.1.a); the second is when it is elongated, forming a prolate ellipsoid then eventually a long cylindrical thread (Figure 6.1.b); and the third is when the interface of the air mass is "roughened", that is, deformation occurs locally resulting in surface irregularities (Figure 6.1.c). In flotation machines, an air mass is subjected to forces from different sources and therefore could break according to any of these three mechanisms.

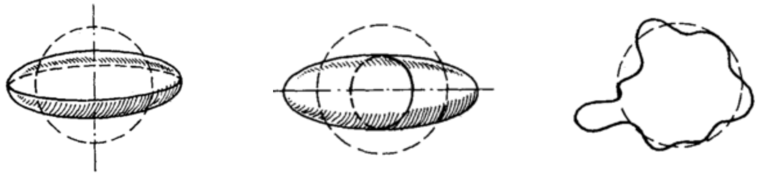

a) Flattened b) Elongated c) Roughened

Figure 6.1 Types of deformation identified by Hinze (1955)

The complex dynamics of small bubble generation in flotation machines suggest that neither coalescence prevention nor enhanced break-up would work alone, rather the two mechanisms are likely complementary (Finch et al., 2008). In recent work, Chu and Finch (2013; 2014) developed an experimental set-up and procedure to mimic bubble formation at the break-up stage. Single bubbles are individually formed by mechanically-induced deformation of a pocket of air. It was demonstrated that the presence of frother and salt reduces the size of bubble that is formed. They speculated that frothers and salts intensified the roughness break-up mechanism (Figure 6.1.c) through surface tension gradients which occur due to local variations in solute surface concentrations. Increasing the number of instabilities along the surface of a finite-volume air mass means that more, and therefore, smaller bubbles will form.

Notwithstanding the mechanism, the presence of the solutes makes the process of small bubble generation more energy efficient: for the same energy input the same mass of air is converted into more and therefore smaller bubbles. This leads to contemplating the role of frother and salt in terms of energy; that is, the presence of frother or salt brings an additional energy component to the mechanical energy needed for a bubble to form. This added energy might also show as a reduction in time for a bubble to form. To test the hypothesis, we adapt the experimental technique of Chu and Finch (2013) to monitor the time elapsed to form a bubble. Different types and concentrations of frothers and salts are investigated.

6.2 Experimental

6.2.1 Apparatus

The experimental set-up (Figure 6.2.a) consists of three components: an 800 mL breaker with a custom-made glass spoon to hold a known volume of air (the “air pocket”), a magnetic stirrer (Corning, PC-420D), and a syringe pump (Fisher Scientific, 78-0100I). The spoon (Figure 6.2.b), with inner diameter 20 mm, is connected to the syringe pump via a hollow handle and plastic tubing. A screw is coupled to the handle to ensure proper sealing of the trapped air. The initial state of the air pocket is shown in Figure 6.2.c.

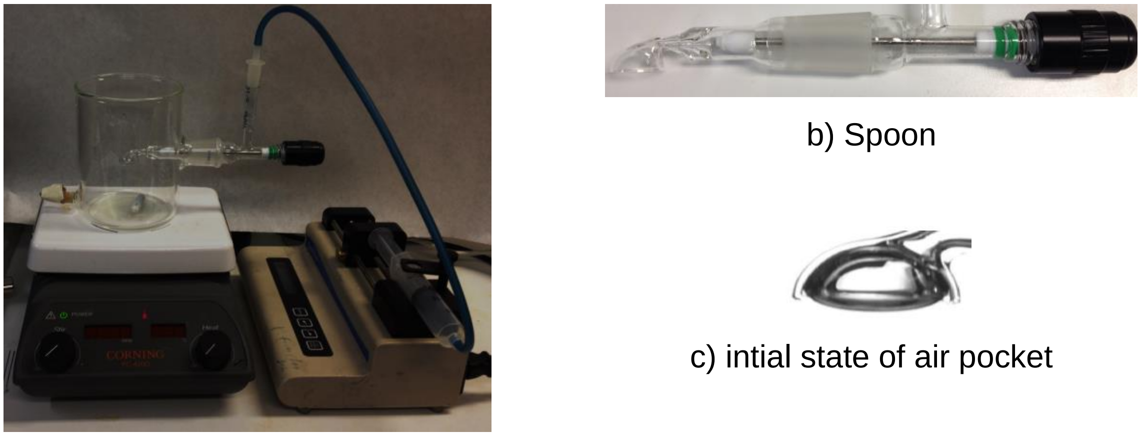

b) Spoon

c) intial state of air pocket

a) The set-up

Figure 6.2 Experimental set-up

6.2.2 Frothers and Salts

Table 6.1 lists the frothers and salts tested. Solutions of 4 L were prepared using Reverse Osmosis (RO) water at room temperature (ca. 23^{o}C). Four separate sets of experiments were conducted on each solution, each consisting of at least five bubble formation experiments. The experimental set-up was thoroughly rinsed with hot tap water followed by RO water between each set of the experiments.

Table 6.1 Frothers and salts tested and concentration range

Name	Formula	Molecular weight (g/mol)	Concentration range	Supplier
Dowfroth 250	$CH_3(PO)_4OH$	264.35	0 – 10 ppm	Aldrich
Flottec 150[a]	$H(PO)_7OH$	425	0 – 10 ppm	Flottec
Sodium Chloride	$NaCl$	58.44	0 – 1 M	Fisher Scientific
Sodium Sulfate	Na_2SO_4	142.04	0 – 1 M	Fisher Scientific

[a] PO is propylene oxide (propoxy) [-O-CH_2-CH_2-CH_2-]

6.2.3 Procedure

The breaker was filled with 750 mL test solution and placed on the magnetic stirrer. The screw was lightly loosened to allow the spoon to be filled with 2 mL of air, and then tightened. The magnetic stirrer (1.5 in. bar) was set at 900 RPM to provide the mechanical energy. The rotation of the liquid causes a vortex that draws down air from the pocket forming a bulge. When sufficient energy input is reached, that is, sufficient stirring time has elapsed, the bulge breaks away to form a bubble. A digital high speed camera (Fastec Imaging HiSpec5 8G Mono/Color) captured the bulging and breaking-away events. The frame frequency was set at 200 Hz, the maximum available. The time to form a bubble is obtained by taking the difference between the starting frame when the stirrer was switched on and the finishing fame when break-away occurred. The image showing the newly formed bubble is processed (software ImageJ) to acquire the sphere-volume equivalent diameter, using the major (a) and minor (b) semi-axes of an ellipse fitted to the projected bubble area (Equation 1) and assuming the bubble to be symmetric about the minor axis:

$$\boldsymbol{d} = \sqrt[3]{(2\boldsymbol{a})^2 \times (2\boldsymbol{b})} \qquad \text{Equation 6.1}$$

6.3 Results

6.3.1 Visual

Figure 6.3.a is an example of bubble formation in the presence of frother, showing the air pocket deforming due to the induced mechanical energy and forming a bubble. Bubble

creation follows the sequence: formation of bulge, elongation of bulge, and bubble break-away. The sequence was observed in all types of solutions, although the shape of the bulge was variable, as illustrated in Figure 6.3.b for a salt solution.

a) 7 ppm DF250

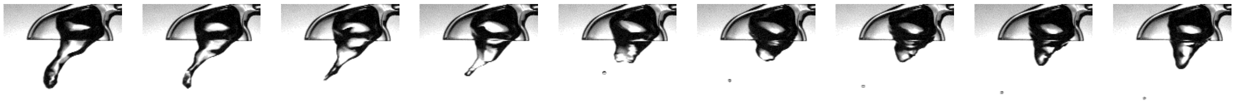

b) 1 M NaCl

Figure 6.3 Sequence of images showing bubble formation

6.3.2 Quantitative

This section reports the average bubble diameter, the time required to form a bubble, and the energy savings in forming a bubble relative to RO water, resulting from the presence of the solutes.

Average bubble diameter

The results in the four systems tested are shown in Figure 6.4. The effect of both frother types (Figure 6.4.a) is similar, resulting in a bubble size decrease of ca. 0.4 mm (1.9 mm to 1.5 mm), or ca. 20%. For the two salts, however, the trend is different (Figure 4b): with sodium sulphate, bubble size rapidly reduces to ca. 1.1 mm (or by ca. 40%), then reversing at concentrations above ca. 0.4 M, while with sodium chloride, the decrease is gradual to reach ca. 1.3 mm. The fact that frothers reduce surface tension and salts increase it (in both cases to a very small extent at the concentration used) rules out surface tension as an explanation of the decrease in bubble size.

Time

The time to form a bubble is shown in Figures 6.5.a, b, for the frothers and salts, respectively. Three features are apparent. First, a bubble forms more quickly in the presence of either solute than in RO water (the time at zero dosage), which took, on average, 14.7 s. Second, frothers seem to have different ‘accelerating’ strengths, DF250 giving faster bubble formation than F150. Third, bubble formation with increasing solute concentration shows different trends, gradual for frothers, but rapid and plateauing for salts at ca. 0.2 M and ca. 13 s.

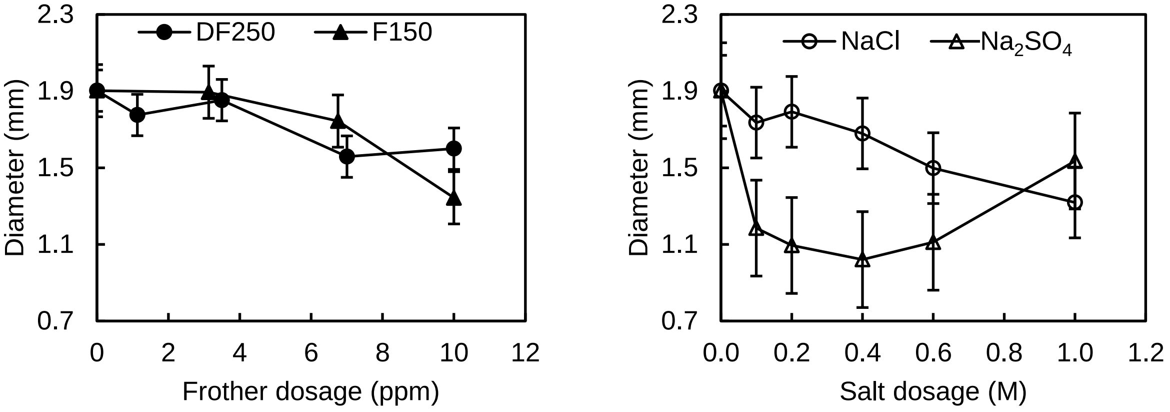

a) frother solutions b) salt solutions

Figure 6.4 Average bubble diameter (error bar is 95% confidence interval on the mean)

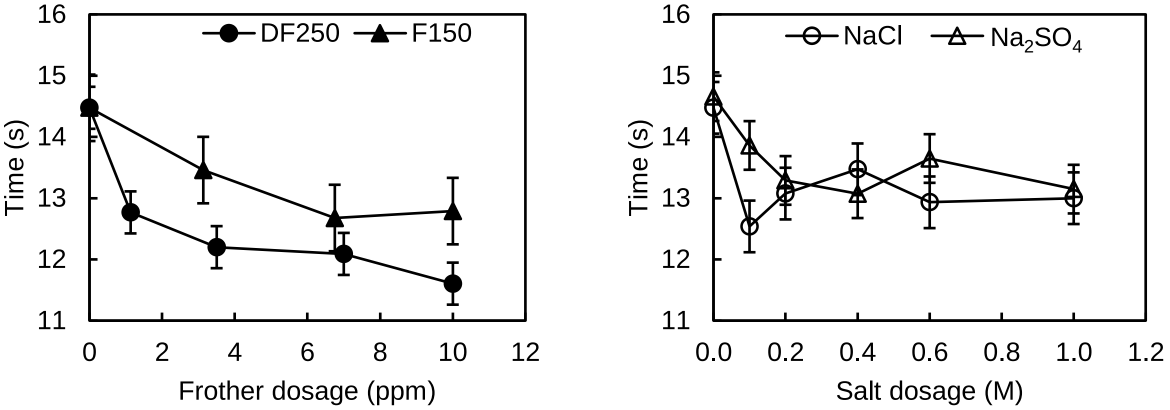

a) frothers b) salts

Figure 6.5 Time to form a bubble (error bar is 95% confidence interval on the mean)

Energy saving

For a constant power input, the case here, the energy to form a bubble can be estimated from the time. The reduction in time required compared to RO water is an “energy saving”, and is shown in Figure 6.6.a, b for the frothers and salts, respectively. The energy savings are about 10%.

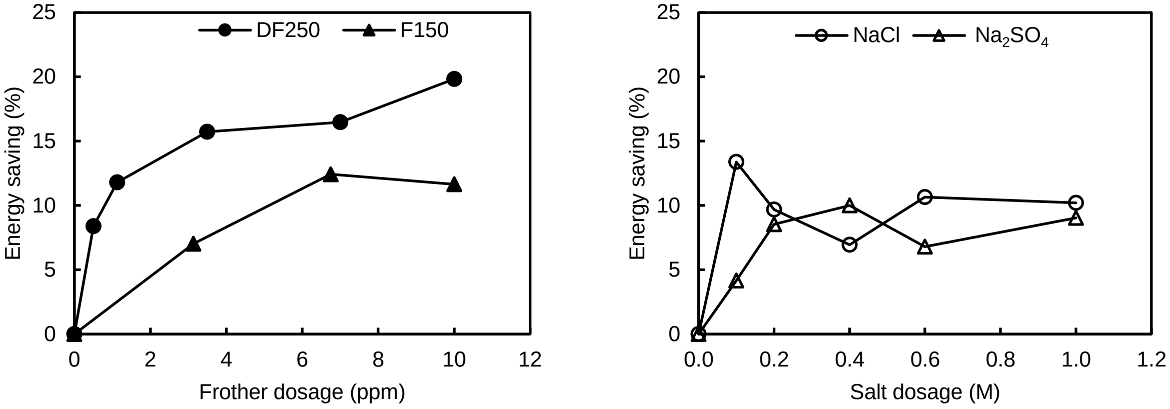

a) frothers b) salts

Figure 6.6 Energy savings

6.4 Discussion

The results show that the presence of frothers and salts not only creates smaller bubbles but also accelerates bubble formation compared to water only. This supports the hypothesis that their presence can be interpreted as introducing a “chemically-derived energy” that augments the mechanical energy required to form a bubble. The impact of frother and salt on enhancing break-up complements their known effect on retarding coalescence in the formation of small bubbles.

We can view the air mass break-up process from the energy standpoint. In the current set-up, the mechanical (kinetic) energy imparted by the rotating bar is dispersed into the water causing turbulence (from the dimensions of the stirrer bar and rotation speed, the Reynolds Number is about 22 000, i.e., in the turbulent regime (Sinnott, 2005).) The turbulence eddies interact with the air/water interface, perturbing it and causing surface irregularities (bulges) which grow and eventually break away to from a bubble. The mechanical energy required in water, indicated by the time required to form a bubble, can be used as a basis to assess the impact of the solutes. Relative to water alone, it appears that about 10% less time, meaning 10% less mechanical energy, is required in the presence of frother and salt; in other words, the solutes have contributed about 10% of the total energy required for the bubble to form.

One application of this energy approach is in models to predict bubble size. In CFD simulations, for example, bubble size is either predicted from the mechanical energy input, or is simply a value is inputted, but in either case no allowance for the important impact of solute is included. The suggestion is to model the effect of solute by an energy term in addition to the mechanical energy input.

The way this “chemical energy” is introduced may be through the surface tension gradients, as speculated by Chu and Finch, (2013; 2014). These force gradients cause local stresses which add to the irregularities produced by the mechanical energy. Consequently, with the same mechanical energy input, the irregularities will take less time to reach the point where break-away occurs. A combination of solute inducing more irregularities and hastening their growth gives smaller bubbles as well. The observed bubble formation sequence supports the roughened mechanism of bubble formation (Figure 6.1.c).

Development of surface tension gradients requires that the bulk concentration not be sufficient to restore concentration uniformity at the interface over the time intervals involved. Conversely, if there is enough solute available, surface tension gradients will not be supported and their contribution to bubble formation will be lost. The result in sodium sulfate solution, where the bubble size re-approaches that in water alone (i.e., the condition of zero surface tension gradients), hints at this idea. The effect of high frother and salt concentration is currently being explored.

6.5 Conclusions

The effect of the presence of frothers and salts on the time to form a bubble via break-up was determined. It is shown that the presence of these solutes accelerates the break-up process. The effect is viewed as an “add-on” energy to the mechanical energy required to form a bubble. Based on the reduced time to form a bubble, the solutes contribute about 10% of the energy required.

References

Acuña, C.A., Nesset, J.E., Finch, J.A., 2007. Impact of frother on bubble production and behaviour in the pulp zone, In Proceedings of the Sixth International Copper-Cobre Conference, ed. de Villar, R., Nesset, J.E., Gomez, C.O., Strading, A.W. MetSoc CIM, Toronto, Ont.

Cho, Y.S., Laskowski, J.S., Bubble coalescence and its effect on dynamic foam stability. The Canadian Journal of Chemical Engineering, 2002, 80(2), 299-305.

Chu, P., Finch, J.A., 2013. Frother and breakup in formation of small bubbles, In Materials Science & Technology. CIM, Montreal, pp. 2034-2043.

Chu, P., Finch, J.A., 2014. Break-up in formation of small bubbles: Salts and frothers, In XXVII International Mineral Processing Congress, ed. J., Y. Gecamin, Santiago, Chile, pp. 312-321.

Craig, V.S.J., Ninham, B.W., Pashley, R.M., The effect of electrolytes on bubble coalescence in water. Journal of Physical Chemistry, 1993, 97(39), 10192-10197.

Finch, J.A., Gelinas, S., Moyo, P., Frother-related research at McGill University. Minerals Engineering, 2006, 19(6–8), 726-733.

Finch, J.A., Nesset, J.E., Acuña, C., Role of frother on bubble production and behaviour in flotation. Minerals Engineering, 2008, 21(12–14), 949-957.

Grau, R.A., Laskowski, J.S., Role of Frothers in Bubble Generation and Coalescence in a Mechanical Flotation Cell. The Canadian Journal of Chemical Engineering, 2006, 84(2), 170-182.

Gupta, A., Yan, D.S., Mineral Processing design and operations: an introduction. 2006, Elsevier, Amsterdam.

Harris, P.J., 1982. Frothing phenomenon and frothers, In Principles of Flotation, ed. King, R.P. S. African IMM, pp. 237-250.

Hinze, J.O., Fundamentals of the hydrodynamic mechanism of splitting in dispersion processes. AIChE Journal, 1955, 1(3), 289-295.

Laskowski, J.S., 2003. Fundamental properties of flotation frothers, In XXIInd International Mineral Processing Congress, ed. Lorenzen, L., Bradshaw, D.J., South Africa, pp. 788-797.

Rao, S.R., Leja, J., Surface Chemistry of Froth Flotation. 2 edn. 2004, Kluwer Academic Publication, New York.

Sinnott, R.K., 2005. Coulson and Richardson's Chemical Engineering Volume 6 - Chemical Engineering Design (4th Edition). Elsevier, p. 73.

CHAPTER 7 UNIFYING DISCUSSION

Frothers are universally employed in mineral flotation to aid bubble size reduction. The bulk of the literature considers the action is related to frother's ability to prevent coalescence (Cho and Laskowski, 2002; Harris, 1976; Laskowski, 2003b; Pugh, 1996). Others have speculated that frothers may also play a role in aiding the break-up of the injected air mass (Acuña, 2007; Finch, 2006; Grau and Laskowski, 2006; Gupta and Yan, 2006; Javor et al., 2013; Kracht and Finch, 2009a), but experimental evidence is lacking. One obstacle hindering such studies is that break-up and coalescence are simultaneous coupled processes. This thesis has established two experimental techniques that allow break-up to be isolated from coalescence.

The topics covered fall under two procedures. In one, bubbles were produced quasi-statically at a capillary. By establishing an acoustic technique combined with high speed cinematography, the effect of frothers on bubble break-away from the capillary tip was determined. In the second, bubbles were produced through mechanically-induced deformation of a trapped air volume ("air pocket"). The set-up mimics break-up of the air-filled cavity behind an impeller blade in a mechanical cell. The impact of frothers and inorganic salts on break-up was determined along with the effect of input mechanical energy and volume of the air pocket. The decrease in time taken for a break-up event was used to estimate the apparent energy contributed by solutes.

The thesis provides the first unambiguous evidence that frothers and inorganic salts do affect the break-up process by generally producing smaller bubbles. It is argued that the unifying mechanism derives from the force arising from surface tension gradients.

Under quasi-static conditions, a bubble at a capillary grows to its maximum volume and subsequently breaks away. The break-away indicates that surface tension at that moment cannot sustain a balance against buoyancy. Frothers reduce surface tension and hence are expected to cause a decreased bubble size. This is seen to be the case in Chapter 3. However, it is noted that the overall reduction in bubble size was too small (e.g., maximum 4% for F150 at 144 μM), for it to be explained solely by the decrease in equilibrium surface tension. Hernandez-Aguilar et al. (2006) noted the same and postulated several factors to explain the apparent inconsistency; failure to reach equilibrium is one which implies the existence of surface tension gradients which may be the origin of a mechanism in break-away.

The surface tension gradient-derived mechanism can be illustrated in Figure 7.1. When an air bubble grows at a capillary, the moment its surface is introduced to a frother solution it will have a surface concentration reflective of the bulk concentration. As the bubble grows, its surface expands which means a tendency for the surface concentration to decrease. Countering this is that the expanding surface encounters more bulk frother molecules and mass transfer occurs from the bulk. Even so it can be argued that a uniform surface concentration is difficult to sustain and therefore gradients in surface tension exist around the bubble surface. A likely arrangement is depicted in Figure 7.1.c, that is, the surface concentration is higher at the leading part of the bubble, than at the bubble rear where surface is “newer”. The consequence of such difference in surface concentration is the generation of a surface tension gradient directed to the bubble rear (i.e., Figure 7.1.d). Under that arrangement, the surface tension gradients will produce a net force pointing downwards which resists the formation of new surface, and thus gives a reduced bubble size. The magnitude of the surface tension gradients is expected to be small and exist more so in low bulk concentrations than high concentrations where achieving equilibrium is easier (more molecules encountered and higher mass transfer rate).

It is proposed, therefore, that the effect of frother concentration on reducing the bubble size in quasi-static conditions is through two possible mechanisms: a surface tension gradient-dominated mechanism when frother concentration is low, and an equilibrium surface tension-dominated mechanism when frother concentration is high. This proposal accommodates the observation of Hernandez-Aguilar et al. (2006) who reported that low frother concentrations gave smaller bubbles than predicted from equilibrium surface tension.

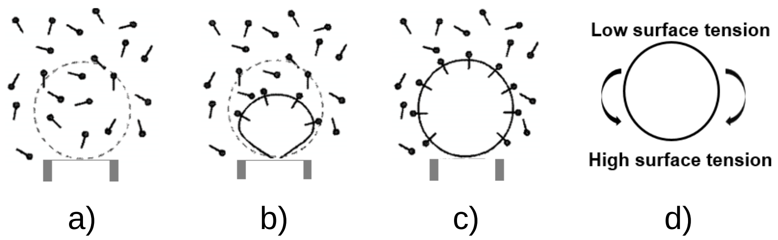

Figure 7.1 Schematic of initial concentration of frother molecules at bubble surface: a) before bubble starts growing (dashed circle represents volume to be occupied by bubble), b) during bubble growth, c) bubble immediately after detachment, and d) generation of surface tension gradients. Modified from Kracht (2008).

Other evidence that supports the notion that surface tension gradients play a role is the fact that the acoustic emission accompanying the break-away event in Chapter 3 was influenced by the presence of frother. The addition of frothers influenced the decay of the liquid jet thereby affecting the dissipation of the emitted acoustic signal and that of the capillary wave. Visual observation revealed that slow decay of the acoustic signal upon addition of frother was associated with damping of the capillary wave which is a known effect resulting from surface tension gradients.

In turbulent conditions, the break-up of a trapped air volume (Chapter 4) was not affected by the input mechanical energy or the volume of initially trapped air pocket, but was dependent on presence of frothers. The size of the bubble produced generally decreased as frother concentration was increased. This was attributed to surface tension gradients at the bulge neck aiding in the break-up process. The proposed mechanism is that for a finite volume of air the number of interfacial instabilities (or surface waves) depends on the magnitude of the surface tension gradients. The higher the magnitude the more, smaller instabilities that form resulting in smaller break-up bubbles.

Since the magnitude of surface tension gradients depends on the bulk concentration, Chapter 5 tested a hypothesis that surface tension gradients would not be produced if the bulk concentration was sufficient for mass transfer rate to allow uniform surface concentration to keep pace with the expanding bubble surface. It was demonstrated that the bubble size passed through a minimum then increased, supporting the notion that surface tension gradients were being indeed lost. The concentration giving minimum bubble size was termed a “critical break-up concentration” (CBC). The argument based on loss of surface tension gradient is at the same time evidence that gradients do occur under other circumstances, that is, when concentration is low.

A reduced bubble size represents an increase in surface energy. Based on this, Chapter 6 examined the apparent energy contributed by frothers to the mechanical energy required for break-up. By applying the fundamental concept that energy is a product of power and time, the energy can be estimated from the time elapsed during break-up provided the power is kept constant, which is the case (stirring speed was constant). It was shown that the presence of frother accelerated the break-up process, and the average saving in mechanical energy over the tested frother concentration range was ca.10%. The study also extended the case to two inorganic salts, and a similar conclusion was reached. The results complement the proposed mechanism that the presence of solutes produce surface tension gradients that decrease the produced bubble size by suggesting the gradients also accelerate the break-up process.

The reader probably notices in the discussion that the impact of surface tension gradients on surface waves (instabilities) is to ‘dampen’ them in the quasi-static condition and ‘promote’ them in the turbulent condition. This seems contradictory but actually is not the case. The evidence in the thesis mirrors the two known actions of surfactants, namely that they can act to either dampen or promote air/water interfacial instabilities (Hühnerfuss et al., 1985; Lemaire and Langevin, 1992; Lucassen, 1982; Miller and Neogi, 1985). Which occurs, promotion or suppression of instabilities, appears to depend on the intensity of the disturbance: minor disturbance (minor deformation) and surface tension gradients oppose growth of the deformation; major disturbance, and the gradients increase the number and growth rate of the deformations. The latter phenomenon would seem to fit the case for bubble swarm generation in a flotation machine and thus is postulated to be the mechanism by which frothers (and salts) aid formation of fine bubbles.

References

Acuña, C.A., Nesset, J.E., Finch, J.A., 2007. Impact of frother on bubble production and behaviour in the pulp zone, In Proceedings of the Sixth International Copper-Cobre Conference, ed. de Villar, R., Nesset, J.E., Gomez, C.O., Strading, A.W. MetSoc CIM, Toronto, Ont., pp. 197-210.

Cho, Y.S., Laskowski, J.S., Bubble coalescence and its effect on dynamic foam stability. The Canadian Journal of Chemical Engineering, 2002, 80(2), 299-305.

Finch, J.A., Gelinas, S., Moyo, P., Frother-related research at McGill University. Minerals Engineering, 2006, 19(6–8), 726-733.

Grau, R.A., Laskowski, J.S., Role of Frothers in Bubble Generation and Coalescence in a Mechanical Flotation Cell. The Canadian Journal of Chemical Engineering, 2006, 84(2), 170-182.

Gupta, A., Yan, D.S., Mineral Processing design and operations: an introduction. 2006, Elsevier, Amsterdam.

Harris, C., Flotation machines. Flotation, A. M. Gaudin Memorial Volume, 1976, 2, 753-815.

Hernandez-Aguilar, J.R., Cunningham, R., Finch, J.A., A test of the Tate equation to predict bubble size at an orifice in the presence of frother. International Journal of Mineral Processing, 2006, 79(2), 89-97.

Hühnerfuss, H., Lange, P.A., Walter, W., Relaxation effects in monolayers and their contribution to water wave damping: I. Wave-induced phase shifts. Journal of Colloid and Interface Science, 1985, 108(2), 430-441.

Javor, Z., Schreithofer, N., Comez, C.O., Finch, J.A., Heiskanen, K., 2013. Effect of scale dependent dynamic properties on bubble size, In Materials Science and Technology, Montreal.

Kracht, W., 2008. Effect of frother on bubble coalescence, break-up, and initial rise velocity. McGill University, Department of Mining and Materials Engineering.

Kracht, W., Finch, J.A., Bubble break-up and the role of frother and salt. International Journal of Mineral Processing, 2009, 92(3–4), 153-161.

Laskowski, J.S., 2003. Fundemental properties of flotation frothers, In Proceedings XXIInd International Mineral Processing Congress, ed. Lorenzen, L., Bradshaw, D.J. S. African IMM, pp. 788-797.

Lemaire, C., Langevin, D., Longitudinal surface waves at liquid interfaces: Measurement of monolayer viscoelasticity. Colloids and Surfaces, 1992, 65(2–3), 101-112.

Lucassen, J., Effect of surface-active material on the damping of gravity waves: A reappraisal. Journal of Colloid and Interface Science, 1982, 85(1), 52-58.

Miller, C.A., Neogi, P., 1985. Interfacial phenomena: equilibrium and dynamic effects, pp. 240-298.

Pugh, R.J., Foaming, foam films, antifoaming and defoaming. Advances in Colloid and Interface Science, 1996, 64(0), 67-142.

CHAPTER 8 CONCLUSIONS, CONTRIBUTIONS, AND FUTURE WORK

8.1 Conclusions

This thesis established two experimental techniques to isolate break-up from coalescence, allowing the effect of frothers or inorganic salts on air mass break-up to be investigated. The thesis is comprised of four studies, viz: establishing an acoustic technique to determine the effect of frothers on bubble break-away at a capillary; establishing a technique to study the break-up of a trapped air mass in a confined volume; a comparison between high and low frother concentrations on size of bubble generated on break-up;, and the estimation of apparent energy contributed by frothers and inorganic salts to the break-up process. The main conclusions from the individual studies are as follows:

- The acoustic frequency and damping ratio associated with bubble generation at a capillary is influenced by frother type and concentration.
- A liquid jet formed during break-away is responsible for stimulating the acoustic emission by initially exciting the bubble then decaying to form a surface wave.
- The presence of frother did not affect the formation of the liquid jet but did increase its decay rate and dampen the surface wave.
- A mechanism based on surface tension gradients to account for the frother effects was proposed.
- Comparing F150 and DF250, the former has stronger effect in increasing the acoustic frequency and in decreasing the acoustic damping ratio. This agrees with the general understanding that the longer chain F150 will be more surface active than the shorter chain DF250.
- Break-up of an air mass trapped in a confined volume was affected by the presence of frothers but not by the input mechanical energy and the initial volume of the air mass.
- Break-up in the presence of frothers generally produced smaller sized bubbles compared to water alone.

- Break-up at high frother concentrations does not necessarily produce smaller bubble size. The trend is that bubble size initially deceases to a minimum then increases.
- The same mechanism based on surface tension gradients to account for the frother effects on break-up was proposed.
- Comparing the ‘break-up’ strength, the tested frothers can be ranked as MIBC < DF250 < F150, again following the expected order of increasing surface activity associated with increased chain length.
- The presence of frothers and salts accelerates the break-up process in turbulent conditions.
- Based on the reduced time to form a bubble, the solutes contributed about 10% of the energy required.
- The mechanism to explain frother effects in both break-away from a capillary and break-up of the air mass was the non-uniformity of the surface concentration as the incipient bubble grows under dynamic conditions that produces surface tension gradients which exert a force.

8.2 Contribution to original knowledge

- A passive acoustic technique has been established to determine the acoustic damping ratio. It offers a novel way to study the role of frothers in bubble formation.
- It is found that the decay of the liquid jet not only stimulates the acoustic emission but also generates a capillary wave that initially excites the bubble surface.
- The results indicate the dissipation of the acoustic wave and that of the capillary wave is inversely related.
- An experimental technique mimicking the break-up of an air-filled cavity behind an impeller blade in a mechanical flotation machine has been developed.
- The study achieved an unambiguous demonstration, for the first time, that the presence of frothers and inorganics salts does affect the break-up process by generally producing smaller bubbles.

- A critical break-up concentration is introduced to characterize the ‘break-up’ strength of frothers.
- The study recognized that the presence of solutes accelerates the break-up process which can be regarded as an apparent energy added to the mechanical energy required.
- This thesis interpreted that the frother action during the break-up is related to the generation of surface tension gradients. The thesis provided strong evidence to advance the argument.

8.3 Suggestions for future work

- Model (simulate) the formation and decay of the liquid jet in the presence of frothers. By using high speed cinematography, relevant information can be obtained to validate the simulation.
- Re-design the acoustic experimental set-up to add acoustic shielding. A useful attachment to the set-up would be a temperature-controlled water bath to allow the effect of temperature to be investigated. Temperature effects on the acoustic parameters would test the surface tension gradient argument and provide further input to the simulation.
- Explore the effect of inorganic salts on acoustic emission. A preliminary test with sodium chloride (in Appendix 3) shows there is a trend which is worthy of further investigation.
- Explore the possible effect of solids on the acoustic emission.
- The acoustic damping ratio seems to adopt a stepwise trend. Currently, the data were only fitted with one sinusoidal decay function. A suggestion could be to fit the data with more than one function. This might provide insight on whether frother molecules form small aggregates (dimers, trimers) as speculated in the background review.
- The offset between bubble size predicted from acoustic frequency by the Minnaert relationship and that measured by imaging should be resolved. Reasons

considered range from the size of the bubble being too large for the prediction to difficulty in fitting the projected area of the bubble image. An independent ‘gold standard’ measure is the displaced-volume method.

- Continue exploring the possibility of using the acoustic frequency to estimate bubble size in a swarm. A preliminary work (a conference paper) with some observations is included in Appendix 4. A suggestion is to use a small hydrophone (e.g., a needle hydrophone) to improve the localization of acoustic monitoring.
- Re-design the geometry of the confined volume set-up (i.e., the air pocket) to introduce liquid flow across the air pocket to better simulate the action on the cavity trailing the impeller. This might open a way to examine different impeller shapes to feed data into computer-aided design.
- Re-design the stirring vessel by adding some baffles on the wall to generate different turbulent conditions.

REFERENCES

Acuña, C.A., Nesset, J.E., Finch, J.A., 2007b. Impact of frother on bubble production and behaviour in the pulp zone, In Proceedings of the Sixth International Copper-Cobre Conference, ed. de Villar, R., Nesset, J.E., Gomez, C.O., Strading, A.W. MetSoc CIM, Toronto, Ont., pp. 197-210.

Acuña, C.A., Radman, J., Finch, J.A., Measurement of flow visualized on surface of bubble blown in air. Colloids and Surfaces A: Physicochemical and Engineering Aspects, 2008, 330(2–3), 112-115.

Adamson, A.W., Physical chemistry of surfaces. 5 edn. 1990, John Wiley & Sons, Inc., New York.

Ahmed, N., Jameson, G.J., The effect of bubble size on the rate of flotation of fine particles. International Journal of Mineral Processing, 1985, 14(3), 195-215.

Al-Masry, W.A., Ali, E.M., Aqeel, Y.M., Effect of antifoam agents on bubble characteristics in bubble columns based on acoustic sound measurements. Chemical Engineering Science, 2006, 61(11), 3610-3622.

Aldrich, C., Feng, D., The effect of mothers on bubble size distributions in flotation pulp phases and surface froths. Minerals Engineering, 2000, 13(10–11), 1049-1057.

Alexander, S., Quinn, J., van der Spuy, J., Finch, J., 2012. Correlation of graphite flotation and gas holdup in saline solutions, In Water in Mineral Processing: Proceedings of the First International Symposium, SME, Englewood, pp. 41-50.

Amini, E., Bradshaw, D.J., Finch, J. A. and Brennan, M., Influence of turbulence kinetic energy on bubble size in different scale flotation cells. Minerals Engineering, 2013, 45, 146-150.

Ata, S., Coalescence of Bubbles Covered by Particles. Langmuir, 2008, 24(12), 6085-6091.

Ata, S., The detachment of particles from coalescing bubble pairs. Journal of Colloid and Interface Science, 2009, 338(2), 558-565.

Barigou, M., Greaves, M., Bubble-size distributions in a mechanically agitated gas—liquid contactor. Chemical Engineering Science, 1992, 47(8), 2009-2025.

Blanchard, D., Syzdek, L., Production of air bubbles of a specified size. Chemical Engineering Science, 1977, 32(9), 1109-1112.

Blander, M., Katz, J.L., Bubble nucleation in liquids. AIChE Journal, 1975, 21(5), 833-848.

Bolaños-Jiménez, R., Sevilla, A., Martínez-Bazán, C., Gordillo, J.M., Axisymmetric bubble collapse in a quiescent liquid pool. II. Experimental study. Physics of Fluids, 2008, 20(11), 112104.

Bonner, O.D., Jumper, C.F., Effect of ions on water structure. Infrared Physics, 1973, 13(3), 233-242.

Bournival, G., Ata, S., Karakashev, S.I., Jameson, G.J., An investigation of bubble coalescence and post-rupture oscillation in non-ionic surfactant solutions using high-speed cinematography. Journal of Colloid and Interface Science, 2014, 414, 50-58.

Chandler, D., Interfaces and the driving force of hydrophobic assembly. Nature, 2005, 437(7059), 640-647.

Chang, C.-H., Franses, E.I., Adsorption dynamics of surfactants at the air/water interface: a critical review of mathematical models, data, and mechanisms. Colloids and Surfaces A: Physicochemical and Engineering Aspects, 1995, 100, 1-45.

Cho, Y.S., Laskowski, J.S., Bubble coalescence and its effect on dynamic foam stability. The Canadian Journal of Chemical Engineering, 2002, 80(2), 299-305.

Chu, P., Finch, J.A., 2013. Frother and breakup in formation of small bubbles, In Materials Science & Technology. CIM, Montreal, pp. 2034-2043.

Chu, P., Finch, J.A., 2014. Break-up in formation of small bubbles: Salts and frothers, In XXVII International Mineral Processing Congress, ed. J., Y. Gecamin, Santiago, Chile, pp. 312-321.

Chu, P., Waters, K.E., Finch, J.A., Break-up in formation of small bubbles: Comparison between low and high frother concentrations. Minerals Engineering, 2016, 96–97, 15-19.

Clift, R., Grace, J.R., Weber, M.E., Bubbles, drops, and particles. 2005, Courier Corporation.

Coulaloglou, C.A., Tavlarides, L.L., Description of interaction processes in agitated liquid-liquid dispersions. Chemical Engineering Science, 1977, 32(11), 1289-1297.

Craig, V.S.J., Bubble coalescence and specific-ion effects. Current Opinion in Colloid & Interface Science, 2004, 9(1–2), 178-184.

Craig, V.S.J., Ninham, B.W., Pashley, R.M., Effect of electrolytes on bubble coalescence. Nature, 1993a, 364(6435), 317-319.

Craig, V.S.J., Ninham, B.W., Pashley, R.M., The effect of electrolytes on bubble coalescence in water. Journal of Physical Chemistry, 1993b, 97(39), 10192-10197.

Crozier, R.D., Klimpel, R.R., Frothers: Plant Practice. Mineral Processing and Extractive Metallurgy Review, 1989, 5(1-4), 257-279.

Danov, K.D., Kralchevsky, P.A., Ivanov, I.B., Equilibrium and dynamics of surfactant adsorption monolayers and thin liquid films. Surfactant science series, 1999, 303-418.

Davies, J.T., Vose, R.W., On the Damping of Capillary Waves by Surface Films. Proceedings of the Royal Society of London. Series A. Mathematical and Physical Sciences, 1965, 286(1405), 218-234.

Dawson, P., The physics of the oscillating bubble made simple. European Journal of Radiology, 2002, 41(3), 176-178.

de Bruijn, R.A., 1989. Deformation and break-up of drops in simple shear flows. Eindhoven Univ. Technol., The Netherlands.

De Gennes, P.-G., Brochard-Wyart, F., Quéré, D., Capillarity and wetting phenomena: drops, bubbles, pearls, waves. 2013, Springer Science & Business Media.

Defay, R., Petre, G., Dynamic surface tension. Surface and Colloid Science, 1971, 3, 27.

Dickinson, E., Adsorbed protein layers at fluid interfaces: interactions, structure and surface rheology. Colloids and Surfaces B: Biointerfaces, 1999, 15(2), 161-176.

Dominguez, A., Fernandez, A., Gonzalez, N., Iglesias, E., Montenegro, L., Determination of Critical Micelle Concentration of Some Surfactants by Three Techniques. Journal of Chemical Education, 1997, 74(10), 1227.

Drelich, J., Miller, J.D., Induction time measurements for air bubbles on chalcopyrite, bornite, and gold in seawater. Water in Mineral Processing, 2012, 73-85.

Duineveld, P., 1998. Bouncing and coalescence of bubble pairs rising at high Reynolds number in pure water or aqueous surfactant solutions, In In Fascination of Fluid Dynamics. Springer, pp. 409-439.

Dukhin, S.S., Miller, R., Loglio, G., 1998. Physico-chemical hydrodynamics of rising bubble, In Studies in Interface Science, eds. MÖbius, D., Miller, R. Elsevier, pp. 367-432.

Eastoe, J., Dalton, J.S., Dynamic surface tension and adsorption mechanisms of surfactants at the air–water interface. Advances in Colloid and Interface Science, 2000, 85(2–3), 103-144.

Enderby, J.E., Howells, W.S., Howe, R.A., The structure of aqueous solutions. Chemical Physics Letters, 1973, 21(1), 109-112.

Finch, J.A., Dobby, G.S., Column flotation: A selected review. Part I. International Journal of Mineral Processing, 1991, 33(1), 343-354.

Finch, J.A., Gelinas, S., Moyo, P., Frother-related research at McGill University. Minerals Engineering, 2006, 19(6–8), 726-733.

Finch, J.A., Nesset, J.E., Acuña, C., Role of frother on bubble production and behaviour in flotation. Minerals Engineering, 2008, 21(12–14), 949-957.

Fritz, W., Berechnung des Maximalvolume von Dampfblasen. Phys. Z., 1935, 36, 379-388.

Fruhner, H., Wantke, K.D., A new oscillating bubble technique for measuring surface dilational properties. Colloids and Surfaces A: Physicochemical and Engineering Aspects, 1996, 114(0), 53-59.

Fu, X.Y., Ishii, M., Two-group interfacial area transport in vertical air–water flow: I. Mechanistic model. Nuclear Engineering and Design, 2003, 219(2), 143-168.

Fuerstenau, D.W., 2007. A century of developments in the chemistry of flotation processing, In Froth Flotation: A Century of Innovation, ed. Maurice C. Fuerstenau, G.J., Roe-Hoan Yoon. SME, Littleton CO, USA pp. 3-64.

Gélinas, S., Finch, J.A., Gouet-Kaplan, M., Comparative real-time characterization of frother bubble thin films. Journal of Colloid and Interface Science, 2005, 291(1), 187-191.

Goetz, R., Lipowsky, R., Computer simulations of bilayer membranes: Self-assembly and interfacial tension. The Journal of Chemical Physics, 1998, 108(17), 7397-7409.

Grace, H.P., Dispersion phenomena in high viscosity immiscible fluid systems and application of static mixers as dispersion devices in such systems. Chemical Engineering Communications, 1982, 14(3-6), 225-277.

Grainger-Allen, T.J.N., Bubble Generation in Froth Flotation Machines. 1969, Warren Spring Laboratory.

Grau, R.A., Laskowski, J.S., Role of Frothers in Bubble Generation and Coalescence in a Mechanical Flotation Cell. The Canadian Journal of Chemical Engineering, 2006, 84(2), 170-182.

Gupta, A., Yan, D.S., Mineral Processing design and operations: an introduction. 2006, Elsevier, Amsterdam.

Hancer, M., Celik, M.S., Miller, J.D., The Significance of Interfacial Water Structure in Soluble Salt Flotation Systems. Journal of Colloid and Interface Science, 2001, 235(1), 150-161.

Harris, C., Flotation machines. Flotation, A. M. Gaudin Memorial Volume, 1976, 2, 753-815.

Harris, P.J., 1982. Frothing phenomenon and frothers, In Principles of Flotation, ed. King, R.P. S. African IMM, pp. 237-250.

Hernandez-Aguilar, J.R., Cunningham, R., Finch, J.A., A test of the Tate equation to predict bubble size at an orifice in the presence of frother. International Journal of Mineral Processing, 2006, 79(2), 89-97.

Hinze, J.O., Fundamentals of the hydrodynamic mechanism of splitting in dispersion processes. AIChE Journal, 1955, 1(3), 289-295.

Hofmeier, U., Yaminsky, V.V., Christenson, H.K., Observations of Solute Effects on Bubble Formation. Journal of Colloid and Interface Science, 1995, 174(1), 199-210.

Holmberg, K., Jönsson, B., Kronberg, B., Lindman, B., 2003. Phase Behaviour of Concentrated Surfactant Systems, In Surfactants and Polymers in Aqueous Solution. John Wiley & Sons, Ltd, pp. 67-96.

Horozov, T.S., Kralchevsky, P.A., Danov, K.D., Ivanov, I.B., Interfacial Rheology and Kinetics of Adsorption from Surfactant Solution. Journal of Dispersion Science and Technology, 1997, 18(6-7), 593-607.

Hsieh, C.-S., Campen, R.K., Vila Verde, A.C., Bolhuis, P., Nienhuys, H.-K., Bonn, M., Ultrafast Reorientation of Dangling OH Groups at the Air-Water Interface Using Femtosecond Vibrational Spectroscopy. Physical Review Letters, 2011, 107(11), 116102.

Hühnerfuss, H., Lange, P.A., Walter, W., Relaxation effects in monolayers and their contribution to water wave damping: I. Wave-induced phase shifts. Journal of Colloid and Interface Science, 1985, 108(2), 430-441.

Israelachvili, J.N., Intermolecular and surface forces: revised third edition. 2011, Academic press.

Israelachvili, J.N., Mitchell, D.J., Ninham, B.W., Theory of self-assembly of hydrocarbon amphiphiles into micelles and bilayers. Journal of the Chemical Society, Faraday Transactions 2: Molecular and Chemical Physics, 1976, 72(0), 1525-1568.

Jameson, G.J., Nam, S., Moo Young, M., Physical factors affecting recovery rates in flotation. Minerals Science Engineering, 1977, 9(3), 103-118.

Javor, Z., Schreithofer, N., Comez, C.O., Finch, J.A., Heiskanen, K., 2013. Effect of scale dependent dynamic properties on bubble size, In Materials Science and Technology, Montreal.

Keim, N.C., Perturbed breakup of gas bubbles in water: Memory, gas flow, and coalescence. Physical Review E, 2011, 83(5), 056325.

Kitchener, J.A., Cooper, C.F., Current concepts in the theory of foaming. Quarterly Reviews, Chemical Society, 1959, 13(1), 71-97.

Klimpel, R.R., Use of chemical reagents in flotation. Chemical Engineering, 1984, 91(18), 75-79.

Klimpel, R.R., Isherwood, S., Some industrial implications of changing frother chemical structure. International Journal of Mineral Processing, 1991, 33(1), 369-381.

Kolmogorov, A.N., On the disintegration of drops in a turbulent flow. Dokl. Akad. Nauk SSSR, 1949, 66, 825-828.

Kracht, W., 2008. Effect of frother on bubble coalescence, break-up, and initial rise velocity. McGill University, Department of Mining and Materials Engineering.

Kracht, W., Finch, J.A., Bubble break-up and the role of frother and salt. International Journal of Mineral Processing, 2009a, 92(3-4), 153-161.

Kracht, W., Finch, J.A., Using sound to study bubble coalescence. Journal of Colloid and Interface Science, 2009b, 332(1), 237-245.

Larson, R.G., Self-assembly of surfactant liquid crystalline phases by Monte Carlo simulation. The Journal of Chemical Physics, 1989, 91(4), 2479-2488.

Laskowski, J.S., Frothers and Flotation Froth. Mineral Processing and Extractive Metallurgy Review, 1993, 12(1), 61-89.

Laskowski, J.S., Frothers and Frothing. Frothing in Flotation II: Recent Advances in Coal Processing, 1998, 2, 1.

Laskowski, J.S., 2001. Chapter 8 Flotation machines, In Developments in Mineral Processing. Elsevier, pp. 225-262.

Laskowski, J.S., 2003. Fundemental properties of flotation frothers, In Proceedings XXIInd International Mineral Processing Congress, ed. Lorenzen, L., Bradshaw, D.J. S. African IMM, pp. 788-797.

Laskowski, J.S., Testing flotation frothers. Fizykochemiczne Problemy Mineralurgii/Physicochemical Problems of Mineral Processing, 2004(38), 13-22.

Laskowski, J.S., Cho, Y.S., Ding, K., Effect of Frothers on Bubble Size and Foam Stability in Potash Ore Flotation Systems. The Canadian Journal of Chemical Engineering, 2003, 81(1), 63-69.

Laughlin, R.G., The aqueous phase behavior of surfactants. 1994, Academic Pr.

Leberman, R., Soper, A.K., Effect of high salt concentrations on water structure. Nature, 1995, 378(6555), 364-366.

Lee, C.-H., Erickson, L.E., Glasgow, L.A., Bubble Breakup and Coalescence in Turbulent Gas-Liquid Dispersions. Chemical Engineering Communications, 1987a, 59(1-6), 65-84.

Lee, C.-H., Erickson, L.E., Glasgow, L.A., Dynamics of Bubble Size Distribution in Turbulent Gas-Liquid Dispersions. Chemical Engineering Communications, 1987b, 61(1-6), 181-195.

Leighton, T.G., The Acoustic Bubble. Academic Press, 1994. ISBN 0-12-441920-8.

Leighton, T.G., Fagan, K.J., Field, J.E., Acoustic and photographic studies of injected bubbles. European Journal of Physics, 1991, 12(2), 77.

Leighton, T.G., Walton, A., An experimental study of the sound emitted from gas bubbles in a liquid. European Journal of Physics, 1987, 8, 7.

Lemaire, C., Langevin, D., Longitudinal surface waves at liquid interfaces: Measurement of monolayer viscoelasticity. Colloids and Surfaces, 1992, 65(2–3), 101-112.

Lessard, R.R., Zieminski, S.A., Bubble coalescence and gas transfer in aqueous electrolytic solutions. Industrial and Engineering Chemistry Fundamentals, 1971, 10(2), 260-269.

Levich, V.G., Physicochemical hydrodynamics. 1962, Prentice-Hall, Englewood Cliffs, N.J.

Liao, Y., Lucas, D., A literature review of theoretical models for drop and bubble breakup in turbulent dispersions. Chemical Engineering Science, 2009, 64(15), 3389-3406.

Lin, J.N., Banerji, S.K., Yasuda, H., Role of Interfacial Tension in the Formation and the Detachment of Air Bubbles. 1. A Single Hole on a Horizontal Plane Immersed in Water. Langmuir, 1994, 10(3), 936-942.

Longuet-Higgins, M.S., Kerman, B.R., Lunde, K., The release of air bubbles from an underwater nozzle. Journal of Fluid Mechanics, 1991, 230, 365-390.

Lucassen, J., Effect of surface-active material on the damping of gravity waves: A reappraisal. Journal of Colloid and Interface Science, 1982, 85(1), 52-58.

Lucassen, J., Van Den Tempel, M., Dynamic measurements of dilational properties of a liquid interface. Chemical Engineering Science, 1972, 27(6), 1283-1291.

Luo, H., Svendsen, H.F., Theoretical model for drop and bubble breakup in turbulent dispersions. AIChE Journal, 1996, 42(5), 1225-1233.

Machon, V., Pacek, A.W., Nienow, A.W., Bubble Sizes in Electrolyte and Alcohol Solutions in a Turbulent Stirred Vessel. Chemical Engineering Research and Design, 1997, 75(3), 339-348.

Maldarelli, C., Jain, R.K., The hydrodynamic stability of thin films. 1988, Marcel Dekker, New York.

Marrucci, G., A theory of coalescence. Chemical Engineering Science, 1969, 24(6), 975-985.

Martinez-Bazan, C., Montañés, J.L., Lasheras, J.C., On the breakup of an air bubble injected into a fully developed turbulent flow. Part 1. Breakup frequency. Journal of Fluid Mechanics, 1999a, 401, 157-182.

Martinez-Bazan, C., Montañés, J.L., Lasheras, J.C., On the breakup of an air bubble injected into a fully developed turbulent flow. Part 2. Size PDF of the resulting daughter bubbles. Journal of Fluid Mechanics, 1999b, 401, 183-207.

McBain, J.W., Martin, H.E., XCII.-Studies of the constitution of soap solutions: the alkalinity and degree of hydrolysis of soap solutions. Journal of the Chemical Society, Transactions, 1914, 105(0), 957-977.

McComb, W.D., Ayyash, S., The production, pulsation and damping of small air bubbles in dilute polymer solutions. Journal of Physics D: Applied Physics, 1980, 13(5), 773.

Meguro, K., Adachi, T., Fukunishi, R., Esumi, K., Formation of multiple adsorption layers of surfactants on particle surfaces. Langmuir, 1988, 4(5), 1160-1162.

Menger, F.M., The structure of micelles. Accounts of Chemical Research, 1979, 12(4), 111-117.

Meunier, J., Langevin, D., Boccara, N., Physics of Amphiphilic Layers: Proceedings of the Workshop, Les Houches, France February 10–19, 1987. 2012, Springer Science & Business Media.

Miller, C.A., Neogi, P., 1985. Interfacial phenomena: equilibrium and dynamic effects, pp. 240-298.

Minnaert, M., On musical air-bubbles and the sounds of running water. Philosophical Magazine, 1933, 16, 235-248.

Monroy, F., Giermanska Kahn, J., Langevin, D., Dilational viscoelasticity of surfactant monolayers. Colloids and Surfaces A: Physicochemical and Engineering Aspects, 1998, 143(2–3), 251-260.

Monteux, C., Williams, C.E., Meunier, J., Anthony, O., Bergeron, V., Adsorption of Oppositely Charged Polyelectrolyte/Surfactant Complexes at the Air/Water Interface: Formation of Interfacial Gels. Langmuir, 2004, 20(1), 57-63.

Mouat, J., The development of the flotation process: technological change and the genesis of modern mining, 1898-1911. Australian Economic History Review, 1996, 36, 27.

Nagarajan, R., Molecular Packing Parameter and Surfactant Self-Assembly: The Neglected Role of the Surfactant Tail. Langmuir, 2002, 18(1), 31-38.

Napier-Munn, T., Wills, B.A., Wills' mineral processing technology: An introduction to the practical aspects of ore treatment and mineral recovery. 2006, Elsevier.

Nesset, J.E., Finch, J.A., Comez, C.O., 2007. Operating variable affecting the bubble size in forced-air mechanical flotation machines, In AusIMM 9th Mill Operators' Conference, Fremantle, Australia, pp. 66-75.

Pandit, A.B., Varley, J., Thorpe, R.B., Davidson, J.F., Measurement of bubble size distribution: an acoustic technique. Chemical Engineering Science, 1992, 47(5), 1079-1089.

Prince, M.J., Blanch, H.W., Bubble coalescence and break-up in air-sparged bubble columns. AIChE Journal, 1990, 36(10), 1485-1499.

Problestein, R., 1994. Physicochemical Hydrodynamics, An introduction. John Wiley & Sons New York.

Pugh, R.J., Foaming, foam films, antifoaming and defoaming. Advances in Colloid and Interface Science, 1996, 64(0), 67-142.

Pugh, R.J., 2007. The physics and chemistry of frothers, In Froth Flotation: A Century of Innovation, eds. Fuerstenau, M.C., Jameson, G.J., Yoon, R.H. Society for Mining, Metallurgy, and Exploration, pp. 259-282.

Pugh, R.J., Weissenborn, P., Paulson, O., Flotation in inorganic electrolytes; the relationship between recover of hydrophobic particles, surface tension, bubble coalescence and gas solubility. International Journal of Mineral Processing, 1997, 51(1), 125-138.

Quinn, J.J., Kracht, W., Gomez, C.O., Gagnon, C., Finch, J.A., Comparing the effect of salts and frother (MIBC) on gas dispersion and froth properties. Minerals Engineering, 2007, 20(14), 1296-1302.

Rao, S.R., Leja, J., Surface Chemistry of Froth Flotation. 2 edn. 2004, Kluwer Academic Publication, New York.

Reay, D., Ratcliff, G.A., Removal of fine particles from water by dispersed air flotation: Effects of bubble size and particle size on collection efficiency. The Canadian Journal of Chemical Engineering, 1973, 51(2), 178-185.

Risso, F.R., FABRE, J., Oscillations and breakup of a bubble immersed in a turbulent field. Journal of Fluid Mechanics, 1998, 372, 323-355.

Rodgers, T.L., Cooke, M., Rotor–stator devices: The role of shear and the stator. Chemical Engineering Research and Design, 2012, 90(3), 323-327.

Romsted, L.S., 2012. Introduction to Surfactant Self-Assembly, In Supramolecular Chemistry. John Wiley & Sons, Ltd.

Rowlinson, J.S., Widom, B., Molecular theory of capillarity. 2013, Courier Corporation.

Rusanov, A., Krotov, V., Gibbs elasticity of liquid films. Prog. Surf. Memb. Sci, 1979, 13, 415-524.

Sagert, N.H., Quinn, M.J., The coalescence of gas bubbles in dilute aqueous solutions. Chemical Engineering Science, 1978, 33(8), 1087-1095.

Sarma, T.K., Chattopadhyay, A., Simultaneous Measurement of Flowing Fluid Layer and Film Thickness of a Soap Bubble Using a UV−Visible Spectrophotometer. Langmuir, 2001, 17(21), 6399-6403.

Schubert, H., On the turbulence-controlled microprocesses in flotation machines. International Journal of Mineral Processing, 1999, 56(1–4), 257-276.

Sinnott, R.K., 2005. Coulson and Richardson's Chemical Engineering Volume 6 - Chemical Engineering Design (4th Edition). Elsevier, p. 73.

Sovechles, J.M., Waters, K.E., Effect of ionic strength on bubble coalescence in inorganic salt and seawater solutions. AIChE Journal, 2015, 61(8), 2489-2496.

Stone, H., Leal, L., The effects of surfactants on drop deformation and breakup. Journal of Fluid Mechanics, 1990, 220, 161-186.

Stone, H.A., Dynamics of Drop Deformation and Breakup in Viscous Fluids. Annu. Rev. Fluid Mech., 1994, 26(1), 65-102.

Strasberg, M., Gas Bubbles as Sources of Sound in Liquids. The Journal of the Acoustical Society of America, 1956, 28(1), 20-26.

Sulman, H.L., Kirkpatrick-Picard, H.F., Ballot, J., 1906. Ore concentration. Bristih Patent.

Sweet, C., van Hoogstraten, J., H., M., , Laskowski, J.S., 1997. The effect of frothers on bubble size and frothability of aqueous solutions, In 2nd UBC-McGill Symposium Series on Fundemental in Mineral Processing, ed. Finch, J.A., Rao, S.R., Holubec, I. The Metallurgical Society of CIM, pp. 235-246.

Szatkowski, M., Some comments on flotation kinetics. Chemical Engineering Science, 1987, 42(10), 2475-2478.

Talanquer, V., Oxtoby, D.W., Nucleation of bubbles in binary fluids. The Journal of Chemical Physics, 1995, 102(5), 2156-2164.

Tan, Y.H., Finch, J.A., Frother structure–property relationship: Effect of alkyl chain length in alcohols and polyglycol ethers on bubble rise velocity. Minerals Engineering, 2016, 95, 14-20.

Tanford, C., The hydrophobic effect: formation of micelles and biological membranes. 1973, Wiley, New York.

Taylor, G.I., The Viscosity of a Fluid Containing Small Drops of Another Fluid. Proceedings of the Royal Society of London. Series A, 1932, 138(834), 41-48.

Taylor, G.I., The Formation of Emulsions in Definable Fields of Flow. Proceedings of the Royal Society of London. Series A, 1934, 146(858), 501-523.

Thomas, R.K., Penfold, J., Multilayering of Surfactant Systems at the Air–Dilute Aqueous Solution Interface. Langmuir, 2015, 31(27), 7440-7456.

Tromp, R.H., Neilson, G.W., Soper, A.K., Water structure in concentrated lithium chloride solutions. The Journal of Chemical Physics, 1992, 96(11), 8460-8469.

Tsang, Y.H., Koh, Y.-H., Koch, D.L., Bubble-size dependence of the critical electrolyte concentration for inhibition of coalescence. Journal of Colloid and Interface Science, 2004, 275(1), 290-297.

Tsao, H.K., Koch, D.L., Collisions of slightly deformable, high Reynolds number bubbles with short-range repulsive forces. Physics of Fluids, 1994, 6(8), 2591-2605.

Tsouris, C., Tavlarides, L.L., Breakage and coalescence models for drops in turbulent dispersions. AIChE Journal, 1994, 40(3), 395-406.

Tucker, C.L., Moldenaers, P., Microstructural evolution in polymer blends. Annu. Rev. Fluid Mech., 2002, 34, 177-210.

Tulin, M.P., Mechanics of Underwater Noise. By DONALD Ross. Pergamon Press, 1976.

Vanegas, C., Holtham, P.N., 2010. Possibilities for flotation acoustics monitoring-A review, In International Mineral Processing Congress 2010. Australasian Institute of Mining and Metallurgy, pp. 2457-2470.

Vargaftik, N.B., Volkov, B.N., Voljak, L.D., International Tables of the Surface Tension of Water. Journal of Physical and Chemical Reference Data, 1983, 12(3), 817-820.

Walter, J.F., Blanch, H.W., Bubble break-up in gas—liquid bioreactors: Break-up in turbulent flows. The Chemical Engineering Journal, 1986, 32(1), B7-B17.

Wang, B., Peng, Y., The effect of saline water on mineral flotation – A critical review. Minerals Engineering, 2014, 66–68, 13-24.

Wang, T., Wang, J., Jin, Y., A novel theoretical breakup kernel function for bubbles/droplets in a turbulent flow. Chemical Engineering Science, 2003, 58(20), 4629-4637.

Wills, B.A., Finch, J.A., 2016. Chapter 12 - Froth Flotation, In Wills' Mineral Processing Technology (Eighth Edition), ed. Finch, B.A.W.A. Butterworth-Heinemann, Boston, pp. 265-380.

Yoon, R.H., Luttrell, G.H., The Effect of Bubble Size on Fine Particle Flotation. Mineral Processing and Extractive Metallurgy Review, 1989, 5(1-4), 101-122.

Zeitling, M.A., Tavlarides, L.L., Fluid-fluid interactions and hydrodynamics. Can. J. Chem. Engng, 1972, 50, 207-215.

Zhao, H., Ge, W., A theoretical bubble breakup model for slurry beds or three-phase fluidized beds under high pressure. Chemical Engineering Science, 2007, 62(1–2), 109-115.

Appendix 1 MATLAB script for analyzing the acoustic signals

```
%%%%%%%%%%%%%%%%%%%%%%%%%%%%%%%%%%%%%%%%%%%%%%%%%%%%%%%%%%%%%%%%%%%%%%%%%%%%%
The following commands import raw data
%%%%%%%%%%%%%%%%%%%%%%%%%%%%%%%%%%%%%%%%%%%%%%%%%%%%%%%%%%%%%%%%%%%%%%%%%%%%%

clear all; close all; clc

filename = 'E:\AcousticAnalysis\500kHz_refined_1_ChemEngF150_3.32ppm.lvm';
delimiter = '\t';
formatSpec = '%*s%f%[^\n\r]';
fileID = fopen(filename,'r');
dataArray = textscan(fileID, formatSpec, 'Delimiter', delimiter,
'EmptyValue' ,NaN, 'ReturnOnError', false);
fclose(fileID);

A = dataArray(Wills and Finch, 2016); %import data
clearvars filename delimiter formatSpec fileID dataArray ans;

Fs = 500000; % data acquistion rate
L = length(A);
zoom_frq = 0.5; %zooming the frequency axis, unit is in kHz and 1 corresponds
to 10kHz
fn = zoom_frq*420000;

T = L/Fs;
t = linspace(0,T,L);

%%%%%%%%%%%%%%%%%%%%%%%%%%%%%%%%%%%%%%%%%%%%%%%%%%%%%%%%%%%%%%%%%%%%%%%%%%%%%
FFT analysis to identify bubble frequency and noise frequency. Data to be
filtered with an 8th order bandpass filter
%%%%%%%%%%%%%%%%%%%%%%%%%%%%%%%%%%%%%%%%%%%%%%%%%%%%%%%%%%%%%%%%%%%%%%%%%%%%%

Y = fft(A);
P2 = abs(Y/L);
P1 = P2(1:L/2+1);
P1(2:end-1) = 2*P1(2:end-1);
f = 0.001*Fs*(0:(L/2))/L; %in kHz

d = fdesign.bandpass('N,F3dB1,F3dB2',8,1.25e3,1.43e3,50e4); %filter
Hd = design(d,'butter');

y = filter(Hd,A); % filtered acoustic data
ydft = fft(y);
p2 = abs(ydft/L);
p1 = p2(1:L/2+1);
p1(2:end-1) = 2*p1(2:end-1);

figure (01)%plot of the unfiltered data
subplot(2,1,1)
plot(t, A)
title('Raw data')
xlabel('Time (s)')
ylabel('Amplitude')
```

```
subplot(2,1,2)
plot(t, y)
title('Filtered data')
xlabel('Time (s)')
ylabel('Amplitude')

figure(02)
subplot(221) %FFT of the original data
plot(f, P1)
title('FFT of the acoustic data')
xlabel('Frequency (kHz)')
ylabel('|P1(f)|')

subplot(222) %FFT of the original data but only the first 10kHz
plot(f(1:fn), P1(1:fn))%420000 points correspond 10 kHz
title('FFT of the acoustic data')
xlabel('Frequency (kHz)')
ylabel('|P1(f)|')

subplot(223)
plot(f,p1)
title('FFT of the filtered acoustic data')
xlabel('Frequency (kHz)')
ylabel('|P1(f)|')

subplot(224)
plot(f(1:fn), p1(1:fn))
title('FFT of the filtered acoustic data')
xlabel('Frequency (kHz)')
ylabel('|P1(f)|')

%%%%%%%%%%%%%%%%%%%%%%%%%%%%%%%%%%%%%%%%%%%%%%%%%%%%%%%%%%%%%%%%%%%%%%%%%%%%%%%%%
Isolating individual peaks. ‘Peakfinder’ script is an open source matlab code
developed by Nathanael Yoder. It is given at the end of this script.
%%%%%%%%%%%%%%%%%%%%%%%%%%%%%%%%%%%%%%%%%%%%%%%%%%%%%%%%%%%%%%%%%%%%%%%%%%%%%%%%%

[yy_loc, yy]= peakfinder(y); % identify the peaks associated with the
filtered bubble sounds
[Max, Max_loc] = findpeaks(yy);

Num_peak = length(Max); % identify the number of peaks, e.g., number of
bubbles

Peak_delta = 40; % Estimated peak time-step, initial as 50 ms but should be
adjusted accordingly

Peak_duration = t(1:(0.001*Peak_delta*Fs+1))'; % shifted time, which always
starts at 0 ms
Peak_amplitude = [];

figure(03)

for i = 1: Num_peak
```

```
    Peak_initial = yy_loc(Max_loc(i));
    Peak_final = Peak_initial + 0.001*Peak_delta*Fs;
    Peak_ampli = y(Peak_initial:Peak_final);
    Peak_amplitude(1:length(Peak_ampli),i) = Peak_ampli; % storing the
amplitude of each peak individually
end

%%%%%%%%%%%%%%%%%%%%%%%%%%%%%%%%%%%%%%%%%%%%%%%%%%%%%%%%%%%%%%%%%%%%%%%%%%%%%
Curve fitting. The fitted value can be found in S
%%%%%%%%%%%%%%%%%%%%%%%%%%%%%%%%%%%%%%%%%%%%%%%%%%%%%%%%%%%%%%%%%%%%%%%%%%%%%

S = [];

figure(05)

for j = 1:Num_peak

      Y_amplitude = Peak_amplitude(:,j);
      [p, p_loc] = findpeaks(Y_amplitude);
      p_ratio = p/max(p);
      p_index = find(p_ratio < 0.20,1);
      Peak_duration_cutoff = find(Y_amplitude == p(p_index));

      peak_duration = Peak_duration(1:Peak_duration_cutoff);
      y_amplitude = Y_amplitude(1:Peak_duration_cutoff);

      yu = max(y_amplitude);
      yl = min(y_amplitude);
      yr = (yu-yl);  % Range of ?y?
      yz = y_amplitude-yu+(yr/2);
      zx = peak_duration(yz .* circshift(yz,[1 0]) <= 0); % Find zero-
      crossings

      per = 2*mean(diff(zx)); % Estimate period
      ym = mean(y_amplitude); % Estimate offset

      fit = @(b,peak_duration)  b(1).*(cos(2*pi*peak_duration./b(2) +
      2*pi/b(3))) .* exp(b(4).*peak_duration) + b(5); % Function to fit

      fcn = @(b) sum((fit(b,peak_duration) - y_amplitude).^2); % Sum-squared-
      error cost function

      s = fminsearch(fcn, [yr;  per;  0.5;  20; ym]); % Minimise Least-
      Squares. the b(4) should be bigger than 1. (1,2,2.75,3 work)

      fitted_Peak = fit(s,peak_duration);

      error = y_amplitude - fitted_Peak;

      subplot(Num_peak,2,2*j-1)
      plot(peak_duration,y_amplitude,'.','Markersize', 1)

      hold on
```

```
      plot(peak_duration,fitted_Peak, 'r-','LineWidth', 1.5)

      hold off
      xlabel('Time (s)')
      ylabel('Amplitude')

      subplot(Num_peak,2,2*j)
      mmmmm = histfit(error,50);

      S(j,:)= [s(1),1/s(2),1/s(3),-s(4),s(5),-100*s(4)/((1/s(2))^2 +
      (s(4))^2)^0.5];

end

%%%%%%%%%%%%%%%%%%%%%%%%%%%%%%%%%%%%%%%%%%%%%%%%%%%%%%%%%%%%%%%%%%%%%%%%%%%%%
Peakfinder script. The Peakfinder should be used a calling function, if the
above script is going to be used.
%%%%%%%%%%%%%%%%%%%%%%%%%%%%%%%%%%%%%%%%%%%%%%%%%%%%%%%%%%%%%%%%%%%%%%%%%%%%%

function varargout = peakfinder(x0, sel, thresh, extrema, includeEndpoints,
interpolate)
%PEAKFINDER Noise tolerant fast peak finding algorithm
%   INPUTS:
%       x0 - A real vector from the maxima will be found (required)
%       sel - The amount above surrounding data for a peak to be,
%           identified (default = (max(x0)-min(x0))/4). Larger values mean
%           the algorithm is more selective in finding peaks.
%       thresh - A threshold value which peaks must be larger than to be
%           maxima or smaller than to be minima.
%       extrema - 1 if maxima are desired, -1 if minima are desired
%           (default = maxima, 1)
%       includeEndpoints - If true the endpoints will be included as
%           possible extrema otherwise they will not be included
%           (default = true)
%       interpolate - If true quadratic interpolation will be performed
%           around each extrema to estimate the magnitude and the
%           position of the peak in terms of fractional indicies. Note that
%           unlike the rest of this function interpolation assumes the
%           input is equally spaced. To recover the x_values of the input
%           rather than the fractional indicies you can do:
%           peakX = x0 + (peakLoc - 1) * dx
%           where x0 is the first x value and dx is the spacing of the
%           vector. Output peakMag to recover interpolated magnitudes.
%           See example 2 for more information.
%           (default = false)
%
%   OUTPUTS:
%       peakLoc - The indicies of the identified peaks in x0
%       peakMag - The magnitude of the identified peaks
%
%   [peakLoc] = peakfinder(x0) returns the indicies of local maxima that
%       are at least 1/4 the range of the data above surrounding data.
%
%   [peakLoc] = peakfinder(x0,sel) returns the indicies of local maxima
%       that are at least sel above surrounding data.
%
```

```
%   [peakLoc] = peakfinder(x0,sel,thresh) returns the indicies of local
%       maxima that are at least sel above surrounding data and larger
%       (smaller) than thresh if you are finding maxima (minima).
%
%   [peakLoc] = peakfinder(x0,sel,thresh,extrema) returns the maxima of the
%       data if extrema > 0 and the minima of the data if extrema < 0
%
%   [peakLoc] = peakfinder(x0,sel,thresh,extrema, includeEndpoints)
%       returns the endpoints as possible extrema if includeEndpoints is
%       considered true in a boolean sense
%
%   [peakLoc, peakMag] = peakfinder(x0,sel,thresh,extrema,interpolate)
%       returns the results of results of quadratic interpolate around each
%       extrema if interpolate is considered to be true in a boolean sense
%
%   [peakLoc, peakMag] = peakfinder(x0,...) returns the indicies of the
%       local maxima as well as the magnitudes of those maxima
%
%   If called with no output the identified maxima will be plotted along
%       with the input data.
%
%   Note: If repeated values are found the first is identified as the peak
%
% Example 1:
% t = 0:.0001:10;
% x = 12*sin(10*2*pi*t)-3*sin(.1*2*pi*t)+randn(1,numel(t));
% x(1250:1255) = max(x);
% peakfinder(x)
%
% Example 2:
% ds = 100;  % Downsample factor
% dt = .001; % Time step
% ds_dt = ds*dt; % Time delta after downsampling
% t0 = 1;
% t = t0:dt:5 + t0;
% x = 0.2-sin(0.01*2*pi*t)+3*cos(7/13*2*pi*t+.1)-2*cos((1+pi/10)*2*pi*t+0.2)-
0.2*t;
% x(end) = min(x);
% x_ds = x(1:ds:end); % Downsample to test interpolation
% [minLoc, minMag] = peakfinder(x_ds, .8, 0, -1, false, true);
% minT = t0 + (minLoc - 1) * ds_dt; % Take into account 1 based indexing
% p = plot(t,x,'-',t(1:ds:end),x_ds,'o',minT,minMag,'rv');
% set(p(2:end), 'linewidth', 2); % Show the markers more clearly
% legend('Actual Data', 'Input Data', 'Estimated Peaks');
% Copyright Nathanael C. Yoder 2015 (nyoder@gmail.com)

% Perform error checking and set defaults if not passed in
narginchk(1, 6);
nargoutchk(0, 2);

s = size(x0);
flipData =  s(1) < s(2);
len0 = numel(x0);
if len0 ~= s(1) && len0 ~= s(2)
    error('PEAKFINDER:Input','The input data must be a vector')
elseif isempty(x0)
    varargout = {[],[]};
```

```
    return;
end
if ~isreal(x0)
    warning('PEAKFINDER:NotReal','Absolute value of data will be used')
    x0 = abs(x0);
end

if nargin < 2 || isempty(sel)
    sel = (max(x0)-min(x0))/4;
elseif ~isnumeric(sel) || ~isreal(sel)
    sel = (max(x0)-min(x0))/4;
    warning('PEAKFINDER:InvalidSel',...
        'The selectivity must be a real scalar.  A selectivity of %.4g will
be used',sel)
elseif numel(sel) > 1
    warning('PEAKFINDER:InvalidSel',...
        'The selectivity must be a scalar.  The first selectivity value in
the vector will be used.')
    sel = sel(1);
end

if nargin < 3 || isempty(thresh)
    thresh = [];
elseif ~isnumeric(thresh) || ~isreal(thresh)
    thresh = [];
    warning('PEAKFINDER:InvalidThreshold',...
        'The threshold must be a real scalar. No threshold will be used.')
elseif numel(thresh) > 1
    thresh = thresh(1);
    warning('PEAKFINDER:InvalidThreshold',...
        'The threshold must be a scalar.  The first threshold value in the
vector will be used.')
end

if nargin < 4 || isempty(extrema)
    extrema = 1;
else
    extrema = sign(extrema(1)); % Should only be 1 or -1 but make sure
    if extrema == 0
        error('PEAKFINDER:ZeroMaxima','Either 1 (for maxima) or -1 (for
minima) must be input for extrema');
    end
end

if nargin < 5 || isempty(includeEndpoints)
    includeEndpoints = true;
end

if nargin < 6 || isempty(interpolate)
    interpolate = false;
end

x0 = extrema*x0(:); % Make it so we are finding maxima regardless
thresh = thresh*extrema; % Adjust threshold according to extrema.
dx0 = diff(x0); % Find derivative
dx0(dx0 == 0) = -eps; % This is so we find the first of repeated values
```

```
ind = find(dx0(1:end-1).*dx0(2:end) < 0)+1; % Find where the derivative
changes sign

% Include endpoints in potential peaks and valleys as desired
if includeEndpoints
    x = [x0(1);x0(ind);x0(end)];
    ind = [1;ind;len0];
    minMag = min(x);
    leftMin = minMag;
else
    x = x0(ind);
    minMag = min(x);
    leftMin = min(x(1), x0(1));
end

% x only has the peaks, valleys, and possibly endpoints
len = numel(x);

if len > 2 % Function with peaks and valleys
    % Set initial parameters for loop
    tempMag = minMag;
    foundPeak = false;

    if includeEndpoints
        % Deal with first point a little differently since tacked it on
        % Calculate the sign of the derivative since we tacked the first
        %  point on it does not neccessarily alternate like the rest.
        signDx = sign(diff(x(1:3)));
        if signDx(1) <= 0 % The first point is larger or equal to the second
            if signDx(1) == signDx(2) % Want alternating signs
                x(2) = [];
                ind(2) = [];
                len = len-1;
            end
        else % First point is smaller than the second
            if signDx(1) == signDx(2) % Want alternating signs
                x(1) = [];
                ind(1) = [];
                len = len-1;
            end
        end
    end

    % Skip the first point if it is smaller so we always start on a
    %   maxima
    if x(1) >= x(2)
        ii = 0;
    else
        ii = 1;
    end

    % Preallocate max number of maxima
    maxPeaks = ceil(len/2);
    peakLoc = zeros(maxPeaks,1);
    peakMag = zeros(maxPeaks,1);
    cInd = 1;
    % Loop through extrema which should be peaks and then valleys
```

```
    while ii < len
        ii = ii+1; % This is a peak
        % Reset peak finding if we had a peak and the next peak is bigger
        %   than the last or the left min was small enough to reset.
        if foundPeak
            tempMag = minMag;
            foundPeak = false;
        end

        % Found new peak that was lager than temp mag and selectivity larger
        %   than the minimum to its left.
        if x(ii) > tempMag && x(ii) > leftMin + sel
            tempLoc = ii;
            tempMag = x(ii);
        end

        % Make sure we don't iterate past the length of our vector
        if ii == len
            break; % We assign the last point differently out of the loop
        end

        ii = ii+1; % Move onto the valley
        % Come down at least sel from peak
        if ~foundPeak && tempMag > sel + x(ii)
            foundPeak = true; % We have found a peak
            leftMin = x(ii);
            peakLoc(cInd) = tempLoc; % Add peak to index
            peakMag(cInd) = tempMag;
            cInd = cInd+1;
        elseif x(ii) < leftMin % New left minima
            leftMin = x(ii);
        end
    end

    % Check end point
    if includeEndpoints
        if x(end) > tempMag && x(end) > leftMin + sel
            peakLoc(cInd) = len;
            peakMag(cInd) = x(end);
            cInd = cInd + 1;
        elseif ~foundPeak && tempMag > minMag % Check if we still need to add
the last point
            peakLoc(cInd) = tempLoc;
            peakMag(cInd) = tempMag;
            cInd = cInd + 1;
        end
    elseif ~foundPeak
        if x(end) > tempMag && x(end) > leftMin + sel
            peakLoc(cInd) = len;
            peakMag(cInd) = x(end);
            cInd = cInd + 1;
        elseif tempMag > min(x0(end), x(end)) + sel
            peakLoc(cInd) = tempLoc;
            peakMag(cInd) = tempMag;
            cInd = cInd + 1;
        end
    end
```

```
    % Create output
    if cInd > 1
        peakInds = ind(peakLoc(1:cInd-1));
        peakMags = peakMag(1:cInd-1);
    else
        peakInds = [];
        peakMags = [];
    end
else % This is a monotone function where an endpoint is the only peak
    [peakMags,xInd] = max(x);
    if includeEndpoints && peakMags > minMag + sel
        peakInds = ind(xInd);
    else
        peakMags = [];
        peakInds = [];
    end
end

% Apply threshold value.  Since always finding maxima it will always be
%   larger than the thresh.
if ~isempty(thresh)
    m = peakMags>thresh;
    peakInds = peakInds(m);
    peakMags = peakMags(m);
end

if interpolate && ~isempty(peakMags)
    middleMask = (peakInds > 1) & (peakInds < len0);
    noEnds = peakInds(middleMask);

    magDiff = x0(noEnds + 1) - x0(noEnds - 1);
    magSum = x0(noEnds - 1) + x0(noEnds + 1)  - 2 * x0(noEnds);
    magRatio = magDiff ./ magSum;

    peakInds(middleMask) = peakInds(middleMask) - magRatio/2;
    peakMags(middleMask) = peakMags(middleMask) - magRatio .* magDiff/8;
end

% Rotate data if needed
if flipData
    peakMags = peakMags.';
    peakInds = peakInds.';
end

% Change sign of data if was finding minima
if extrema < 0
    peakMags = -peakMags;
    x0 = -x0;
end

% Plot if no output desired
if nargout == 0
    if isempty(peakInds)
        disp('No significant peaks found')
    else
        figure;
```

```
        plot(1:len0,x0,'.-',peakInds,peakMags,'ro','linewidth',2);
    end
else
    varargout = {peakInds,peakMags};
end
```

Appendix 2 Design of the data acquisition system (assisted by Dr. Randolph Pax)

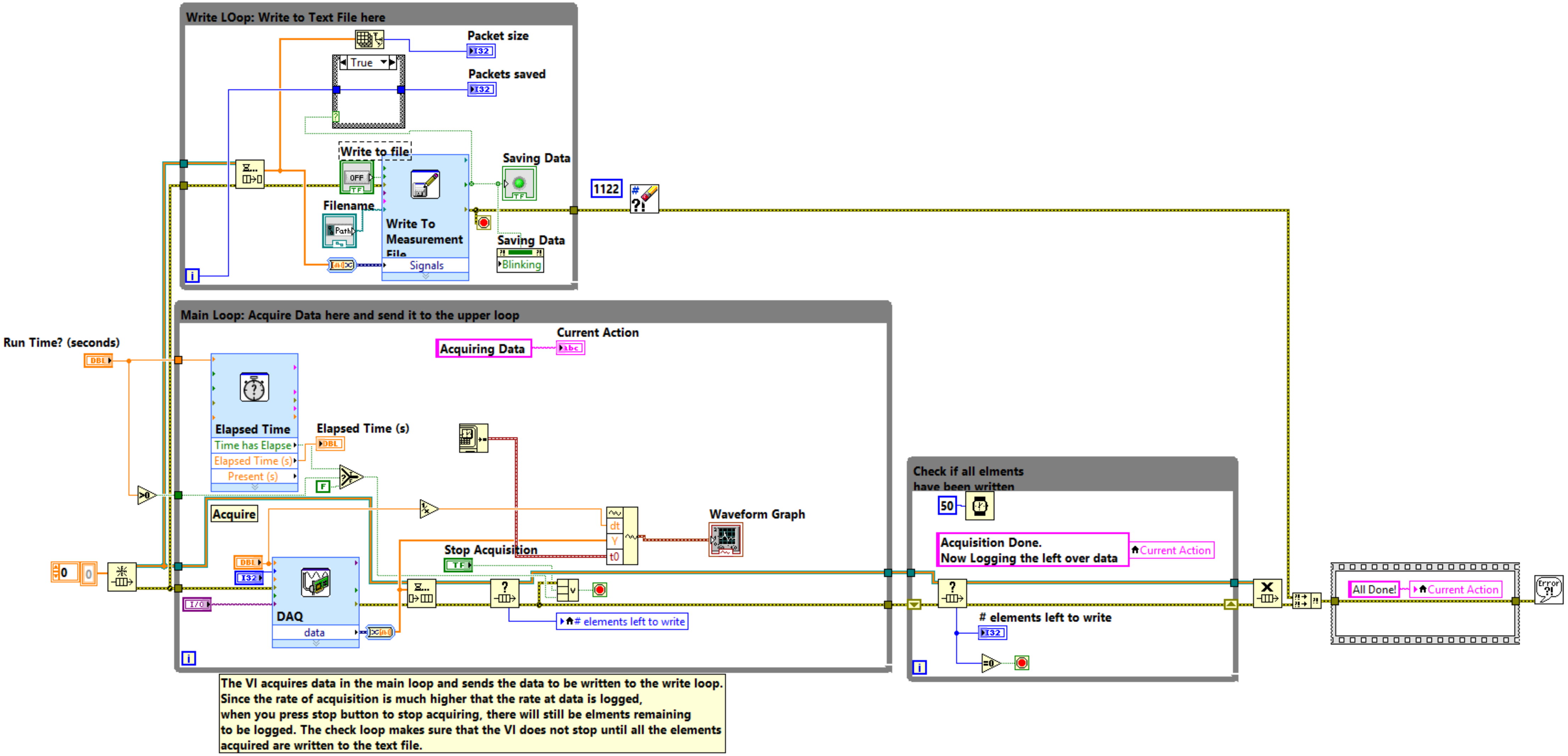

The VI acquires data in the main loop and sends the data to be written to the write loop.
Since the rate of acquisition is much higher that the rate at data is logged,
when you press stop button to stop acquiring, there will still be elments remaining
to be logged. The check loop makes sure that the VI does not stop until all the elements
acquired are written to the text file.

Appendix 3 Acoustic analysis and Imaging analysis

The acoustic analysis generates four types of data, namely, amplitude, damped frequency, phase, and damping ratio. Data presented here includes results for F150, DF250 and a preliminary result for NaCl.

Table A3.1 Amplitude of the fitted acoustic signal for F150

µM	1	2	3	Avg.	95% CI
0.0	0.218	0.260	0.172	0.217	0.016
1.2	0.223	0.249	0.229	0.233	0.005
2.3	0.229	0.243	0.224	0.232	0.003
3.6	0.225	0.241	0.221	0.230	0.004
5.2	0.220	0.237	0.218	0.224	0.004
6.3	0.223	0.235	0.217	0.224	0.003
7.9	0.222	0.233	0.215	0.223	0.003
8.9	0.223	0.233	0.215	0.223	0.003
12.2	0.219	0.230	0.210	0.220	0.004
17.2	0.214	0.227	0.207	0.216	0.004
24.3	0.212	0.221	0.205	0.213	0.003
47.7	0.201	0.215	0.192	0.203	0.004
71.8	0.195	0.204	0.179	0.193	0.005
144.3	0.171	0.186	0.164	0.174	0.004

Table A3.2 Damped frequency (Hz) of the fitted acoustic signal for F150

µM	1	2	3	Avg.	95% CI
0.0	1349	1348	1346	1348	0.6
1.2	1345	1347	1346	1346	0.3
2.3	1347	1349	1347	1348	0.5
3.6	1347	1348	1346	1347	0.4
5.2	1346	1347	1346	1346	0.1
6.3	1344	1347	1344	1345	0.5
7.9	1345	1346	1343	1345	0.5
8.9	1345	1345	1343	1344	0.4
12.2	1346	1345	1344	1345	0.3
17.2	1348	1347	1345	1347	0.4
24.3	1351	1351	1350	1350	0.3
47.7	1364	1365	1364	1364	0.2
71.8	1378	1377	1376	1377	0.5
144.3	1394	1393	1392	1393	0.3

Table A3.3 Phase (radian) of the fitted acoustic signal for F150

µM	1	2	3	Avg.	95% CI
0.0	1.57	1.79	2.00	1.78	0.11
1.2	2.00	2.00	2.00	2.00	0.00
2.3	1.92	2.00	1.86	1.93	0.07
3.6	2.00	2.00	2.00	2.00	0.00
5.2	2.00	1.67	1.58	1.74	0.11
6.3	2.00	1.92	1.58	1.84	0.10
7.9	1.79	2.01	1.94	1.91	0.09
8.9	1.58	1.80	2.01	1.79	0.11
12.2	1.94	2.01	2.01	1.99	0.05
17.2	2.01	2.01	2.01	2.01	0.00
24.3	2.01	2.01	2.01	2.01	0.00
47.7	2.01	2.01	2.01	2.01	0.00
71.8	2.00	2.01	2.00	2.00	0.00
144.3	2.00	2.00	2.00	2.00	0.00

Table A3.4 Damping ratio (%) of the fitted acoustic signal for F150

µM	1	2	3	Avg.	95% CI
0.0	11.49	10.09	10.75	10.78	0.25
1.2	9.60	9.37	9.15	9.39	0.09
2.3	7.84	8.53	8.09	8.14	0.13
3.6	8.04	8.48	8.35	8.29	0.09
5.2	7.83	8.78	8.59	8.35	0.18
6.3	8.11	8.72	8.26	8.33	0.12
7.9	8.23	8.55	8.50	8.43	0.07
8.9	7.82	8.67	8.42	8.30	0.16
12.2	7.93	8.67	8.62	8.41	0.16
17.2	7.82	9.37	8.32	8.50	0.29
24.3	8.08	9.22	9.18	8.88	0.23
47.7	8.02	8.59	8.28	8.31	0.11
71.8	6.98	7.66	7.72	7.48	0.15
144.3	5.68	5.98	5.93	5.87	0.06

Table A3.5 Amplitude of the fitted acoustic signal for DF250

µM	**1**	**2**	**3**	**Avg.**	**95% CI**
0.0	0.236	0.239	0.187	0.222	0.010
1.8	0.228	0.184	0.153	0.190	0.030
4.3	0.231	0.170	0.171	0.192	0.023
11.1	0.196	0.165	0.167	0.176	0.029
18.9	0.224	0.165	0.167	0.186	0.022
26.4	0.217	0.190	0.168	0.193	0.009
38.2	0.214	0.188	0.165	0.190	0.009
56.9	0.211	0.156	0.164	0.177	0.020
79.7	0.210	0.156	0.165	0.177	0.020
97.7	0.204	0.175	0.158	0.180	0.009
115.8	0.202	0.180	0.157	0.181	0.008
133.5	0.198	0.168	0.157	0.175	0.008
151.7	0.194	0.172	0.156	0.175	0.007
175.1	0.190	0.171	0.157	0.174	0.006

Table A3.6 Damped frequency of the fitted acoustic signal for DF250

µM	**1**	**2**	**3**	**Avg.**	**95% CI**
0.0	1339	1344	1349	1344	1.8
1.8	1339	1343	1348	1343	1.7
4.3	1340	1344	1348	1344	1.5
11.1	1338	1343	1347	1343	1.7
18.9	1336	1341	1347	1341	2.2
26.4	1337	1342	1347	1342	1.9
38.2	1338	1344	1349	1344	2.1
56.9	1342	1348	1350	1346	1.6
79.7	1348	1354	1355	1352	1.6
97.7	1352	1357	1363	1357	2.0
115.8	1357	1364	1366	1362	1.8
133.5	1361	1366	1368	1365	1.3
151.7	1365	1369	1370	1368	0.9
175.1	1369	1375	1373	1372	1.1

Table A3.7 Phase of the fitted acoustic signal for DF250

μM	1	2	3	Avg.	95% CI
0.0	2.00	1.86	2.00	1.95	0.07
1.8	2.00	2.00	2.01	2.00	0.00
4.3	2.00	1.91	1.75	1.89	0.09
11.1	1.67	1.83	1.92	1.81	0.12
18.9	2.01	2.00	2.01	2.01	0.00
26.4	1.87	1.72	2.01	1.86	0.10
38.2	2.01	2.01	2.01	2.01	0.00
56.9	2.01	2.01	2.02	2.01	0.00
79.7	2.01	2.01	2.02	2.01	0.00
97.7	2.01	2.01	2.01	2.01	0.00
115.8	2.01	2.00	2.01	2.01	0.00
133.5	2.01	2.01	2.01	2.01	0.00
151.7	2.01	2.01	2.01	2.01	0.00
175.1	2.01	2.00	2.01	2.01	0.00

Table A3.8 Damping ratio of the fitted acoustic signal for DF250

μM	1	2	3	Avg.	95% CI
0.0	9.53	10.52	7.78	9.35	0.50
1.8	8.96	10.06	8.76	9.27	0.27
4.3	8.45	8.75	8.22	8.47	0.10
11.1	8.96	8.74	8.59	8.76	0.08
18.9	9.75	8.54	7.92	8.79	0.36
26.4	9.09	8.60	7.67	8.49	0.26
38.2	9.22	9.47	8.47	9.09	0.19
56.9	9.19	9.08	7.94	8.76	0.26
79.7	9.65	9.50	7.26	8.85	0.50
97.7	9.00	8.72	7.25	8.38	0.34
115.8	9.01	9.04	7.21	8.48	0.38
133.5	8.70	7.69	6.96	7.79	0.32
151.7	8.44	7.65	7.24	7.80	0.23
175.1	8.07	7.98	6.83	7.65	0.24

Table A3.9 Acoustic analysis data for a preliminary test with NaCl

NaCl	**Amplitude**		**Damped frequency**		**Phase**		**Damping ratio**	
M	**Avg.**	**95% CI**	**Avg.**	**95% CI**	**Avg.**	**95% CI**	**Avg.**	**95% CI**
0.00	0.251	0.002	1334	0.1	2.00	0.001	9.62	0.06
0.04	0.236	0.001	1336	0.2	2.00	0.000	9.56	0.07
0.08	0.228	0.001	1335	0.3	2.00	0.001	9.27	0.10
0.11	0.227	0.002	1334	0.2	2.00	0.001	9.28	0.10
0.15	0.225	0.001	1333	0.1	2.00	0.001	9.20	0.05
0.18	0.224	0.000	1332	0.2	2.00	0.001	9.05	0.02
0.21	0.198	0.005	1331	0.3	2.00	0.002	9.26	0.11
0.24	0.200	0.005	1330	0.2	2.00	0.002	9.40	0.13
0.27	0.207	0.006	1329	0.2	2.01	0.002	9.16	0.11
0.30	0.243	0.001	1330	0.2	2.00	0.001	8.86	0.08
0.32	0.244	0.002	1329	0.1	2.00	0.001	8.89	0.10
0.35	0.216	0.004	1328	0.1	2.00	0.002	9.12	0.14
0.38	0.224	0.007	1328	0.2	2.00	0.003	8.90	0.11
0.40	0.221	0.005	1327	0.2	2.01	0.001	8.94	0.12

Table A3.10 Bubble size from imaging analysis for F150

F150	**Bubble size (mm)**				
μM	**1**	**2**	**3**	**Avg.**	**95% CI**
0.0	5.83	5.76	5.72	5.77	0.04
1.2	5.78	5.78	5.73	5.76	0.02
2.3	5.88	5.72	5.75	5.78	0.04
3.6	5.80	5.77	5.74	5.77	0.03
5.2	5.78	5.75	5.74	5.76	0.03
6.3	5.77	5.74	5.75	5.75	0.03
7.9	5.76	5.73	5.74	5.74	0.03
8.9	5.79	5.72	5.76	5.76	0.03
12.2	5.80	5.71	5.75	5.75	0.03
17.2	5.78	5.71	5.74	5.74	0.03
24.3	5.76	5.73	5.71	5.73	0.03
47.7	5.72	5.68	5.67	5.69	0.03
71.8	5.67	5.64	5.71	5.67	0.03
144.3	5.57	5.52	5.57	5.55	0.03

Table A3.11 Bubble size from imaging analysis for DF250

DF250	**Bubble size (mm)**				
µM	**1**	**2**	**3**	**Avg.**	**95% CI**
0.0	5.82	5.78	5.71	5.77	0.04
1.8	5.76	5.77	5.76	5.76	0.02
4.3	5.76	5.78	5.75	5.76	0.03
11.1	5.77	5.74	5.70	5.74	0.02
18.9	5.82	5.86	5.70	5.79	0.04
26.4	5.76	5.78	5.73	5.76	0.03
38.2	5.73	5.77	5.74	5.75	0.03
56.9	5.72	5.76	5.71	5.73	0.02
74.6	5.69	5.74	5.67	5.70	0.02
97.7	5.76	5.74	5.68	5.73	0.04
115.8	5.74	5.68	5.65	5.69	0.03
133.5	5.69	5.69	5.62	5.67	0.03
151.7	5.65	5.69	5.64	5.66	0.03
170.1	5.69	5.65	5.64	5.66	0.04

Appendix 4 2016 XXVIII International Mineral Processing Congress Conference Paper

INVESTIGATION OF THE POSSIBILITY OF USING ACOUSTIC TECHNIQUE TO DETERMINE BUBBLE SIZE IN AN INCLINED CELL

*P. Chu[1], R. Li[1], R.A. Pax[2] and J.A. Finch[1]
[1]*Department of Mining and Materials Engineering, McGill University*
3610 Rue University
Montreal, Canada, H3A 0C1
*(*Corresponding author:pengbo.chu@mail.mcgill.ca)*

[2]*RAP Innovation & Development Pty Ltd*
PO Box 559, Indooroopilly
Qld, Australia, 4068

ABSTRACT

Bubble size plays a key role in flotation. In this paper, we examine the possibility of using passive acoustic sending to determine bubble size. Software based on Short Time Fourier Transformation (STFT) was developed to analyze the frequency of the acoustic signal emitted from the bubble formation event. Bubble size was determined from the Minnaert frequency. It was shown that the acoustic-determined bubble size responded to reagent dosage, but was less sensitive than that given by imaging. The constraints of the current acoustic approach are discussed.

KEYWORDS

Bubble size, acoustic, frothers, salts, imaging

INTRODUCTION

Bubble size is an important factor affecting flotation performance. It determines the maximum available surface area for collecting and transporting mineral particles. Of interest for process control (Gorain et al., 1995), it can be determined by several techniques, such as image analysis (Grau and Heiskanen, 2002; Hernandez-Aguilar et al., 2002); conductivity (Barigou and Greaves, 1992); drift flux analysis using gas rate and gas holdup measurements (Banisi and Finch, 1994); and optical sensors (Randall et al., 1989). However, all these techniques have drawbacks.

Acoustic analysis of the oscillatory behaviour of bubbles to extract bubble size is another possibility (Al-Masry et al., 2005; Leighton, 1987; Leighton and White, 2012; Manasseh and Ooi, 2009; Pandit et al., 1992; Spencer et al., 2012). The fundamental basis is the work of Minnaert (1933) who first correlated the bubble size with its natural frequency, Equation 1:

$$f = \frac{1}{\pi D}\sqrt{\frac{3\gamma P_0}{\rho}} \tag{1}$$

where f is frequency, γ the specific heat of gas to liquid, P_0 the absolute liquid pressure, ρ the liquid density, and D the spherical diameter of the bubble.

An advantage of the acoustic approach is that it is not limited to opaque systems. The purpose of this paper is to examine the possibility of using passive acoustic technique to determine bubble size. An experimental set-up was built and an acoustic analysis program was designed. The study tested two reagents, MIBC and NaCl, at different concentrations. A comparison of bubble size obtained from imaging was made.

EXPERIMENTAL

Apparatus

The set-up comprised an Plexiglas cell with an inclined section (Figure 1), a camera (Canon EF 100 mm 1:1.28 USM macrolens), a hydrophone (Pettit Marine LLC, model

Lab-40-20), an amplifier (Radio Shark, Cat. No. 277-1088c), and a data acquisition board (NI USB-6341, X Series DAQ (16 AI, 24 DIO, 2 AO)).

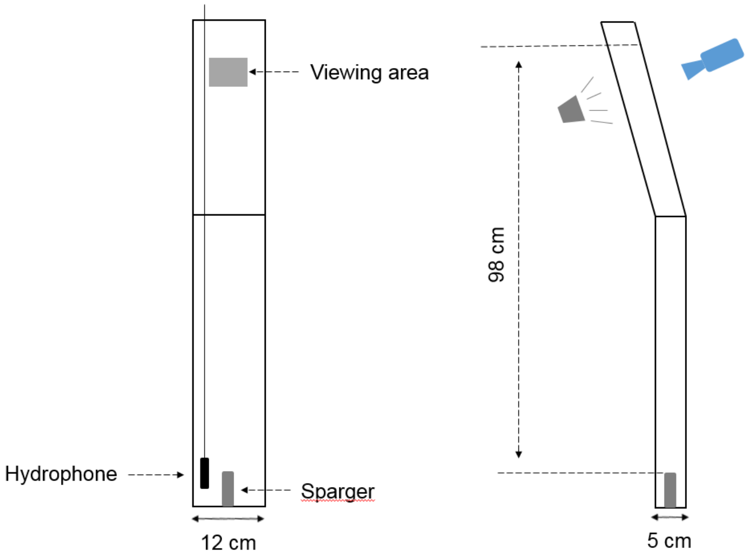

Figure 1 – Schematic of the cell

Software

Framed in LabView, software was developed to analyze the frequency of the acoustic signal emitted from bubble formation event. Frequency extraction is based on Fourier transformation (FT), specifically, fast time FT (FFT) (Equation 2) and short time FT (STFT) (Equation 3). In this work mainly STFT was employed because it also provides information on how the frequency changes over time, which is helpful for identifying noise in the signal. To ensure the resolution of the STFT, the data acquisition (acoustic recording) rate was set to 100 kHz. With the selection of a Hanning window and a window size of 4096, the 100 kHz was divided into 4096 bins with each representing a certain frequency range and therefore a specific range of bubble size. The STFT extracts the frequency from the signal and classifies them according to the pre-divided frequency bins. The number of appearance of each frequency is recorded. The Minnaert frequency (Equation 1) was then applied to each frequency bin to calculate the corronsponding bubble size.

$$\tilde{f}\ (\delta) = \int_{-\infty}^{+\infty} f(t) e^{-2\pi i t \delta}\, dt \qquad (2)$$

where $f(t)$ is a signal variationin time t, and δ represents frequency (in Hz).

$$F(\tau, \omega) = \int_{-\infty}^{+\infty} f(t) w(t-\tau) e^{-j\omega t}\, dt \qquad (3)$$

where $w(t)$ is the window function, typically a Hanning window or Gaussian window centered at *0*, τ the time index or the window size, ω the frequency.

Reagents

Two reagents, MIBC and salt (NaCl) were tested with concentrations listed in Table 1. The solutions were prepared with distilled water at room temperature (18 – 20^{0}C). For each condition, 3 repeat experiments were conducted. Between each experiment, the cell and hydrophone were thoroughly rinsed with tap water followed by distilled water.

Table 1 – Reagent tested

Reagents	Chemical formula	Concentration tested	Supplier
MIBC	$(CH_3)_2CHCH_2CH(OH)CH_3$	0 – 15 ppm	Sigma-Aldrich
Sodium Chloride	NaCl	0 - 0.8 M	Fischer-Scientific

Procedure

After filling the cell with test solution, the hydrophone was slowly lowered to the bottom of the cell next to the sparger. The air was turned on at 66 mL/min to generate bubbles. After the system reached steady state (*i.e..* the pressure stabilized), the acoustic recording was started. Each recording lasted about 1.5 minutes ensuring that enough data were collected. The recording was taken at two locations (left and right side of the sparger) aiming to maximise signal capture and compensate for uneven distributed sensitivity around the hydrophone.

During acoustic recording images were taken at the inclined viewing section of the cell (Figure 1). (The inclined section is used as the bubbles here slide approximately in a single layer avoiding the overlap at the bottom of the cell.) The images were analyzed offline using ImagJ software to obtain the sphere-volume equivalent diameter using the major (*a*) and minor (*b*) semi-axes of an ellipse fitted to the projected bubble area (Equation 4), assuming the bubble to be symmetric about the minor axis. The Sauter mean diameter was then calculated using Equation 5:

$$d = \sqrt[3]{(2a)^2 \times (2\mathrm{b})} \quad (4)$$

$$D_{32} = \frac{\sum d^3}{\sum d^2} \quad (5)$$

RESULTS

Short Time Fourier Transformation (STFT)

Figure 2 shows an example of the acoustic analysis of a bubble formation event in distilled water at air rate of 66 mL/min. It is observed in Figure 2a that the acoustic signature of the bubbly event is rather noisy and not much useful information can be extracted. The STFT analysis in Figure 2b provides a better alternative to examine the acquired acoustic data by showing two distinct frequency bands that are centered around 3 KHz and 3.5 KHz, respectively. The bubble size (Figure 2c) is obtained by applying the Minnaert frequency to the STFT result.

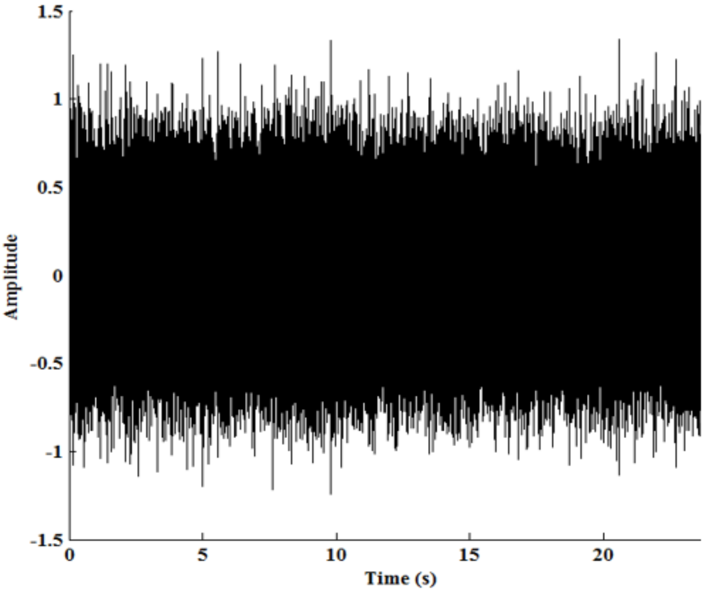

a) Actual acoustic recording of (for clarity, only the first 25s data was shown)

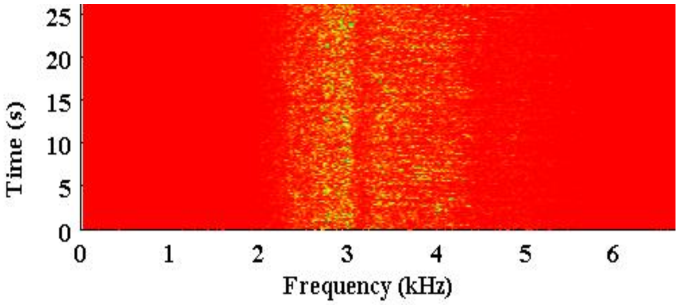

b) Spectrogram analysis

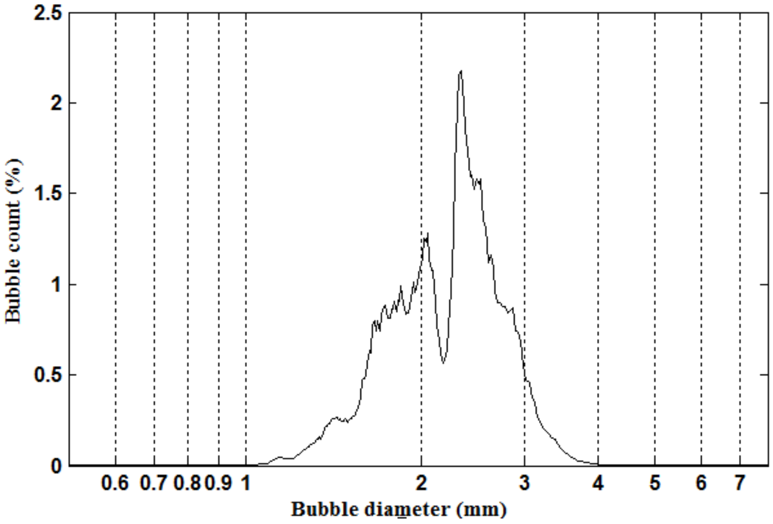

c) Bubble size distribution based on STFT

Figure 2 – Acoustic analysis of a bubble formation event in distilled water at 66 mL/min

Bubble Size

Figure 3 shows the bubble diameter obtained from both acoustic and imaging technique. One general observation is that with the increase in reagent dosage the bubble size obtained from imaging technique shows a significant decrease initially then plateaus while that from the acoustic technique only exhibits a minor decrease.

For MIBC, the bubble size from imaging technique decreases from *ca.* 1.87 mm (±0.03 mm, standard deviation) to *ca.* 083 mm (±0.01 mm), representing a reduction of *ca.* 56%;

while the acoustic only shows *ca.* 4.5% on average. For NaCl, the reduction in bubble size is *ca.*55% for imaging technique and *ca.* 6.5% for acoustic technique.

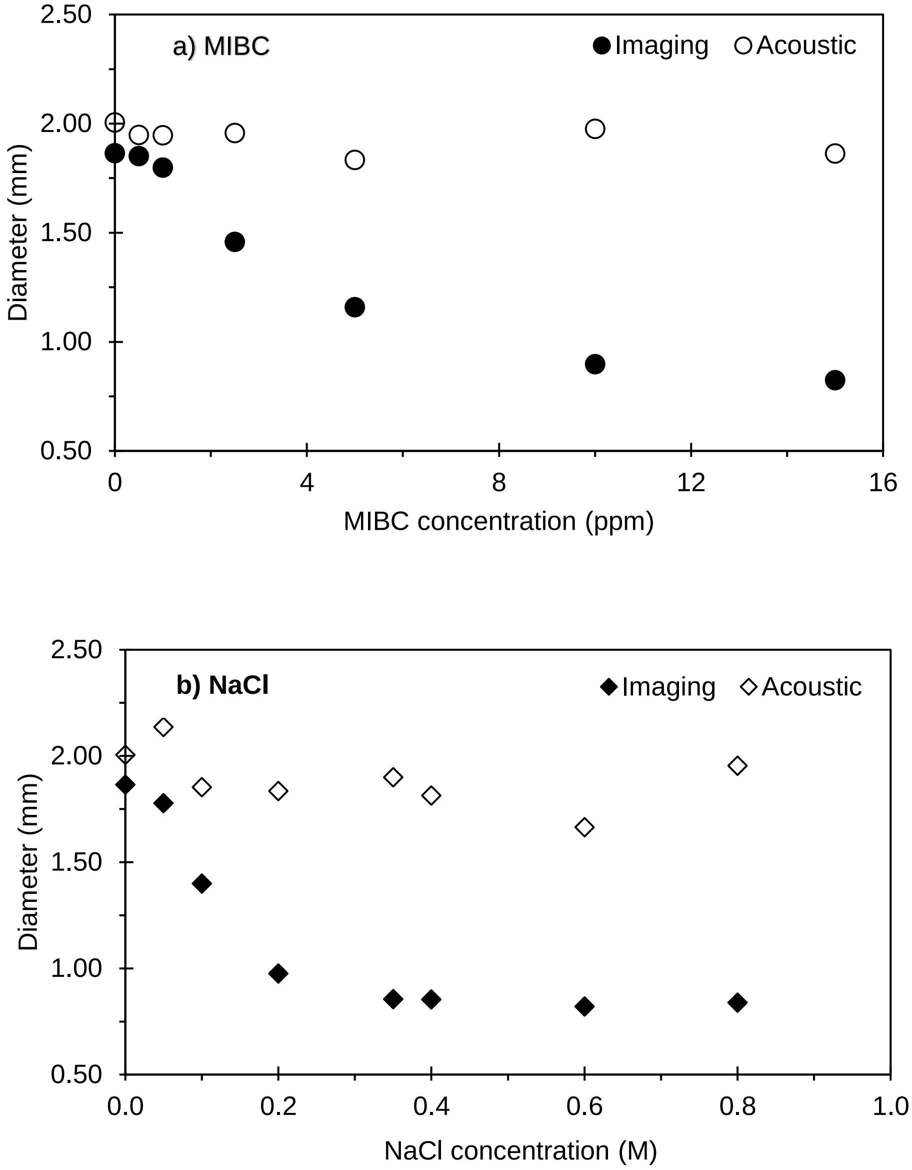

Figure 3 – Bubble diameter in the presence of different reagents at different concentrations

DISCUSSION

Bubble size in an incline cell was determined by both imaging and acoustic technique. It is shown that the imaging technique is more efficient in terms of accurately describing the bubble size than the current acoustic approach.

Results from imaging technique are consistent with experimental data in the literature. The characteristic of the critical coalescence concentration (CCC) (Cho and Laskowski, 2002) is obvious on both plots. With this particular experimental set-up, the CCC for MIBC seems to be 10 ppm and for NaCl 0.35 M. Such observation, however, cannot be made on the acoustic results.

It is noted that the acoustic and imaging measurements take place at two different locations. The bubble size by the imaging technique is a result of the interaction of all the bubbles traveling upwards to the inclined section, while the acoustic technique only focuses on the bubbles that are freshly formed off the sparger. The presence of reagent inhibits coalescence, and this is evidently supported by our imaging results. Additionally, some suspect the reagents also have an impact on bubble size at the creation stage.(Chu, 2013, 2014; Grau and Laskowski, 2006; Kracht and Finch, 2009). During this work, we have visually observed that reagents caused a bubble size reduction around the sparger area. However, the current acoustic approach failed to detect such change.

Perhaps the inefficiency of the current acoustic approach is due to the increasing complexity of the system when the number of bubble rises. It has been demonstrated that the Minnaert frequency reasonably describes the relationship of the volume pulsation and the radius of an isolated bubble (Leighton, 1994; Minnaert, 1933). In many practical circumstances, however, bubbles are entrained in a solid boundary or ‘wall’ (Manasseh and Ooi, 2009). Strasberg (1956) postulated that a bubble pulsating adjacent to a rigid boundary is equivalent to two bubbles pulsating in phase, so that the bubble is effectively coupled to its ‘mirror image’. The result of this coupling lowers the resonance frequency than the same bubble in an unbounded domain, causing an over-estimation of the true bubble size. In addition, adding frother or other chemicals could damp the vibration frequency and amplitude of bubbles, generating false signals. This phenomenon becomes more problematic if the number of bubbles becomes larger. Our acoustic results seem to reflect this occurrence.

The acoustic analysis by STFT only is not a sufficient approach. To improve its accuracy we will attempt several methods, including the zero crossings and auto-correction functions to detect the bubble pulsation count and frequency (Al-Masry et al., 2005) and the use of amplitude of the measured pressure fluctuations to determine the bubble size distribution (Pandit et al., 1992).

CONCLUSIONS

An acoustic analysis based on Short time Fourier Transformation was developed to determine bubble size in an inclined cell. It is shown the current approach is not efficient to accurately determine the bubble size. Further work is required to improve the functionality of this acoustic approach.

ACKNOWLEDGMENTS

The work was supported under the Chair in Mineral Processing at McGill University funded by Vale, Teck, Xstrata Process Support, Barrick Gold, Shell Canada, SGS Lakefield, COREM and Flottec through the NSERC CRD program.

REFERENCES

Al-Masry, W.A., Ali, E.M., Aqeel, Y.M., Determination of Bubble Characteristics in Bubble Columns Using Statistical Analysis of Acoustic Sound Measurements. Chemical Engineering Research and Design, 2005, 83(10), 1196-1207.

Banisi, S., Finch, J.A., Technical note reconciliation of bubble size estimation methods using drift flux analysis. Minerals Engineering, 1994, 7(12), 1555-1559.

Barigou, M., Greaves, M., Bubble-size distributions in a mechanically agitated gas—liquid contactor. Chemical Engineering Science, 1992, 47(8), 2009-2025.

Cho, Y.S., Laskowski, J.S., Bubble coalescence and its effect on dynamic foam stability. The Canadian Journal of Chemical Engineering, 2002, 80(2), 299-305.

Chu, P., Finch, J.A., 2013. Frother and breakup in formation of small bubbles, In Materials Science & Technology. CIM, Montreal, pp. 2034-2043.

Chu, P., Finch, J.A., 2014. Break-up in formation of small bubbles: Salts and frothers, In XXVII International Mineral Processing Congress, ed. J., Y. Gecamin, Santiago, Chile, pp. 312-321.

Gorain, B.K., Franzidis, J.P., Manlapig, E.V., Studies on impeller type, impeller speed and air flow rate in an industrial scale flotation cell — Part 1: Effect on bubble size distribution. Minerals Engineering, 1995, 8(6), 615-635.

Grau, Heiskanen, K., Visual technique for measuring bubble size in flotation machines. Minerals Engineering, 2002, 15(7), 507-513.

Grau, R.A., Laskowski, J.S., Role of Frothers in Bubble Generation and Coalescence in a Mechanical Flotation Cell. The Canadian Journal of Chemical Engineering, 2006, 84(2), 170-182.

Hernandez-Aguilar, J., Gomez, C., Finch, J., 2002. A technique for the direct measurement of bubble size distributions in industrial flotation cells, In the 34th Annual Meeting of the Canadian Mineral Processors, pp. 389–402.

Kracht, W., Finch, J.A., Bubble break-up and the role of frother and salt. International Journal of Mineral Processing, 2009, 92(3–4), 153-161.

Leighton, T.G., The Acoustic Bubble. By T. G. LEIGHTON. Academic Press, 1994. 613 pp. £95. ISBN 0-12-441920-8. Journal of Fluid Mechanics, 1994, 272, 407-408.

Leighton, T.G., Walton, A., An experimental study of the sound emitted from gas bubbles in a liquid. European Journal of Physics, 1987, 8, 7.

Leighton, T.G., White, P.R., Quantification of undersea gas leaks from carbon capture and storage facilities, from pipelines and from methane seeps, by their acoustic emissions. Proceedings of the Royal Society of London A: Mathematical, Physical and Engineering Sciences, 2012, 468(2138), 485-510.

Manasseh, R., Ooi, A., Frequencies of acoustically interacting bubbles. Bubble Science, Engineering & Technology, 2009, 1(1-2), 58-74.

Minnaert, M., On musical air-bubbles and the sounds of running water. Philosophical Magazine, 1933, 16, 235-248.

Pandit, A.B., Varley, J., Thorpe, R.B., Davidson, J.F., Measurement of bubble size distribution: an acoustic technique. Chemical Engineering Science, 1992, 47(5), 1079-1089.

Randall, E.W., Goodall, C.M., Fairlamb, P.M., Dold, P.L., Connor, C.T.O., A method for measuring the sizes of bubbles in two- and three-phase systems. Journal of Physics E: Scientific Instruments, 1989, 22(10), 827.

Spencer, S.J., Bruniges, R., Roberts, G., Sharp, V., Catanzano, A., Bruckard, W.J., Davey, K.J., Zhang, W., An acoustic technique for measurement of bubble solids mass loading: (b) Monitoring of Jameson cell flotation performance by passive acoustic emissions. Minerals Engineering, 2012, 36–38(0), 21-30.

Strasberg, M., Gas Bubbles as Sources of Sound in Liquids. The Journal of the Acoustical Society of America, 1956, 28(1), 20-26.

Wills, B.A., Finch, J.A., 2016. Chapter 12 - Froth Flotation, In Wills' Mineral Processing Technology (Eighth Edition), ed. Finch, B.A.W.A. Butterworth-Heinemann, Boston, pp. 265-380.